AN INVESTIGATION OF GEOTECHNICAL CHARACTERISTICS AND STABILITY OF A TAILINGS DAM

A THESIS SUBMITTED TO
THE GRADUATE SCHOOL OF NATURAL AND APPLIED SCIENCES
OF
MIDDLE EAST TECHNICAL UNIVERSTY

BY

EMİR SAYIT

IN PARTIAL FULFILLMENT OF THE REQUIREMENTS
FOR
THE DEGREE OF MASTER OF SCIENCE
IN
CIVIL ENGINEERING

JUNE 2012

Approval of the thesis:

AN INVESTIGATION OF GEOTECHNICAL CHARACTERISTICS AND STABILITY OF A TAILINGS DAM

submitted by **EMİR SAYIT** in partial fulfillment of the requirements for the degree of **Master of Science in Civil Engineering Department, Middle East Technical University** by,

Prof. Dr. Canan Özgen _________________
Dean, **Graduate School of Natural and Applied Sciences**

Prof. Dr. Güney Özcebe _________________
Head of department, **Civil Engineering**

Assist. Prof. Dr. Nejan Huvaj Sarıhan _________________
Supervisor, **Civil Engineering Dept., METU**

Examining Committee Members:

Prof. Dr. Orhan Erol _________________
Civil Engineering Dept., METU

Assist. Prof. Dr. Nejan Huvaj Sarıhan _________________
Civil Engineering Dept., METU

Prof. Dr. Erdal Çokça _________________
Civil Engineering Dept., METU

Prof. Dr. H. Şebnem Düzgün _________________
Mining Engineering Dept., METU

Inst. Dr. N. Kartal Toker _________________
Civil Engineering Dept., METU

Date: 21.06.2012

I hereby declare that all information in this document has been obtained and presented in accordance with academic rules and ethical conduct. I also declare that, as required by these rules and conduct, I have fully cited and referenced all material and results that are not original to this work.

Name, Last Name : EMİR SAYIT

Signature :

ABSTRACT

AN INVESTIGATION OF GEOTECHNICAL CHARACTERISTICS AND STABILITY OF A TAILINGS DAM

SAYIT, Emir

M.Sc., Department of Civil Engineering

Supervisor: Assist. Prof. Dr. Nejan Huvaj SARIHAN

JUNE 2012, 108 pages

The objective of this study is to investigate the stability problems in tailing (i.e. mine waste) dams. A tailing dam is an embankment dam (made of natural borrow or tailing material) constructed to retain slurry-like mining wastes that are produced as a result of operation of mines. In the last 30 years, the stability of tailing dams has drawn much attention as a significant number of tailing dam failures have been recorded worldwide. These instability problems caused significant loss of life and damage to property in addition to environmental hazards. In this study causes of failure of tailing dams and their stability problems are investigated with respect to their geometric and material characteristics. Seepage and stability of tailing dams are studied through limit equilibrium method and finite element method. The effects of uncertainties in material properties on the stability of tailings dams is investigated. Within this context, Kastamonu-Kure copper tailings dam is used as a case study and material properties are determined by laboratory tests.

Keywords: tailing dam, mine waste, slope stability, seepage.

ÖZ

BİR ATIK BARAJININ GEOTEKNİK ÖZELLİKLERİ VE STABİLİTESİNİN İNCELENMESİ

SAYIT, EMİR
Yüksek Lisans, İnşaat Mühendisliği Bölümü
Tez Yöneticisi: Ydr.Doç. Dr. Nejan Huvaj SARIHAN

HAZİRAN 2012, 108 sayfa

Bu çalışmanın amacı maden atık barajlarındaki şev duraylılığı problemlerini incelemektir. Maden atık barajları aslında değerli cevheri içinden işlenerek alınmış ince taneli çamurumsu maden atıklarını arka tarafta tutmak için, kaba maden atıklarından veya doğal malzemelerden oluşturulmuş setlerdir. Son 30 yılda, dünyada yıkılan çok sayıda atık barajının oluşu dikkatleri bu barajlardaki duraylılık sorunlarına çekmiştir. Bu yıkımlar çok sayıda can kaybına ve maddi hasara yol açmakla beraber çevresel felaketlere neden olmuşlardır. Bu çalışmada öncelikle, atık barajlarının geometrileri, malzeme özellikleri, yıkılma nedenleri ve stabilite problemleri hakkında bir literatür taraması sunulmaktadır. Daha sonra, limit denge ve sonlu elemanlar metodları ile atık barajlarındaki sızma ve stabilite problemleri analiz edilmiştir. Ayrıca malzeme özelliklerindeki belirsizliklerin stabiliteye etkisi incelenmiştir. Örnek çalışma olarak Kastamonu Küre'deki bakır madeni atık barajı seçilmiş ve buradan elde edilen numuneler üzerinde geoteknik laboratuvar deneyleri gerçekleştirilmiştir.

Anahtar Kelimeler: atık barajı, maden atığı, şev duraylılığı, sızma.

To My Family

ACKNOWLEDGEMENTS

I would like to express my appreciation to my committee: Prof. Dr. Orhan Erol, Prof. Dr. Erdal Çokça, Prof. Dr. Şebnem Düzgün and Dr. Kartal Toker. Special thanks to the Assist. Prof. Ayhan Gürbüz and other instructors in department of civil engineering at Atılım University for their precious help. They give me an opportunity to be part of Atılım University. I would like to thank to Assist. Prof. Nejan Huvaj Sarıhan for her guidance, support, patience and understanding.

I would also like to thank to all the people in the department of civil engineering at METU.

I would like to thank to Ulaş Nacar for his help and invaluable advice.

TABLE OF CONTENTS

LIST OF TABLES

TABLES

LIST OF FIGURES

FIGURES

CHAPTER 1

INTRODUCTION

1.1 General

Mining have been done since pre-historic times. At the beginning, digging for ores was pervasive. Today with the spread of modern mining concepts, researching for ores and processing of raw valuable minerals begin to dominate and promote mining industry all over the world. Nowadays, mining industry has been one of the most leading sectors for many developed countries' economies. However, in addition to the benefits, some outcomes of mining process can't be ignored such as environmental pollutions and several health risks. After the early 1900's, mine industry disposal legislation was amended and new stringent laws came in force. According to this new legislation, storage facilities became necessary for mining industry. These restrictions promoted emergence of various type of facilities. One of them is tailings dams. Engineers use waste materials itself as containment of dam structures (EPA, 1994). This type is widely admitted because of its countless precious merits. Above all, it is more economical, safe and effective way of holding enormous amounts of mining disposal with sizes range from sand-sized down to as low as a few microns. Hence, construction of tailing dams had been already spread all over the world.

Today, there are approximately 20000 mines all over the world (UNEP, 2000). In USA, there are about 1000 active metal mines and many of these have one or more tailing impoundment (EPA, 1994). These statistics reveal that the needs for robust, safe and well-operated tailings dams have been gradually increased.

However, these dumping sites and facilities are generally seen as burden by investors. Many of them do not want to invest and allocate budget for these passive facilities. As a consequence, the number of accidents and failures of tailing dam have increased all over the world due to poor maintenance, inaccurate design and bad stewardship. These huge and devastating failures cause serious catastrophic events (see figure 1.1). A recent example of instability in a tailing dam in Turkey (luckily this incident did not cause any human casualties or environmental damage) is shown in fig.1.2.

Figure 1.1 (a) View of the failed section in Hungary tailing dam failure in October 2010, (b) The extent of the environmental damage due to Hungary tailing dam failure in October 2010.

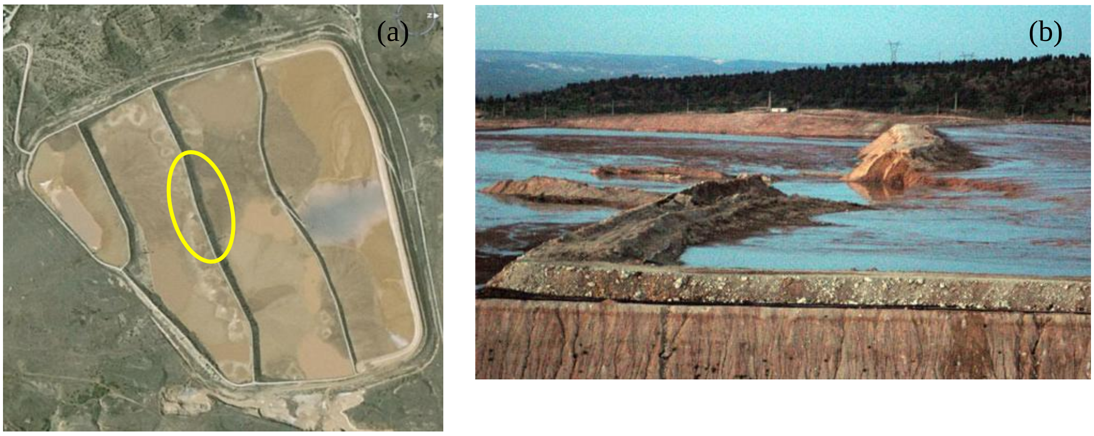

Figure 1.2 (a) Top view of a mine tailing dam in Kutahya, Turkey (Google Earth), (b) A view from the failed section in one of the four dykes in Kutahya, in May 2011 (http://www.emekdunyasi.net/ed/toplum-yasam/12415-ttb-kutahyada-risk-ciddi-boyutlarda)

In this study, firstly historical failures are listed with their consequences to demonstrate the importance of tailing dam stability. Afterwards, the main reasons behind the failures are found out and further investigated. The researches show that majority of these failures occurred in tailing dams which are constructed by upstream construction method, due to slope stability problems. Therefore, this study mainly focuses on the parameters which govern the slope stability of these type of tailing dams. Kastamonu Küre copper tailing dam is used as an example case. Subsequently, important parameters for slope stability are identified via literature survey. Moreover, geotechnical parameters of tailings are obtained from both laboratory tests and literature surveys to use in the analyses. Afterwards, whole ingredients' mean, maximum, minimum, standard deviation values and possible intervals are determined to use in SLIDE and in PLAXIS software. The slope stability analyses are done via these useful softwares to clarify the relative importance of all ingredients in calculated factor of safety. The results are shown in a pie chart to indicate the contributions of the ingredients in the safety of the dam.

1.2 **Scope of the Thesis**

Following the introduction, in the second chapter, firstly, definition of tailing dams is made and their failure trends are revealed by historical catastrophic incidents list. Secondly, the leading reason behind these failures is established as slope stability problem based on the data obtained from relevant institutions. Besides, it is expected that tailing dams constructed by upstream construction method are more vulnerable against this problem than other dams constructed with different methods. Thirdly, Kastamonu Küre copper tailing dam is studied as a case study. Fourthly, the parameters are selected that affect the slope stability. In addition to that, the range of values and basic statistical information about these parameters is researched and gathered by the help of laboratory tests results and literature survey. Finally, slope stability concept and limit equilibrium methods are reviewed.

In the third chapter, details of laboratory tests are explained and the results are shown.

In the fourth chapter, slope stability analyses in SLIDE and PLAXIS software are carried out. Firstly, brief explanation is done regarding the scenarios and then range of all slope stability parameters and intervals of other factors used in analyses, are explicitly shown in tables. The result of each analysis is shown as a graph of factor of safety versus change of the parameter.

In the fifth chapter, relative importance of the parameters that contribute to factor of safety, are shown as a pie chart and comments are made about the results.

CHAPTER 2

LITERATURE REVIEW

2.1 **Review of tailing dam concept all over the world**

Mine tailings can be defined as a part of worthless remaining waste of mine operations after removal of the profitable fraction from the ore. These residues are generally fine-grained particles. These fine grained particles are typically mixed with water until they acquire appropriate viscosity properties for pumping. At the end, slurry like mixture is dumped to storage field and storage processes are done by the help of dam-like structures (tailing dams). According to EPA technical report (1994), mine industry disposal legislation was amended after the early 1900's and new stringent laws came in force. It states that storage facilities are a must for mining industry. These facilities were planed as dams to contain tailings behind.

These impoundments do not only hold the waste mining disposal behind but also keep contaminated waters under control. The main distinction between tailing dam from water retention dams are; tailing dams cannot generate any revenue for their owner and they are designed for retaining their main construction materials, mining residues, behind itself instead of water (Davies, 2002). In contrast to water retention dams, tailing dams also do not have impermeable cores and filter layers; they are generally constructed by dumping fine and coarse grained tailings. It has been reported in the literature that, the failure rate of tailing dams are about ten times the rate of failure of conventional water retention dams (Davies, 2002). Moreover, constructions of tailing dams are continued stage by stage, their height is raised over time. In the light of this information, tailing dams are divided into three types. If raising progress is in direction of flow, this type of construction method is called as “downstream” type, if the dam is raised toward the upstream side of the dam, this method of construction is named “upstream” type, and if the construction raises the dam in both sides, this type is called “centerline” type (Vick, 1990) These different construction methods can be seen in Fig. 2.1.

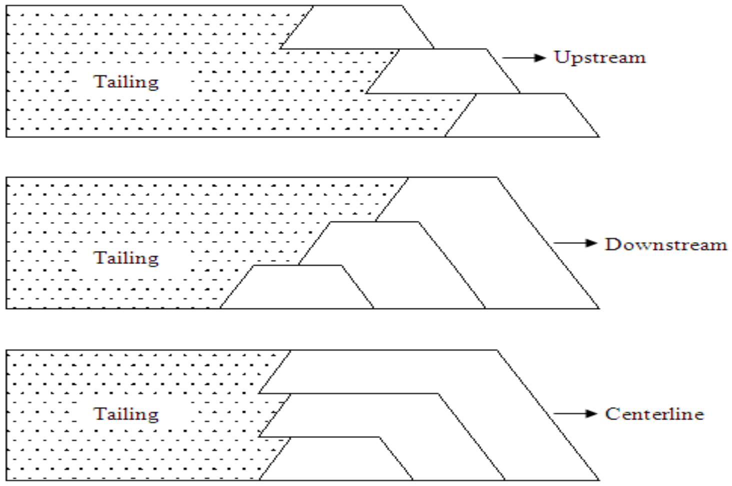

Figure 2.1 Raising type of tailing dams (after Vick, 1983).

In recent decades, upstream method has been the most chosen technique by the prominent mining companies around the world (Zuoan Wei, 2009). These preferences stem from the fact that constructions and operations of upstream dams are commercially viable. Nevertheless, operations of the tailing dam especially become more dangerous in financial turmoil times due to the passive nature of them. Institutional recommendations about vital construction processes and stewardship steps are generally ignored by mining companies to draw down operational costs. Historical failure events demonstrate that the negligence is endangering ecological nature and human life on the vicinity of tailing dams. Unfortunately, failures commonly cause huge and devastative effects which will be categorized directly and indirectly. The aftermath of failures; casualties, injuries, irrecoverable environment calamities can be direct consequences. However, indirect outcomes in some events can be more deplorable. They can result in substantial damages on socioeconomics of societies, such as erasing well-established mining companies from stock exchange markets and bring them to bankruptcies (UNEP, 2000). Some of the most significant failures in history and their consequences are listed in table 2.1.

Table 2.1 The most prominent tailing dams failures (http://www.wise-uranium.org).

Information	Type	Reason	Consequences
Aberfan, Wales, United Kingdom (coal)(1966)	-	Liquefaction due to heavy rain	162,000 m^3 tailings traveled 600 meters, 144 killed
Mufulira, Zambia (copper)(1970)	-	tailings flowed into underground	1 million tons 89 miners killed
Buffalo Creek,USA (coal)(1972)	-	collapse of tailings dam after rain	500,000 m^3 tailings traveled 27 km,125 killed
Bafokeng,South Africa (1974)	upstream	failure by seepage	3000000 m^3 tailing released
Madjarevo,Bulgaria (1975)	upstream	structural deficiency	250000 m^3 tailing released
Stava, Italy (Fluorine Mine) (1984)	upstream	overtopping and domino fashion	destroyed the village of Stava caused considerable damage
Cerro Negro No.4, Chile(copper) (1985)	-	liquefaction due to earthquake	500,000 m^3 tailings flow 8 km downstream
Merriespruit, South Africa (Gold) (1994)	upstream	overtopping (static-liquefaction)	17 people lost their lives
Amatista, Nazca, Peru (1996)	upstream	liquefaction due to earthquake	300,000 m^3 tailings flow 600m spill into river, croplands
Aznalcollar (Los Frailes), Spain (lead-zinc mine) (1998)	-	shallow foundation failure	$5x10^6$ m^3 tailings flows cause finances failure of a company
Baia Mare,Romania (2000)	upstream	structural deficiency	100,000 m^3 cyanide and heavy metal-contaminated liquid spilled into the Lupus stream
Kabadüz,Ordu,Turkey (copper,lead,zinc) (2009)	-	heavy rainfall cause overtopping	Contaminated water mix potable water supply of the city
Ajka, Hungary (red mud)(2010)	-	weak foundation most probably reason but research have still go on	4 killed and at least 120 needed medical treatment.700,000 m^3 of sludge gushed from the Ajkai Timfoldgyar plant in Ajka, 160km from Budapest

Major failures had occurred between 1928 and 2000 and have totally caused at least 1080 deaths. Most of the fatal failure had occurred between 1965 and 1996. In addition to that the records from destroyed or substantially damaged dams have obviously showed that upstream type is the most likely type of tailing dam to fail (Blight, 2010).

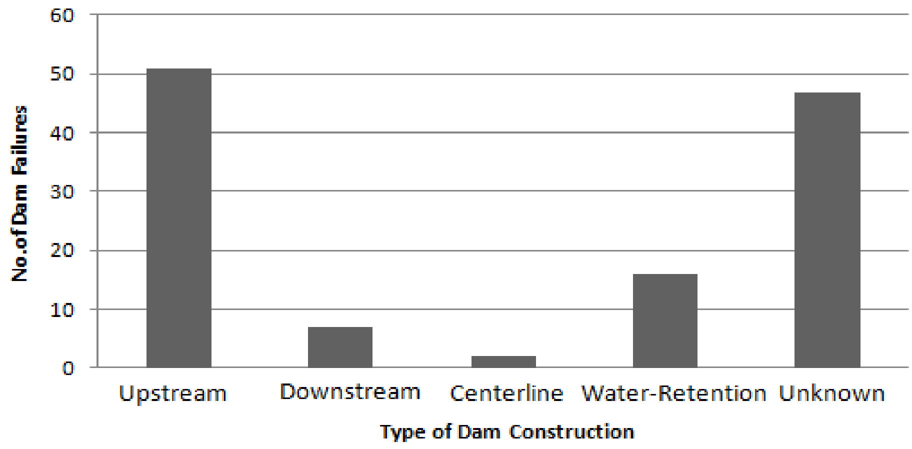

Figure 2.2 Tailings dam failures by dam type (USCOLD, 1994; UNEP, 1996).

For Turkey, one of the most important accident occurred in Turkey-Ordu Karadüz village in 2009. Zinc, lead, copper mining waste flowed into Melet River because of dam failure due to heavy rain. It rendered potable water resources useless and caused serious environmental contamination (http://www.yerbilimleri.com).

According to comprehensive literature researches and the interviews from incumbent institutions, number of substantially large tailing dams was 3500 in 2000 (Davies and Martin, 2000); for instance, there are 130 tailing dams in British Columbia-Canada, 350 in West Australia, 400 in South Africa, 500 in Zimbabwe. These verifications indicate that needs for more storage systems and trends to construct new tailing dams have already reached really serious levels. Their stability problems and possible failure scenarios have been considered and new researches have initially focused on the main reasons behind accidents and failures. According to numerous studies, each year, 2 to 5 "major" tailing dams experience structural stability problems (Davies, 2002). According to ICOLD (2001), the main reasons are listed in figure 2.3. The most predominant factor that causes more accidents and failures among others is slope stability.

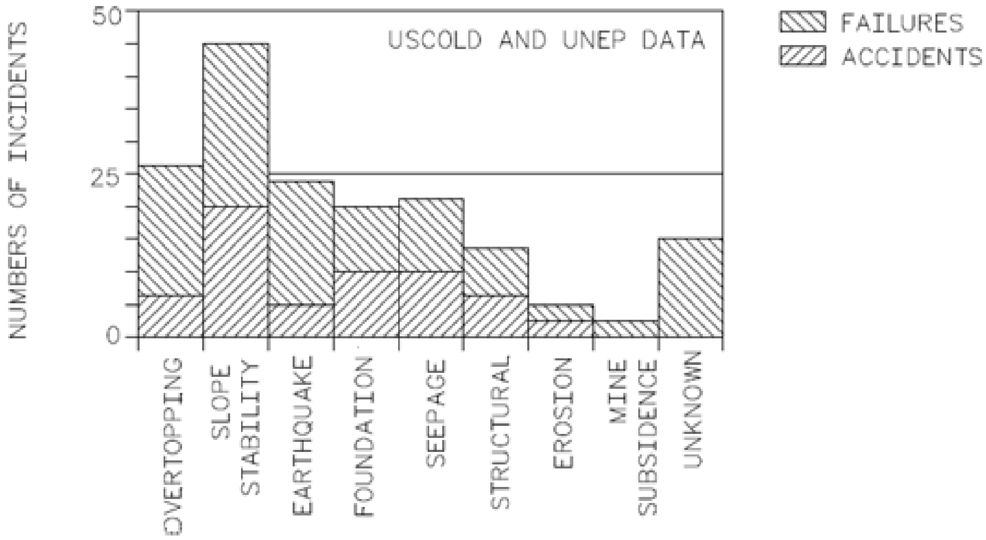

Figure 2.3 Reasons of failures and accidents in tailing dams all over the world (International Commission of Large Dams, 2001).

According to Yin et al. (2004), based on statistical data for China, most of the upstream-type tailing dams higher than 25m have had at least one time failure accidents or at least one time will encounter with potential failure along their service lives. Furthermore, the number of tailing dams in operation or being constructed are increasing day by day. When their long service life are considered, the issue of avert of potential slope stability failure should take priority. Comprehensive searches of all factors that contribute to the slope stability of tailing dams, should be investigated. Also, their relative effect/importance to stability analysis should be found out. So that, site investigations, laboratory of field investigations may be focused on determining one or two most important parameters, hence limited budget can be used more efficiently. Also, it may be a guide for further operations and robust designs of other parts of tailing dams. For instance, according to Fourie et al. (2009), water action has direct profound influences on almost every tailing storage facilities failure.

2.2 **Case Study: Kastamonu Küre Copper Tailing Dam**

Exact coordinate of copper mine in Kastamonu Küre is 41°48’ northern parallel and 33°41’ eastern meridian. This mine has been in operation since 1959; it is the third largest copper reserves in Turkey and total crude copper ore production reached to 700,000 tons in 2003. According to press release of chamber of Turkish mining engineers in 2004, its average copper ore production capacity is 300,000 tons per year.

Technically, the mine is operated with its tailing dam. This dam is a cross-valley tailings impoundment dyke. The building blocks of the dam are tailings, stacked rocks and natural soils. Stage construction process is being continued by the way of stacking of new materials without much compaction on the previously existing embankment. Rock and soil materials are carried by trucks. Tailings are mixed with water and pumped to dam reservoir as slurry and are spread through all over the area by spigots.

Figure 2.4 Kastamonu Küre copper mine waste storage tailing dam and spigotting process.

As of September 2009, the height of the dam was approximately 90 meters and due to intense production, its height has continuously been increased. The rate of increment is estimated to be about 3 meters per year.

2.3 **Characteristics of Mine Tailings**

In this section, firstly, the significant parameters are decided by results of literature reviews regarding the geotechnical properties of copper tailings and, specifically, the main characteristics of copper tailing dams all over the world. Secondly, the laboratory test results and literature review results are combined. Afterwards, final decision about the range of parameters to be used in slope stability analyses is made. The final step is really strenuous because tailing properties exhibit appreciable variability according to their locations in the section of the dam. For instance, grain size distributions of the tailings have direct relationship with the mining operations and discharge choices. The mining operations in the copper tailing dam in this thesis is assumed to be the same as in other copper mines all over the world. The discharge can be done with several methods (i.e single point, spigot and cyclone). In Kastamonu Küre upstream copper tailing dam, spigotting method has been applied. In spigotting method, tailings are piped with small diameter pipes network which is located on the crest of the dam and layed along the whole width of the dam (Lighthall, 1989). This method causes physical separation between the coarser and finer particles because the coarser materials is settling out immediately while the finer particles tend to move away from discharge point and settle away. As a result of less dragging of heavy and big particles, density, shear strength and permeability decreases with increasing distance from spigot points. In theory, with changing the location of discharging points, desired separation of the tailings will be provided behind the embankment. Perfect application is really difficult on field but by the help of this controlled segregation, heavy and coarse grain particles imbricate into each other near the embankment and additional slope stability can be provided. Moreover, big particles take an active role on reduction of pore water pressure by directing water flow path towards embankment. This will play complementary role on tailing dam slope stability by reducing pore water pressure (Lighthall, 1989).

As a natural result of dumping, soil parameters are greatly dependent on the location of specimens in the dam body. Ignoring variations in critical material properties making slope stability analysis with single values of a property, may deteriorate the process of finding out the governing parameter. Therefore, probabilistic analyses are preferred in this thesis to take into account the uncertainties. Samples taken from different depths at different spatial locations in the dam body and in the tailing reservoir might be useful to completely discover the uncertainty of the parameters. Unfortunately, laboratory tests are conducted on surficial disturbed soil samples taken from the dam by manual shallow excavations. These laboratory tests on samples taken from the dam would give an idea about the vital parameters and afterwards we could determine a range for these parameters by the help of literature review. These vital parameters are friction angles, cohesions, elastic modulus, unsaturated strength parameter ($\emptyset^b$) and void ratio of tailings. After the determinations, their probabilistic parameters such as mean and standard deviation values are inputted into SLIDE software for stability analyses. Also, several other characteristic parameters of tailing dam are included in analyses to investigate their effects on slope stability. These parameters are annual height of rise of dam and tailings (Note that the tailings level rises slightly less than dam crest elevation in order to have some air space to prevent overtopping. However as in typical tailing dams, this air space is not much, it is typically 0.5-1m), anisotropy in hydraulic conductivities (k_x/k_y) and location of the water at the upper layer (after settlement of tailings clear water pond can be visible at the surface elevation of the tailing reservoir). Their ranges are totally determined by the means of literature review results or site observations. Also, finite element analysis software PLAXIS, is utilized to study the rise rate effect in the analyses.

In this study, change of saturated hydraulic conductivity of tailings with factors of depth and distance from tailing discharge point are included in finite element seepage analyses. The permeability of tailings is influenced by the distance from spigot point. However, due to consolidation and decreasing void ratio of tailings with depth, saturated hydraulic conductivities of tailings are decreased with depth. The distance factor is considered, while drawing cross sections of Kastamonu Küre upstream copper tailing dam. Tailings are conceptually separated into two main groups as coarser and finer according to their hydraulic conductivity capabilities. According to ANCOLD (2011), coarser tailing beach slope may be up to 5% to 10% near the discharge point and close to horizontal near the slime zone. However, in this study, it is assumed that at the end of each stage, the top level of dam is remained smoothly horizontal and coarse part and fine parts are separated from each other with precise boundaries. It is assumed that coarse and fine tailings are filled half of the reservoir for each increments. Thus, two different tailings, the coarser and finer portions, are separated with forty-five degree line. Furthermore, the full cross-section of rock-fill part is extracted from outline drawing of field coordinates. The heights and slope of the left halves of seven dikes are obviously seen in this drawing. The other halves are assumed to be identical as seen in figure 2.5.

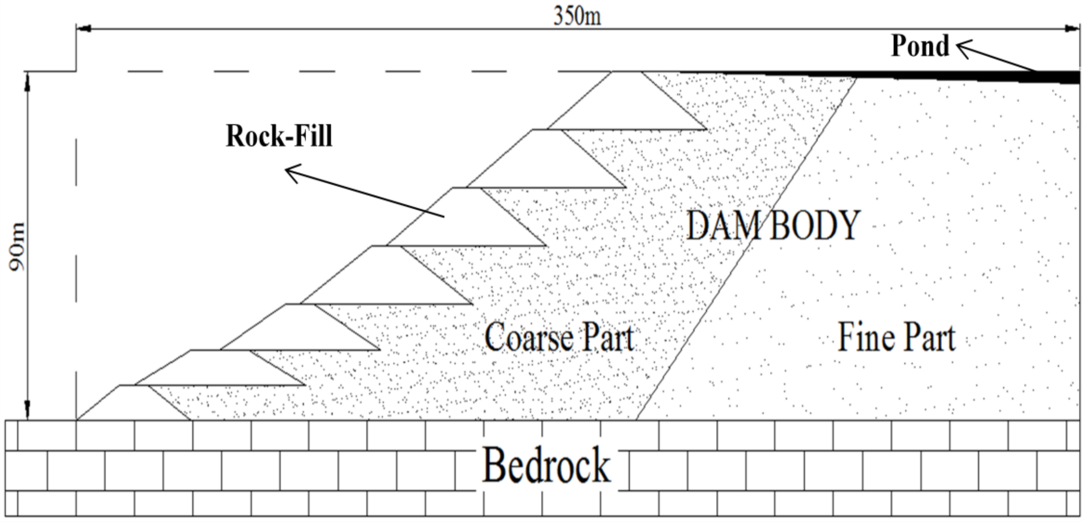

Figure 2.5 General view of the observed materials and shape of the Küre copper tailing dam cross section.

In seepage analysis, anisotropy ratio (k_x/k_y) and hydraulic conductivity ratio of coarser and finer tailings affect both flux and phreatic surface level in dam body. Also, permeability of rock-fill part dominates and governs the process. Moreover, according to Vick (1990), the ratio of permeability of coarser part (Ko) and finer part (Ks) is generally in range of 1-100 for mine tailings. As illustrated in figure 2.6, drastic changes can be observed in phreatic surface position and seepage amounts with Ko/Ks values. These changes naturally affect the factor of safety.

In literature, the hydraulic conductivity of copper tailings is reported to be in a wide range. Their fines content directly impacts the hydraulic properties of the whole tailing dam. According to Johnson (1997), saturated hydraulic conductivity is in the range of 10^{-4} cm/s to 10^{-5} cm/s, however, this value may go down to 10^{-6} cm/s at the some part of the tailing dams. Moreover, as illustrated in figure 2.7, the hydraulic conductivity ranges of copper tailing with amount of fines fraction are plotted against void ratios. In slope stability analyses in SLIDE, permeability of fine tailings at 1.4 void ratio ,which is the maximum void ratio, is taken as 10^{-6}cm/s as read from F200=70 regression line in figure 2.7. The regression line is extended to read the value corresponding to 1.4 void ratio. It will cast doubt on accuracy of the value but according to Bear (1972), it is reasonable for the slurry-like tailing soil consisting of silt and sand.

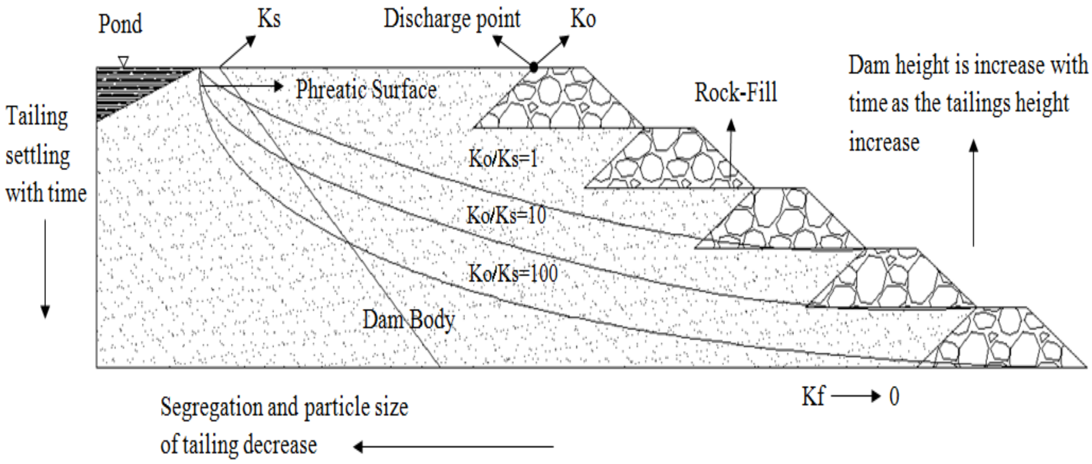

Figure 2.6 A cross section shows that effects of variations in permeability values on phreatic surface, and seepage (modified after Vick, 1990).

Ks: Permeability of the tailing at slimes zone,

Ko: Permeability of the tailing at the spigot point (dam crest),

Kf: Permeability of foundation.

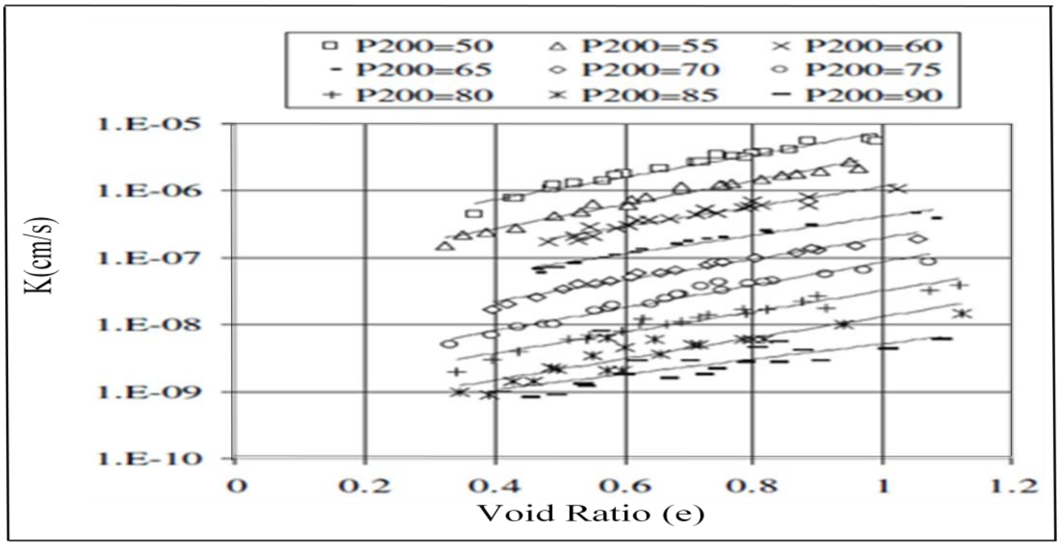

Figure 2.7 Variation of saturated hydraulic conductivity of copper tailing with P_{200} (passing percentage from No.200) varying from 50% to 90%, (Abolfazl, 2007).

In seepage analysis, the permeability of coarse tailings is assumed greater or equal to fines. In other words, to do robust assessment about the effects of Ko/Ks ratio on seepage and slope stability, for each scenario three analyses are done in SLIDE. The coarse tailings' hydraulic conductivities are calculated according to ratios are 1:10:100 respectively. During these analyses, saturated hydraulic conductivity of rock-fill part is assumed the same as unrevised value of coarse tailing.

In addition to that, depth factor is included in saturated hydraulic conductivity calculations. By the help of equation proposed by Taylor (1948), hydraulic conductivity values of tailings are considered to change with depth. Firstly, tailing dam body is transversely divided into four parts and their average void ratio is determined. The details of this process will be mentioned in later paragraphs. Saturated hydraulic conductivities of fine tailings of these parts are altered according to these average void ratios. Initial hydraulic conductivity (k_o) and void ratio (e_o) are taken 10^{-6} cm/s and 1.4 respectively.

According to Taylor (1948),

$$\log k = \log k_o - \frac{e_o - e}{C_k} \tag{2.1}$$

k_o: Hydraulic conductivity at a void ratio e_o.

k: Hydraulic conductivity at a void e.

C_k: hydraulic conductivity change index ($0.5*e_o$).

Anisotropy of saturated hydraulic conductivity ($k_{x/}k_y$) also affects transport processes of water in soil. It is well-known that horizontal conductivity values can be several times bigger than values of vertical conductivity especially in layered clayey soil. According to Bagarello (2009), this ratio barely reaches to two for sandy-loam soil. Therefore, for all analyses kx/ky is taken as 2.0.

The location of the pond has been perpetually changed with mining operations. It may be the most significant factor for pore pressure distributions through the dam slope stability analyses. Hence, three different locations are determined by means of site observations and literature surveys. The analyses are done with these scenarios to make robust decision.

Another important factor is the consolidation of loose tailings under their own weights. Increment of rate of effective compression stress is directly related with depth. Thus, through depth of dam, the rate of consolidation increases. Drainage conditions also accelerate this process. Hence, changes in void ratio with depth are considered in analyses. In geotechnical engineering for mine waste storage facilities, Blight, (2010) plots general void ratio of tailings versus depth as shown in figure 2.8.

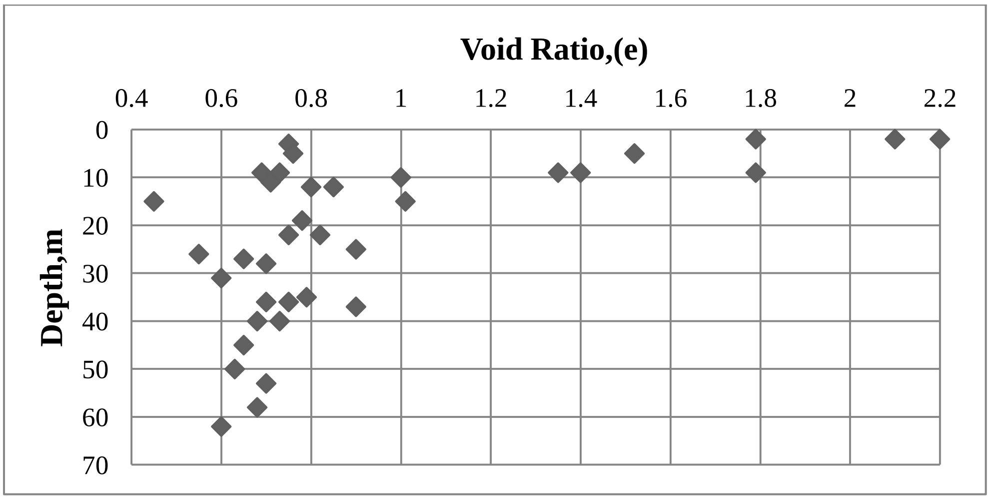

Figure 2.8 General void ratios (e) versus depth in copper tailing dam (Blight, 2010).

Statistical parameters of these values are derived and used in calculation of saturated unit weights of the tailings. Afterwards, probabilistic analysis is done in SLIDE with these unit weight values. The probabilistic parameters of void ratios are listed in table 2.2. The main reason of dividing the void ratio values into fifteen-meter intervals is construction process of rock-fill part. The part is raised with tailings on coarse tailing part. During the construction process, according to field coordinator, up to one and half meters settlements can be observed at coarse part in the first dumping of heavy particles of rock-fill part. Thus, it is assumed that coarse tailing part becomes denser after each increment step of rock-fill part. Also, the height of each embankment is approximately 15 meters. Hence, dividing the dam body into fifteen meters interval to make a comment about their void ratio is supposed as reasonable.

Table 2.2 Mean, maximum, minimum and standard deviation of tailings' void ratios with depth interval (Blight, 2010).

Depth (m)	0-15	15-30	30-45	45-62
Mean	1,18	0,78	0,74	0,66
Max	2,2	1,02	0,91	0,71
Min	0,46	0,56	0,61	0,61
SD	0,56	0,14	0,09	0,04

According to Zardari (2011), after a new dike construction on tailings, pore pressures reach to critical level and completion of the consolidation process take time. After consolidation, coarser tailings become denser. Therefore, usages of decreasing void ratio values in analysis are reasonable. However, at the surface levels (from top to depth of 15 meters), there is a wide gap between maximum and minimum values. Study of Bjelkevik and Knutsson (2005) on surface tailing samples from seven Swedish tailing dams, narrow the gap a bit. That study supports the variation of void ratios with distance from outlet. At all sites except at two, void ratio increase with distance. This indicates that tailing become finer as move away from the discharge point. That study show that, fluctuations of calculated void ratios between 0.6 and 1.3 cause 38-57 percent of changes in dry density. In addition to that, for copper tailings void ratio, Volpe (1979) propose a range between 0.6 and 1.4. Moreover, laboratory test results of maximum void ratio of Küre tailings are about 1.4 (testing procedure by Yamamuro and Lade (1998) is used, this will be explained in later sections. All of them demonstrate that usage of 0.6-1.4 range for surface tailings void ratios is reasonable. Hence, in this study, this min and max values are used for surface void ratios in SLIDE software analysis. The statistical parameters of interval of 45m-90m are assumed as same as that of 45m-62m interval. Void ratios of other intervals are checked by according to Cubrinovski and Ishihara (2002) if they are plausible or not. All maximum and mean void ratios of the intervals are nearly in the conceivable range.

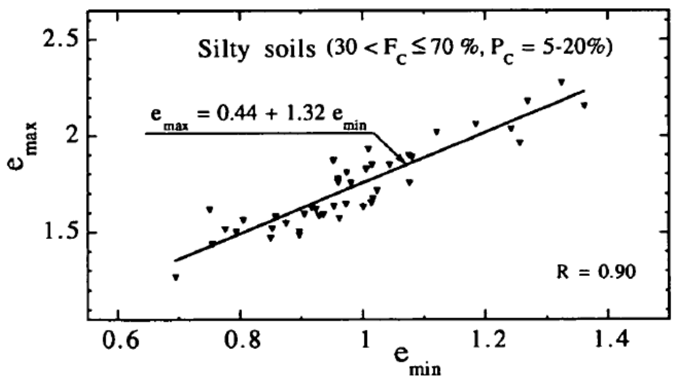

Figure 2.9 Relationship between e_{max} and e_{min} Cubrinovski and Ishihara (2002),.

e_{max}: 0,44+1,32 e_{min} (30%<Fc<70%, Pc=5%-20%) (2.2)

Where;

Fc: Fine fraction, for which grain size is smaller than 0,075mm,

Pc: Clay-size fraction (<0,005).

The palpable effect of distance from outlet on void ratio is not included in analysis; it is assumed that void ratio is continuously changed only with depth. In the model of Küre dam, unit weights of two type tailings that are derived from their average void ratios, are taken as identical at the same depth. Actually, remarkable changes are observed in void ratios for Aitik Swedish copper tailing dam at distance of 1500m and 3000m from the outlet. However, according to results of survey, total maximum reservoir length for Küre dam is barely 350m. Hence, effects of distance on void ratio are ignored. On the contrary, both distance and depth factors are included in prediction of tailings' modulus of elasticity. Modulus of elasticity increases with depth for coarser and finer tailings. In addition, it is expected that coarser tailings compressibility capability is relatively less with respect to finer particles at the same void ratio. This can be attributed to extra compaction efforts which applied by the weight of rock-fill on the coarse tailings.

In this study, moduli of elasticity (E) of the tailings are correlated according to Gurbuz (2007). This paper suggest that modulus of elasticity of cohesive soils can be extracted as two hundred times of the undrained shear strength (cu). According to unconfined compression tests results, modulus of elasticity values of coarse tailings at several different void ratios, are calculated. The modulus of elasticity of the loosest fine tailing, up to 15 meters depth, is cited from Zardari (2011). According to that study, the smallest elasticity modulus of Aitik cooper tailing is about 3000kPa. This value is assigned to fine tailings in 0-15 meters depth. Also, the modulus of elasticity values of the loosest coarse tailing, up to 15 meters depth, is derived from laboratory tests as 6000kPa. The difference between coarse tailing and fine tailing in the same depth interval is used as reference to figure out other modulus of elasticity values of fine tailings. The 'E' values of the rock-fill part are taken 40000kPa as mentioned in Zardari (2011). The bedrock is designed as the most rigid layer hence; its 'E' value is taken 10^6 kPa. The details of modulus of elasticity for the layers are listed in table 2.3.

Table 2.3 Elastic modulus values for parts of the dam for PLAXIS analysis.

Elastic Modulus (kN/m^2)			
Depth (m)	**Rock-fill**	**Coarse Tailing**	**Fine Tailing**
0-15	40000	6000	3000
15-30	40000	9000	6000
30-45	40000	12000	9000
45-90	40000	16000	13000

Other important factors are degree of saturation and water content of tailings and sandy soils in the rock-fill part. These substantial factors are directly related with phreatic surface location in first order, in second order amounts of discharged water, and seasonal precipitation. Seasonal precipitation concept doesn’t participate in scope of this study, and mixing ratio of water and tailing is being debated all over the world for construction of more stabile tailing dams without need for extra effort such as compaction or amendment. In this study, to figure out realistic phreatic surface, firstly the fact is considered which is the last elevated part is almost covered with water. Hence, water table should be located on there and phreatic surface should initiate from here. Therefore, determination of phreatic surface and pore pressures calculations are done by the following two main procedures. In one of them, three ponds are defined all of which have different initial points in the upper layer. Afterwards, phreatic surface and pore pressures are calculated via finite element methods with assumption of validation of steady state flow conditions. Saturated and unsaturated permeability properties of tailings and sandy soils of rock-fill part are included in finite element analysis. According to the results, the accuracy of phreatic surface level is evaluated and checked with field observation. Presence of water at toe and other trace of previous flows are elaborately examined. Also, amount of seepages are controlled for avert possible miscalculations. In other procedures, seepage analyses are not done. Only saturated conditions are considered and phreatic surfaces are stretched from initial points of previously defined ponds to toe. This procedure is applied for the model in which only undrained condition or both of the conditions are valid.

In this study, seepage analyses comprise unsaturated hydraulic conductivities properties of soils. This makes usage of new parameters mandatory. The main reason is, while permeability of saturated soils only depends on void ratio, for unsaturated soils, permeability is also governed by water content (Leong, 1997). According to Fredlund and Rahardjo (1993), it is demonstrated that there is a relationship between net suction pressure and unsaturated properties of soils. This relationship can be explained with soil water characteristic curve (SWCC) which explicitly shows that behavior of volumetric water content with increasing matric suction. In laboratory tests, taking accurate measurements of instantaneous volume changes with increasing matric suctions is very difficult. According to Leong (1997), to find out SSWC, empirical fitting equations can be used, moreover equation of Fredlund and Xing (1994) is recommended to fit the experimental data. In this study, due to lack of available SWCC data, ‘a’, ‘b’, and ‘c’ parameters are derived according to Zapata (2000). Eventually, SWCC curves of sandy soil and tailings are obtained for this study as figure 2.11 and 2.12.

According to Zapata (2000), for fine grained soils, the suction at a constant saturation is governed by specific surface area of the soil and PI (plasticity index) is well indicator about specific surface area. Moreover, clayey soils which have high PI values and small specific surface areas are also considered in Zapata (2000). Weighted PI, wPI, values are used in correlations to be more sensitive for water retention and absorption properties of the soils. For non-plastic soils, D_{60}, gradation parameter is preferred among several other parameters. Regarding to that issue, there is no specific reason stated in the study.

Fitting curve parameters for fine grained soil (Zapata, 2000);

$$\text{wPI} = \text{passing\#200} * \text{PI} \tag{2.3}$$

Passing #200: Specimen passing through 0,075mm in decimal,

PI= Plasticity index (%).

$$a = 0{,}00364 * (\text{wPI})^{3{,}35} + 4 * (\text{wPI}) + 11 \tag{2.4}$$

$$\frac{b}{c} = -2{,}313 * (\text{wPI})^{0{,}14} + 5 \tag{2.5}$$

$$c = 0{,}0514 * (\text{wPI})^{0{,}465} + 0{,}5 \tag{2.6}$$

$$\frac{h_r}{a} = 32{,}44 * e^{0{,}0186} * (\text{wPI}) \tag{2.7}$$

Fitting curve parameters for coarse grain soil (Zapata, 2000);

$$a = 0{,}8627 * (D_{60})^{-0{,}751} \tag{2.8}$$

$$\bar{b} = 7.5 \tag{2.9}$$

$$c = 0,1772*\ln(D_{60})+0,7734 \tag{2.10}$$

$$\frac{h_r}{a} = \frac{1}{D_{60}+9,7*e^{-4}} \tag{2.11}$$

a: A soil parameter which is primarily a function of the air entry value of soil (kPA),

b: A soil parameter which is primarily a function of the rate of water extraction from soil, once the air entry value has been exceeded,

$\bar{b}$: Average value of fitting parameter b,

c: A soil parameter which is primarily a function of the residual water content,

hr: A soil parameter which is primarily a function of the suction at which residual water content occurs (kPa).

D_{60}: Grain diameter corresponding to 60% passing by weight or mass (mm),

Frendlund and Xing (1994) equation fits the experiment data to standardized curve. The most distinctive difference of this equation from others is having well-defined mathematical equations to achieve the best fitting. In the original equation, 'a', 'm' and 'n' values are used. These are basically fitting parameters which indicate the shape of the curve. For instance, 'a' value indicates that matric suction at the inflection point. 'a' values should be taken greater than air entry value. It is insistently recommended in the articles. Zapata estimation satisfies this rule. Other coefficients, 'm' and 'n', are derived from slope of the curve. Instead of this values Zapata (2000) uses 'a', 'b', 'c' and additionally 'hr' value in own equations. Finally, Frendlund and Xing (1994) define correction factor 'C(ψ)' to reset volumetric water content at 10^6 kPa matric suction,. Zapata (2000) is also able to estimate that value.

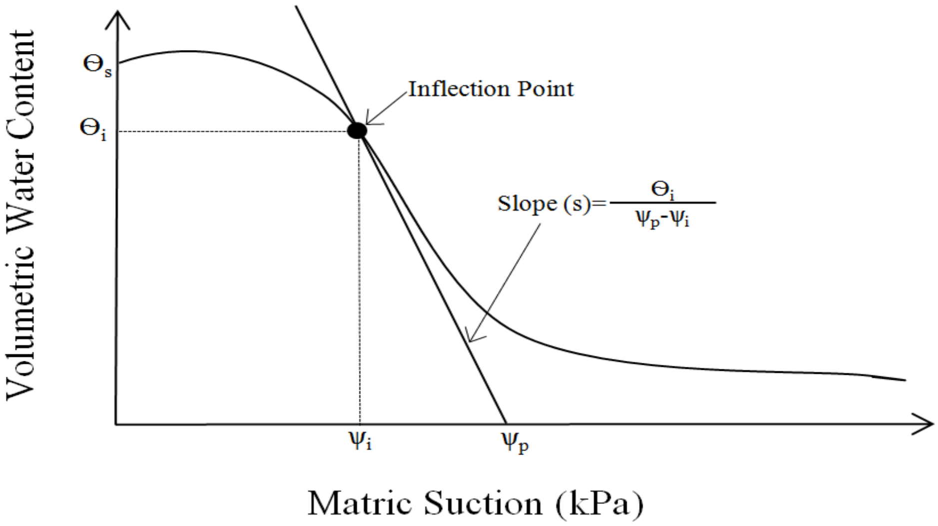

Figure 2.10 Explanation of parameters in graphic. (Fredlund and Xing, 1994).

Fredlund and Xing (1994) SWCC equation is used to fit experimental data;

$$\Theta w = C(\psi) * \left[\frac{\Theta s}{\left[Ln\left[e + \left[\frac{\psi}{a}\right]^{b} \right] \right]^{c}} \right] \tag{2.12}$$

a: Matric suction at inflection point (kPA),

b: Shape factor relate with upper part of SWCC,

c: Shape factor relate with lower part of SWCC.

$$C(\psi) = 1 - \left[\frac{Ln\left[1+\frac{\psi}{h_r}\right]}{Ln\left[1+\frac{10^6}{h_r}\right]} \right] \tag{2.13}$$

Θw: Volumetric water content,

Θs: Saturated volumetric water content, ψ: Matric Suction,

C(ψ): Correction factor.

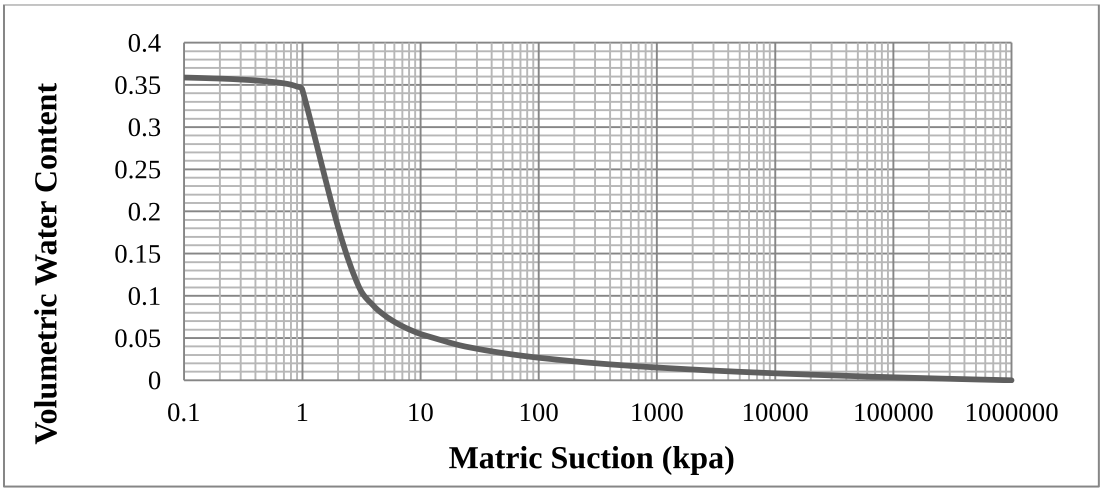

Figure 2.11 SWCC of sandy part of rock-fill.

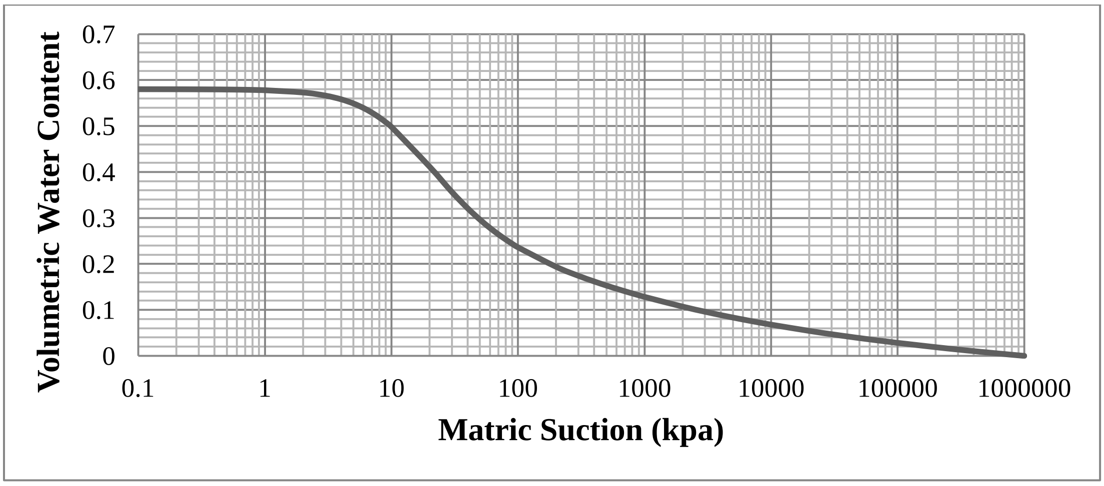

Figure 2.12 SWCC of slurry tailings.

According to Leong (1997), coefficient of unsaturated permeability can be written as a function of matric suction. Coefficients of unsaturated permeability are calculated for tailings and sandy soil with the formulas 2.14. Afterwards, these values are inputted in SLIDE software and by the help of finite element methods, calculation of phreatic surface and pore pressure is done. Coefficient of 'p' is taken as 4,32 according to recommendations of Leong (1997) for wetting tailing samples.

$$k_r = \frac{1}{\left[Ln \left[e + \left[\frac{\psi}{a} \right]^b \right] \right]^{c'}} \tag{2.14}$$

k_r: Ratio of unsaturated permeability and saturated permeability.

c’: c*p,

p=fitting parameter for permeability.

Finally, the last considerations are done on the most critical geotechnical parameters for slope stability analysis. The range of cohesion and drained friction angle values are revealed by the help of direct shear tests and literature survey. Furthermore, because of usually encountered unsaturated conditions in the nature, additionally modified Mohr-Coulomb parameters are involved in analysis. These are matric suction and unsaturated shear strength parameter ($\emptyset^b$) which is the angle indicating the rate of increase in shear strength relative to the matric suction. Fredlund (1978) states that matric suction will provide extra bonding stress and consequent increasing shear strength. In this study, unsaturated part of dam has crucial importance on the slope stability. Although water table almost covers the entire upper layer, there is high expectation from seepage analysis that substantial part of layers keep above the water table. Hence, linear form of shear strength equation proposed by Fredlund (1978) for unsaturated soil is used in analyses.

$$\tau_f = c' + (\sigma_n - u_a) * \tan\emptyset' + (u_a - u_w) * \tan\emptyset^b \tag{2.15}$$

τ_f : Shear strength of an unsaturated soil,

c': Effective cohesion of saturated soil,

$\emptyset'$: Effective angle of shearing resistance for a saturated soil,

$\emptyset^b$: Angle of shearing resistance with respect to matric suction,

$(\sigma_n - u_a)$: Net normal stress on the plane of failure, at failure,

$(u_a - u_w)$: Matric suction of the soil at the time of failure,

According to Fredlund (1995) once SWCC is obtained, shear strength of unsaturated soil can be easily determined via relationship between the matric suction and shear strength. Air entry value is essential for proper estimation because beyond this point, $\emptyset^b$ decrease as the matric suction increases. When the saturation is one, $\emptyset^b$ is equal to the effective friction angle ($\emptyset'$) and then decreases as saturation decreases. According to formula 2.15, shear strength increase permanently as suction increases. However, in case of low confining pressure, and depending on type of soil, the shear strength-matric suction curve will drop down to lower values. This behavior is usually nonlinear but in this study, the analysis bases on linear estimation. Hence, only, air entry value is read from SWCC and $\emptyset^b$ values are reasonable estimated. The maximum value of $\emptyset^b$ has to be decided as smallest value of effective friction angle due to software restrictions. The software does not allow definition of coefficient of correlation between $\emptyset^b$ and $\emptyset'$. It can be only defined between cohesion and effective friction angle ($\emptyset'$) for Mohr-Coulomb strength type. If the value of $\emptyset^b$ is taken greater than or equal to $\emptyset'$ at any unsaturated condition, it will cast doubt on accuracy of the analyses. Therefore, upper value of $\emptyset^b$ is concluded as equal to the minimum effective friction angle at air entry value and the lower value of $\emptyset^b$ is taken as 14^o which is proposed by Wohler (1974) as a possible minimum effective friction angle for copper slimes. Statistical parameters of effective friction angle and cohesion can be seen in table 2.4.

Table 2.4 Direct shear test results of tailings and their probabilistic parameters.

-	Friction Angle (^{o})	Cohesion (kPA)	$e_{average}$
Dry	35.9	8	1.34
	36.2	14.7	1.17
	36.5	24	1.11
	36.8	12.2	1
	37.0	30	0.77
w=%6.16	34.5	30	1.06
w=%8.68	33.6	21	0.89
w=%11.21	32.5	31	0.95
Saturated	30.4	6	0.75
Mean	34.8	19.7	-
SD	2.28	9.8	-
Maximum	37.0	31	-
Minimum	30.4	8	-

According to Abolfazl (2007), copper slimes effective friction angle ($\emptyset'$) is between 24^o-37^o and Guangzhi Yin (2011) supports this study and proposes that saturated friction angle is between 31^o-28^o. Hence, in analysis, mean, standard deviation and maximum value of friction angle are kept as same as test results but minimum value is pulled down to 24^o. Also, Abolfazl (2007) adds regarding cohesion values that the range is approximately 8 to 3030 kPa. The cohesion values obtained from tests are almost in this range, hence 30kpa and 8kpa values are used as minimum and maximum and values. Also, standard deviation and mean value of cohesion obtained from direct shear test are used in analyses without any changes.

The other shear strength parameters, have same degree of importance, are undrained shear strength parameters. The slip surfaces and factor of safeties, obtained with usage of them, are clearly more critical than that obtained with usage of effective strength parameters. Also, possibility of occurrence of a failure situation in undrained condition is really high. However, according to Vick (1983), less than 9m/yr of rising rate for upstream dams do not pose a problem for accumulation of excess pore water pressure to hazardous level. Therefore, expectation on formation of fully undrained condition from the dam which has 3m/yr rising rate, is considered as very few. While, making comments regarding stability of the dam via results of the analyses based on totally drain conditions, is not realistic. Consequently, all of the possible conditions are taken into consideration. The undrained shear strengths (cu) of coarse tailings are listed in table 2.5.

Table 2.5 Undrained shear strength of coarse tailings.

Undrained Shear Strength (cu) (kN/m^2)	
Depth (m)	**cu**
0-15	30
15-30	45
30-45	60
45-90	80

2.4 **Slope Stability Analyses Methodologies**

Nowadays the problems of slope stability have been addressed by deterministic or probabilistic approaches. In this study, limit equilibrium technique is coupled with Monte-Carlo probabilistic approaches in SLIDE analyses. Also, finite element method is used in slope stability calculation in PLAXIS analysis. Monte Carlo analysis is performed using 1000 and 10000 samples respectively. However, the results of analyses used 1000 samples are only showed due to negligible differences between mean factor of safeties of the analyses and also to minimize the consumption of time. Moreover, in this study, for a simple analysis, all input parameters are normally distributed. While distribution process, we made sure that negative values are not used for all parameters such as cohesion, friction angle, unit weight etc. The reliability indices are also calculated on the assumption that the factors of safety values are distributed both log normal and normal.

$$\beta_{ln} = \frac{\ln\left[\frac{\mu}{\sqrt{1+v^2}}\right]}{\sqrt{\ln(1+v^2)}} \tag{2.16}$$

β_{ln}: Log-normal reliability index,

μ: The mean of factor of safety,

v: Coefficient of variation of factor of safety.

$$v = \frac{\sigma}{\mu} \tag{2.17}$$

σ: Standard deviation.

$$\beta = \frac{\mu_{FS}-1}{\sigma_{FS}} \tag{2.18}$$

β: Normal reliability index,

μ_{FS}: Mean safety factor,

σ_{FS}: Standard deviation of safety factor.

Recommended reliability index of SLIDE software manual is at least 3 for minimal assurance of a slope design. Reliability of the results is evaluated with respect to this reference value.

In this study, limit equilibrium methods is preferred because of being one of the most popular approaches to slope stability analysis. This reason can be attributed to calculations simplicity and being a purely static method. In this method, deterministic slope stability analysis is provided as a factor of safety which depends on geotechnical characteristics of soil and conditions. The alleged failing part of the slope is divided into a series of vertical slices and considering separately but calculation of the factor of safety is done by considering all of them as one. Factor of safety will be defined as the ratio of the resisting shear strength to the mobilized shear stress. The static equilibrium of the slices and the mass as a whole are used to elucidate the slope components. However, due to methods of slices intrinsic properties, equilibriums are generally statically indeterminate and, as a result, require assumptions in order to solve the equations. Some of these assumptions demonstrate differences according to chosen method; this issue is discussed in next subtitles. The others are peculiar to method of slice. For instance, assumption of potential slips surface type. According to Ning (2008), at heterogeneous soil layer with non-complex profile, the slip surface can be assumed as circular. Therefore, critical slip surfaces are sought with method of grid search as though they have circular shape.

2.5 **Methodology of Choosing one of the Limit Equilibrium Methods**

There are many comprehensive procedures on methods of slices in order to solve slope stability problems. These procedures have their own assumptions to render the problem determinate. Especially, assumptions on correlations of inter-slice forces are decisive features which distinguish methods to each other. However, this distinction is not explicit for Morgenstern-Price and Spencer method, although correlations are very different from each others. The factor of safety values with respect to moment equilibrium, are substantially similar. For instance, ratio of horizontal normal forces and lateral shear forces on slices are defined by constant value 'λ' and function f(x) in Morgenstern-Price method. While in Spencer method, this ratio is only defined by tangent of the angle between the horizontal and the resultant inter-slice force. Comparative studies demonstrate that for two methods, the correlations have not profound influence on FS of moment equilibrium. The differences are not bigger than %1 therefore they are perfectly usable in practice.

Table 2.6 Description of slope stability analysis method (Pockoski & Duncan, 2000).

Method	Overall Moment Equilibrium	Individual Slice Moment Equilibrium	Horizontal Force Equilibrium	Vertical Force Equilibrium	Assumptions	Comments
Swedish Circle	Yes	No	No	No	Circular Slip Surface	Only for ϕ=0
Ordinary Method of Slices (Fellenius 1927)	Yes	No	No	No	Circular Slip Surface Side Forces Parallel to Base	Conservative Very inaccurate for high pore water pressures
Bishop's Modified Method (Bishop 1955)	Yes	No	No	Yes	Circular Slip Surfaces Side Forces Horizontal	Very inaccurate for high pore water pressures
Morgenstern and Price's Method (Morganstern and Price 1965)	Yes	Yes	Yes	Yes	Slip surface of any shape Pattern of Side Force Orientations	Much engineering time required to vary side force assumptions.
Spencer's Method (Spencer 1967)	Yes	Yes	Yes	Yes	Slip surface of any shape Side Forces Parallel	Simplest Method
Corps of Engineers Modified Swedish (1970)	No	No	Yes	Yes	Slip surface of any shape Side Forces Parallel to Slope	High factor of safety
Lowe & Karafiath (1960)	No	No	Yes	Yes	Slip surface of any shape Side Force Orientations Average of Slope and Slip Surface	Best side force assumption
Janbu Simplified (Janbu 1954)	No	No	Yes	Yes	Slip surface of any shape Side Forces Horizontal	Low Factor of Safety
GLE - General Limit Equlibrium	Yes	Yes	Yes	Yes	Slip surface of any shape Pattern of Side Force Orientations	Much engineering time required to vary side force assumptions.
GoldNail Method* (Golder)	Yes	*	Yes	Yes	Slip surface of any shape Normal Stress Distribution	Toe circles only
SNAIL Method (CALTRANS)	No	No	Yes	Yes	Slip surface of any shape Two or three wedges, with side force angle = ϕ	Limited shapes of slip surfaces

Table 2.6 concisely shows that merits of the methods. The most outstanding ones among them are Morgenstern Price method, Spencer method. According to American Society of Civil Engineers (SCEC, 2002) due to difficulties in selecting appropriate force function for Morgenstern Price method and entails strenuous efforts, it is not practically suitable for engineers. Hence, SCEC guideline for analyzing and mitigating landslide hazards in California (2002) recommend that Spencer Method be used for analysis of failure surfaces of any shape. The Spencer Method assumes that relative changes of the lateral shear forces and horizontal normal forces, which are acting on each side of all slices, are constant for all the sliding section. The most important merit of this method is able to do calculation of the horizontal force and moment equilibriums independently. So that it is able to give both force equilibrium factor of safety (F_f) and moment equilibrium factor of safety (F_m) which are identical to each other. Therefore, in this study, factor of safety is calculated with Spencer Method and the results are evaluated according to Sowers (1979).

Table 2.7 Significance of factor of safety (Sowers, 1979)

Factor of Safety	**Significance**
Less than 1,0	Unsafe
1,0-1,2	Questionable safety
1,3-1,4	Satisfactory for cuts, fills, questionable for dams
1,5-1,75	Safe for dams

2.6 Comparison Criteria of the Slope Stability Results

The changes of the results in SLIDE analyses are stemmed from the fact that they are directly dependent on the variations of the used slope stability parameters. As already mentioned, these parameters are cohesion, effective friction angle, unit weight, unsaturated shear strength ($\emptyset^b$) and Ko/Ks ratio for SLIDE analyses. One of the changed parameters can cause differences in contribution of other parameters to the results and consequently changes factor of safety itself. Hence, while considering relative effects of these parameters to the results in this study; firstly, the details of relationships between the parameters and factor of safeties (FOS) are figured out. Scatter plots assist to make these relationships concrete. Initially, it is assumed that there are linear relationships between the parameters and FOS values because linear Mohr-Coulomb shear strength criteria are preferred in the analyses and according to them; the parameters are directly proportional to shear strength. Subsequently, the equations of linear regression lines are individually derived from scatter plots of FOSs and values of each parameter. The slopes of the lines show those parameters' capabilities to change FOS. However, these equations mostly do not properly fit the scatters of the values of parameters and FOSs. Moreover, some equations fit better than others. Therefore, correlation coefficients of these lines are appraised as criteria for fitting succession. These slopes of the lines and correlation coefficients render calculations possible to find out relative contributions of the parameters to FOSs for any scenarios. The contributions can be calculated by formula 2.19 and 2.20 except Ko/Ks parameter. The total absolute effects of Ko/Ks parameter are noticed only via scatter plots of Ko/Ks values and corresponding mean factor of safeties. Therefore, only one scatter plot are generated by using three Ko/Ks values and corresponding mean factor of safeties for each scenario. Hence, the total absolute effect of this parameter is calculated by multiplying only one slope value and one correlation coefficient value for each scenario.

$$Z_{p,c}=\sum_{f=1}^{N_t} (cc)_{t,d}*S_{t,d} \tag{2.19}$$

$Z_{p,c}$: Total absolute effects of the parameter under one of the (Ko/Ks) conditions for the scenario,

$cc_{t,d}$: Correlation coefficient of the soil in the depth interval,

$S_{t,d}$: Slope of the linear regression line of the soil in the depth interval,

p: Indicates that one of the parameters, c: Indicates that one of the (Ko/Ks) conditions,

N_t: Indicates that number of depth intervals of the soil (for instance, coarse tailing have four depth intervals),

t: Indicated that type of the soil (i.e coarse tailing, fine tailing or rock-fill),

f: It is a counter for depth intervals of the soil.

Absolute effects of each parameter on FOS can be individually calculated for any scenario by the means of cumulative summations of the multiplications of these slopes and correlation coefficients. However, in this study, some parameters have more depth interval than others. For instance, while twenty seven cohesion effects are being summed for a scenario, only one Ko/Ks effect or twenty four unsaturated shear strength effects are being summed. Therefore, all parameters average effects are calculated to provide equal change in formula 2.20. In addition, the percentage of each parameter can be represented as a piece of pie in the charts for any scenario via formula 2.20. It is based on an assumption that the cumulative summations of total absolute effects of all parameter constitute the FOS. If total absolute effects of a parameter are divided by all cumulative effects, the width of a piece in whole pie can be determined.

$$R_i = \frac{\dfrac{\left[\sum_{c=1}^{3} Z_{p,c}\right]}{N_j}}{\sum_{i=1}^{4} \dfrac{\left[\sum_{c=1}^{3} Z_{pi,c}\right]}{N_j}} \text{ X } 100 \qquad (2.20)$$

R_i: Indicates that percent contribution of a parameter to FOS for the scenario,

$Z_{pi,c}$: Indicates that all absolute effects of one of the parameter under the (Ko/Ks) condition for the scenario,

N_j: Summation of depth intervals in three (Ko/Ks) condition,

i: It is a counter for the parameters,

c: It is a counter for (Ko/Ks) conditions.

The absolute effects of the Ko/Ks parameters should be additionally summed with denominator of the formula 2.20 while calculation of all percentages. In case of calculation of percent distribution for Ko/Ks parameter, inputting of its absolute effects as numerator of the formula 2.20 is enough.

The percents contributions of each parameter are utilized while making assessments on the results of all scenarios. Also, the uncertainties of the parameters are included in this evaluation process. In the framework, uncertainties are represented by coefficient of variation (COV) values and computed as the ratio between parameters' standard deviations and their mean values. Consequently, a criterion is generated by combining both of them into formula 2.21 to compare the results of scenarios among each other. In this process, percents contribution of each parameter is multiplied with their COV square values individually. Afterwards, all multiplications are summed and finally, a unique evaluation factor is defined for a scenario (Ang and Tang, 2007).

$$H_j=\sum_{i=1}^{5} R_i*(COV_i)^2 \quad (2.21)$$

H_j: Unique evaluation factor for a scenario,

R_i: Indicates that percent contribution of a parameter to FOS,

COV_i: Indicates that coefficient of variation of a parameter.

The evaluation process is carried out according to the reduction factors for PLAXIS analyses. The factors indicate the maximum allowable reduction ratios for cohesions and effective friction angles at the critical condition. While the dam is being raised, the successive phi/c reduction calculations are done. Afterwards, the heights of dam and reduction values are plotted. The linear regression line of the plot is tapped to make a prediction about the reachable maximum height of the dam in future.

CHAPTER 3

LABORATORY TESTS

3.1 **Sample Used In This Study**

Various laboratory tests have been conducted to identify and find out mechanical and geotechnical properties of tailings from Kastamonu Küre copper tailing dam. These tests results and procedures are briefly explained and discussed in this chapter. Firstly tailing sample is brought from Kastamonu Küre copper tailing dam side which is located at the middle north of Turkey.

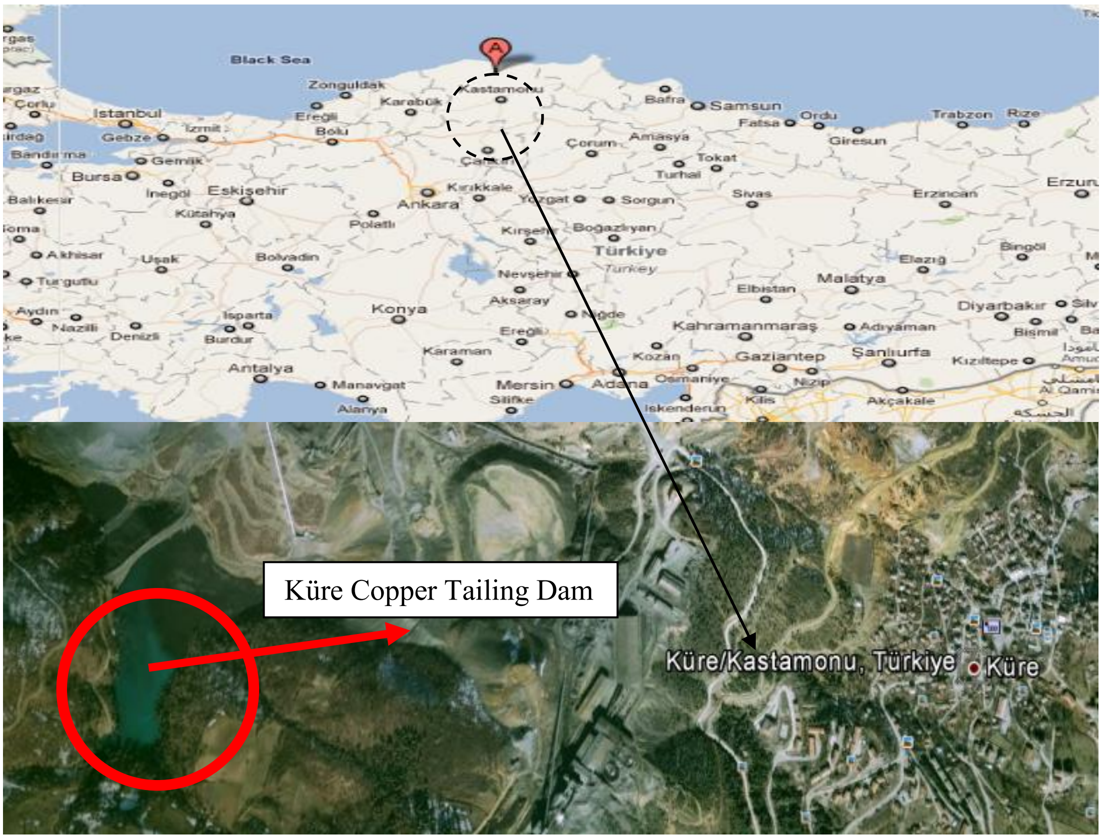

Figure 3.1 Location of Kastamonu Küre Copper Tailing Dam. (Google Earth).

The tailing dam is approximately spread over an area of 0.1 square kilometers. This wide storage facility area makes the specimen handling difficult, laborious and expensive. For instance, during the sample handling, opening bore holes at different locations on tailing dam body is required. It could not be done due to lack of special equipments designed to move on slurry like soil. Despite all of these issues, the disturbed samples are taken as much as possible from close to discharge point and rock-fill. Although disturbed and superficial sampling is done for this study, this does not mean that they are useless or worthless because the tailings are homogenously dispersed by spigotting method over the dam reservoir. Coarse and fine tailing particles properly separate from each others as increasing the distance from discharge point. In addition to that, due to the fact that they are continuously passed through the same mining operations, making an assumption about their homogeneity is reasonable (Lighthall, 1989). Moreover, rock fill materials (cobbles and sands) used as buttressing loads at the downstream side of the dam for each steps, are quite homogeneous and well graded. Hence, the samples of coarse tailings and rock-fill are adequate for classical geotechnical tests and classification procedure.

This chapter describes the soils using visual-manual methods. This classifies formally the soil according to Unified Soil Classification System (UCSC). Initially, the samples can easily be separated to three groups. The first two are from around rock fill region. One of them is unprocessed natural granular soils, containing wide range of soil type such as cobbles, gravels and sands. The other 'Sand' is from transition zone between rock fill and tailing part. Due to the fact that it is not a mining operational disposal, its mechanical properties are similar to mainly the coarse part of rock-fill and in this study, it is named as "sandy part of rock-fill". The last one is fine grained slurry tailings from dam body.

The coarse part of rock fill sample of which maximum particle size is 12 cm, is obtained from angular cobbles, gravels and sub rounded sands particles. The maximum particle size of sub-rounded sandy rock fill particles is 2 mm. Whereas more than %50 of the tailing passes through the no.200 sieve, even though determining the visual maximum particle size is impossible. It seems like fly-ash and can easily mix up with air on air-dry conditions and causes high risk for health. Therefore, using standard dust masks are not able to provide proper protection to avoid inhaling. Its moisture condition is wet at the field; even visible free water can be clearly detected. Its consistency is slurry like due to excessive water which used to provide proper consistency for spigotting methods. In laboratory, its consistency is determined as very soft by the help of quick test, thumb is penetrated into the soil more than 25 mm. The other physical specific property is its characteristic odor, when it is mixed with water; the odor emanates from tailing and does not smell earthy. Its cementation is described as weak; it is crumbled and broken with little finger pressure. Its dry strength is low; 12 mm diameter soil ball is crumbled into powder with mere pressure of handling. Low grade is more suitable for its plasticity, the thread can barely be rolled and the lump cannot be formed when it is drier than the plastic limit. Determine the quick soil type for tailing, the settling time in a field dispersion test is done. The results show that the settling is completed in nearly 60 minutes. It is found out that most of the suspension is silt. After performing, the quick index tests to determine the visual classification according to USCS, quantitative laboratory tests are conducted.

Figure 3.2 Coarse rock-fill from Kastamonu Küre copper dam.

Figure 3.3 Air-dry tailing and sandy part of rock fill (Soil) (D_{max}<2 mm) from storage part of Kastamonu Küre copper tailing dam.

3.2 **Specific Gravity Tests**

The aim of this test is to determine the ratio of the mass of a given volume of soil particles to the mass of an equal volume of distilled water. In this test, the way of measuring the accurate and precise volume of soil particles goes to temperature equilibrium, perfectly distilled water and sufficient deairing. According to ASTM reference of soils and testing program, the accepted standard deviation for reproducibility of this test on the same soil should be 0.007.

In this test, liquid submersion technique is used. One of the reason why this technique is used, is the expectation of sample's specific gravity to be more than water, and the second reason is the slight possibility to be able changed with undesired chemical reaction, which can cause serious damages and changes on inherent properties of the sample. When a little of water is mixed with the sample in iodine flask, air molecules are inevitably trapped between soil particles as visible or invisible bubbles. Shaking and stirring the iodine flask is not enough and useful method to get rid of them. A pump with sufficient strength is used to suck off the air bubbles. They hinder the proper filling of water into the flask. This process takes more time for tailings than soil, since the consistency of tailings is slurry. This does not allow to release entrapped air. When the samples are perfectly deaired, the water temperature is measured as 28^{o}C and water-filled weight of iodine flask is measured carefully.

Table 3.1 Set-1 and set-2 Specific Gravity Data of Slurry Samples at 28^{o}C.

Sample	No of Test	Gs	Gs Average
Slurry-1	1	3.646	3,706
	2	3.706	
	3	3.766	
Slurry-2	1	3.610	3,706
	2	3.717	
	3	3.742	
	4	3.754	

Table 3.2 Set-1 and set-2 Specific Gravity Data of Sandy Samples at 28^oC.

Sample	No of Test	Gs	Gs Average
Soil-1	1	2.926	2.957
	2	2.998	
	3	2.939	
	4	2.965	
Soil-2	1	2.949	2.965
	2	3.049	
	3	2.883	
	4	2.980	

Temperature correction to 20^oC by accounting for the change in water density;

$$GS = GS_t * \frac{Pw_{28}}{Pw_{20}} \tag{3.1}$$

GS: Specific gravity of sample at 20^oC.

GS_t: Specific gravity of sample at 28^oC.

Pw_{28}: Water density at 28^oC, (0.9962371g/cm^3).

Pw_{20}: Water density at 20^oC, (0.9982063g/cm^3).

Specific gravity of soil and slurry at 20^oC :

Gs of set-1 slurry=3.699

Gs of set-2 slurry=3.698

Gs of set-1 sandy soil=2.951

Gs of set-2 sandy soil=2.959

Temperature correction factor is applied to specific gravity values and corrected to 20^oC with respect to the changes in water density. Finally, the set-1 and set-2 results of sandy soil and slurry soil show that standard deviations in acceptable bounds are

0.006 and 0.0001 respectively. High specific gravity results correspond with the expectations which stem from possible presence of various high concentrated heavy metals. Some of filtered heavy metals from copper tailing extenders are lead, zinc, barium etc (Mohini Saxena, 2005). Their specific gravities change from 2.85 to 4.5 so that values in Table 3.1. and 3.2 are reasonable results for a copper tailing and heavy metal containing soil.

3.3 **Atterberg Limits Tests**

The purpose of this test is to determine the liquid limit (LL) and plastic limit (PL) of tailing and soil samples from Kastamonu Küre copper tailing dam. It is well known that consistency and resistance of the soil fluctuate between solid phases to liquid phase with water. Dedication of these transitional water content values render possible to use some correlations to estimate soil water characteristic curve (SWCC) in flow analysis. Also, determination of characteristic optimum water contents for the best reclamation will drastically decrease tailing dam slope failure and accidents. Moreover, by the help of these values, many strength parameters and coefficient of consolidation can be correlated. The specimens are pulverized and dehydrated along 1 day. Sandy soil is sieved and finer than 0.425 mm (No.40) particles are used. Liquid limits are determined by Casagrande device. PL, LL values are used to determine their group symbol by the help of Casagrande plasticity chart. Both of them are below the A-line. Group symbol of slurry tailing is ML. It corresponds to inorganic silts and low plasticity. Low plasticity index values confirm quick test results “low grade of plasticity”. During the test some quick tests are conducted and important details are notified. For instances, toughness is determined as low. Only slight pressure is required to roll the thread near the plastic limit. Also, the thread and the lump are weak and soft. Dilatancy characteristic is slow, water disappear while shaking. These observations are exactly corresponding to ASTM inferences about ML soils. The other important property is sensitivity. It is essential factor for proper interpretation of its long term stability. However, one of the key parameter for this, natural water content, cannot be obtained due to disturbance. However, upper part of tailings is known under water at the loose state in the field. Under laboratory tests, some empirical studies are conducted to determine natural water content. Under the lights of it, most probably slurry tailing LI (Liquidity Index) value is estimated above the unity, this refers that tailing exists is in fluid range and likely to be sensitive (Germaine, 2009). Relatively high PL and LL values indicate that sandy soil specimen obtains silty and clayey particles. Its plasticity might be evaluated as intermediate.

Table 3.3 Atterberg parameters for Kastamonu Küre copper tailing .

LIQUID LIMIT	SLURRY-1	SLURRY-2
LL (%)	22	22
PL (%)	21	21
PI (%)	1	1

Table 3.4 Atterberg parameters for Kastamonu Küre sandy soil.

LIQUID LIMIT	SOIL-1	SOIL-2
LL (%)	45	46
PL (%)	40	40
PI (%)	5	6

$$PI = LL - PL \tag{3.2}$$

Where:

PL: Plastic Limit,

PI: Plasticity Index,

LL: Liquid Limit.

$$LI = \frac{Wc - PL}{PI} \tag{3.3}$$

Wc: Water Content (%),

LI: Liquidity Index,

According to ASTM reference soils and testing program, the laboratory repeatability requirements should also be satisfied for validation of the results. Standard deviation of the results must be 0.7 for liquid limit and 0.5 for the plastic limit. For slurry tailing, LL and PL standard deviations are 0.14 and 0.3 respectively, in desired interval. For sandy soil, LL and PL standard deviation are 0.29 and 0.26 respectively and these are acceptable too. Accuracy of the results of tailing specimens is demonstrated by literature survey. According to Mittal and Morgenstern (1976), copper tailing’s liquid limit range can be 0-30 and plasticity index can be 0-11.

3.4 **Standard Proctor Test**

The main purpose is establishing a characteristic compaction curve for the sample with standard proctor method. Maximum dry density and optimum moisture content values can be deduced from this curve. It is well known that while applying standard compaction energy with hammer to soil at various water contents, the dry density increases with water content to the peak point and further attempt to increase dry density with adding water do not work. Dry density curve begin to fall. Actually every point on this curve indicates the highest possible dry density with its water content under standard proctor energy. If desired, these peak points can be used for calculation of compaction levels. Especially, it can be useful while preparing direct shear test specimens. It may render possible making a comparison among compaction level of prepared specimen and others. This comparison has been already done with respect to the void ratio but this can be an alternative approach without need for specific gravity value.

This test is conducted only on slurry tailing sample due to lack of sample. The same specimen is used for each test after dehydration and pulverization process. These situations naturally affect shape of curves. The curves slightly slide to right and up. The optimum moisture content values so close to each other, also the differences among dry density results are not exceed 0.01 gr/cm^3. According to ASTM reference soils and testing program the standard deviation should be 0.01 Mg/m^3 for maximum dry density and 0.3 percent for optimum water content. Hence the results are acceptable. In this study average maximum dry density 2.3gr/ml is reported as maximum dry density of the slurry tailings.

In this test, the method A is followed according to sample maximum particle size limitations. The sample satisfies the condition of “%25 or less retained on the 4.75mm (No.4) sieve” so that 101.6mm diameter mold is used. During the test, especially proper implementation of energy to the specimen at 3 layers with 25 drops is very important. In these tests manual compactions are done. Especially, while compaction process, hammer drop pattern is followed carefully and wooden basement is used to absorb the recoil reaction.

Table 3.5 Test-1 Dry density and moisture content data for slurry tailing.

TEST-1					
Test Number	1	2	3	4	5
Dry Density (gr/ml)	2.07	2.19	2.3	2.23	2.1
Moisture Content (%)	5.32	7.61	10.5	13.6	17.1

Table 3.6 Test-2 Dry density and moisture content data for slurry tailing.

TEST-2						
Test Number	1	2	3	4	5	6
Dry Density (gr/ml)	2.05	2.27	2.3	2.24	2.19	2.11
Moisture Content (%)	4.17	9	10.5	13.5	14.9	17.2

Table 3.7 Test-3 Dry density and moisture content data for slurry tailing.

TEST-3						
Test Number	1	2	3	4	5	6
Dry Density (gr/ml)	2.08	2.19	2.3	2.25	2.19	2.13
Moisture Content (%)	4.19	6.9	10.1	13.5	15.5	17.2

The peak dry density values and optimum moisture content values can be easily read from figure 3.8. The average value of the maximum dry density is 2.3 gr/ml and moisture content is 10.5 percentage.

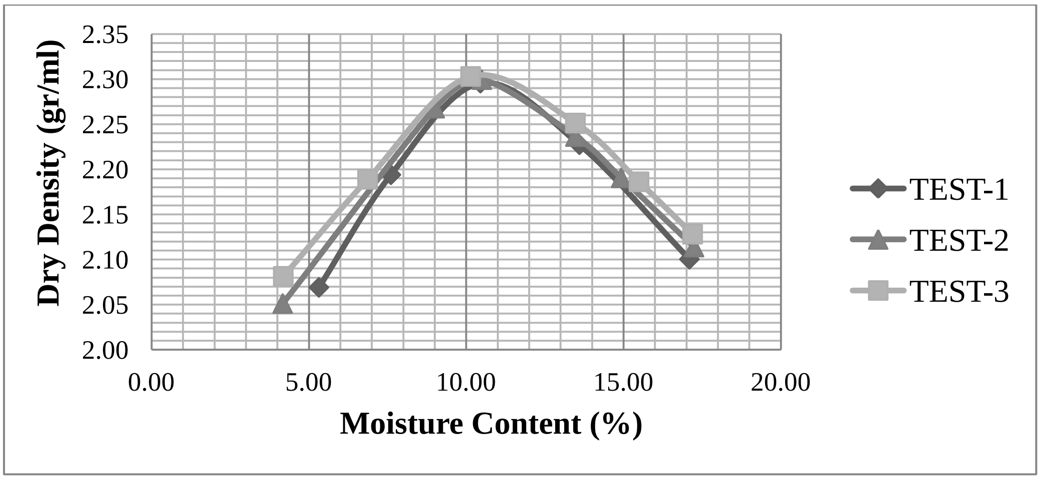

Figure 3.4 Test-1, test-2, test-3 Moisture content versus dry density graphic for slurry tailing.

3.5 **Sieve Analysis and Hydrometer Test**

Sieve analysis and hydrometer tests are key factors for classification of the samples according to USCS system. Sieve analyses are conducted on coarse part of rock-fill and sandy soil. While hydrometer analyses are applied on sandy soil finer than 0.075 mm (No.200) and on fine part of tailings.

Sieving processes are carried out by hand, this way is more effective for coarse grained size soil. The samples have been sieved in dry state and cleaning process has been skipped because of the weight of small size particles are negligibly small. During simple sieving process, special attention is paid to avoid exceeding of the overloading limits for various sieve sizes. Also a brush with appropriate-stiffness has been used to remove the remaining particles in the mesh. Firstly, grain size distribution graphs of three samples from coarse part of rock-fill are plotted. D_{60}, D_{30}, D_{10} values are determined as 62 mm, 36 mm, 18 mm respectively by taking average of them. By the help of these useful information, group symbol and group name are read as GW and well graded gravel from coarse grained soil flow chart of USCS. Secondly, only one grain size distribution graph of sandy soil is plotted due to lack of sample. D_{60} D_{30}, D_{10} values are determined as 0.5 mm, 0.27 mm, 0.09 mm respectively. Afterwards, by the help of these information, group symbol and group name are determined as SW-SM and well graded sand with silt respectively. Unlike the other analysis, the sample is firstly washed with water on No.200 sieve, and then dried and sieved. Fine particles are used in hydrometer analysis.

Table 3.8 Sieve analysis of sandy soil part of the rock fill.

Sandy Soil	
Mass of Dry Sample	623 gr
Losses	10.49 gr
Sieve(mm)	Cumulative Percentage Passing (%)
2	100
0.6	66.61
0.3	38.20
0.212	17.82
0.15	13.48
0.075	8.83

Table 3.9 TEST-1 and TEST-2, Sieve analysis of coarse part of rock fill.

TEST-1		TEST-2	
Mass of Dry Sample	19898gr	Mass of Dry Sample	20618gr
Losses	21.3gr	Losses	21.5gr
Sieve(mm)	Cumulative Percentage Passing(%)	Sieve(mm)	Cumulative Percentage Passing(%)
100	100.00	120	100.00
50	52.26	50	23.50
37.5	41.70	37.5	12.21
25	34.93	25	6.06
19	31.88	19	4.24
12.5	26.11	12.5	2.36
9.5	23.07	9.5	1.85
6.3	18.06	6.3	1.24
4.75	14.33	4.75	0.95
2	8.39	2	0.59
0.6	3.88	0.6	0.33
0.3	2,01	0.3	0.22
0.212	1.62	0.212	0.17
0.15	1.27	0.15	0.13
0.075	1.20	0.075	0.13

Table 3.10 TEST-3, Sieve analysis of coarse part of rock fill.

TEST-3	
Mass of Dry Sample	7403.88 gr
Losses	24.21
Sieve(mm)	Cumulative Percentage Passing(%)
100	100.00
50	53.55
37.5	30.68
25	15.91
19	11.44
12.5	7.62
9.5	6.31
6.3	4.93
4.75	4.08
2	3.06
0.6	1.60
0.3	0.98
0.212	0.77
0.15	0.59
0.075	0.30

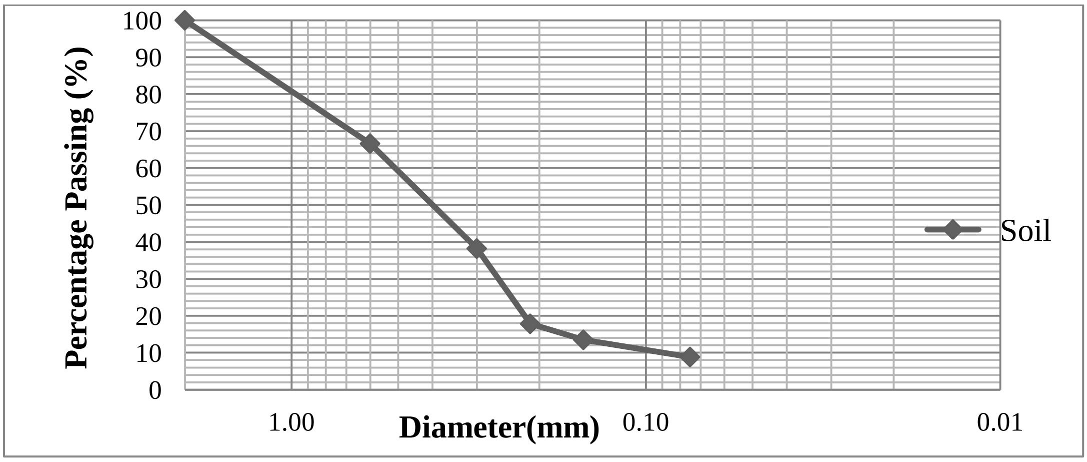

Figure 3.5 Grain size distribution graphic of sandy soil from nearby rock-fill region.

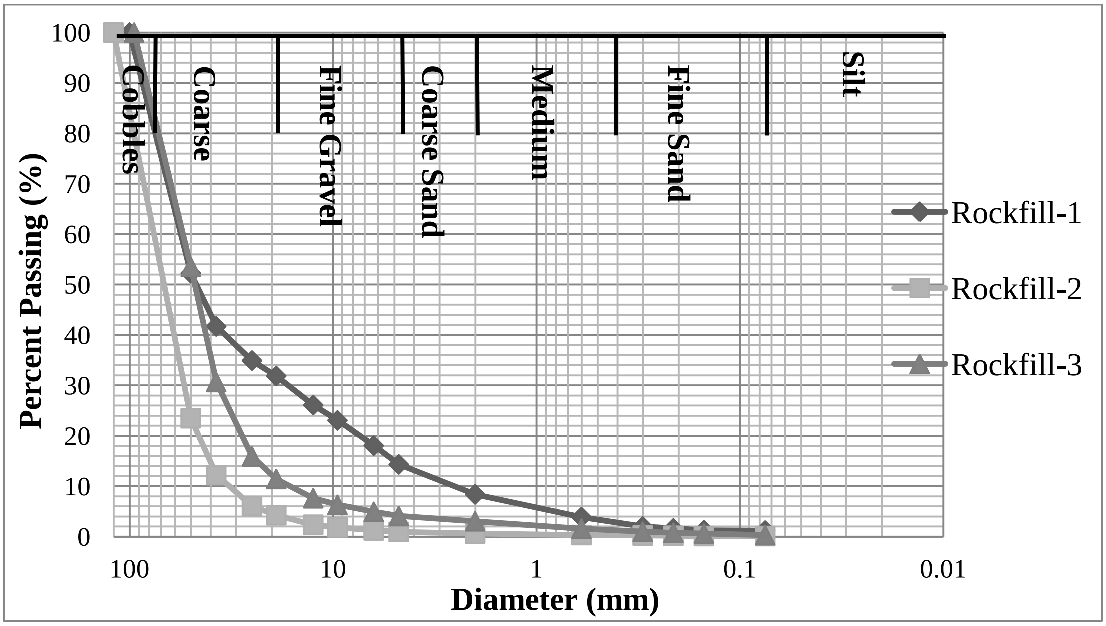

Figure 3.6 According to USCS definition of particle size, rock-fill-1, rock-fill-2 and rock fill-3 grain size distribution graphic.

Simple sedimentation analyses are done on finer than 0.075mm slurry tailings and sandy soil samples. 151-H type hydrometer placed in suspension within a graduated cylinder. This type of hydrometer capacity is about 50 gr soil in suspension so that the dry weights are measured thereabouts. Firstly, the hydrometer calibration values are dedicated and plotted. Equation of this line has been used to converting the corrected hydrometer reading to calibrated effective depth. Secondly, dispersion agent correction is determined as 4 because of concentration of sodium hexametaphosphate are 5 gr per liter. This dispersant neutralizes the surface charges on the particles and thwarts floc formation. Thirdly, temperature correction value is read from monographic chart solution of Stokes' law. Temperature is significant factor for the sedimentation because viscosity of the suspension change with temperature and this seriously change the force acting on a particle falling through a fluid. Therefore, suspension cylinder has been putted into water bath to eliminate these disruptive effects. Temperature correction has been done according to average temperature of all reading. Finally, the hydrometer is left slowly in suspension without agitation because small particles can be easily dragged to upward and density of suspension can be spoiled. Moreover, after the all reading, hydrometer has been carefully removed out of the suspension and cleaned to avoid undesired attachments of small size particles. This may cause more sinking than normal and the gradation curve will gradually decrease (Germaine, 2009). Also, all reading has been taken at the top of the meniscus and explicit meniscus correction (Cm) is applied to the distance of fall. All related test datas, readings and details of calculations are shown in the tables.

$$K=\frac{100*Gs}{Wb*(Gs-1)}*(Rh+Mt-x) \tag{3.4}$$

$$D=\sqrt{\frac{18*\mu*Hr}{Pw*g*(Gs-1)*t}} \tag{3.5}$$

$$B=\frac{18}{Pw*g*(Gs-1)} \tag{3.6}$$

K: Percentage of particle that the corresponding particles diameter (%),

Wb: Weight of dry specimen,

Rh: Corrected hydrometer reading,

Mt: Temperature correction,

x: Dispersing agent correction,

D: Diameter of grain (mm),

μ: Viscosity of liquid (mPa.sec),

Hr: Calibrated effective depth (cm),

Pw: Mass density of water (g/cm^3),

t: time (sec),

B: Density correction with respect to temperature.

g: Acceleration of gravity (cm/sec2),

Table 3.11 Calibration values for hydrometer used in the test.

Corrected Hydrometer Reading (Rh)	Calibrated Effective Depth (Hr)
40	8.951
30	11.401
20	13.881
10	16.361

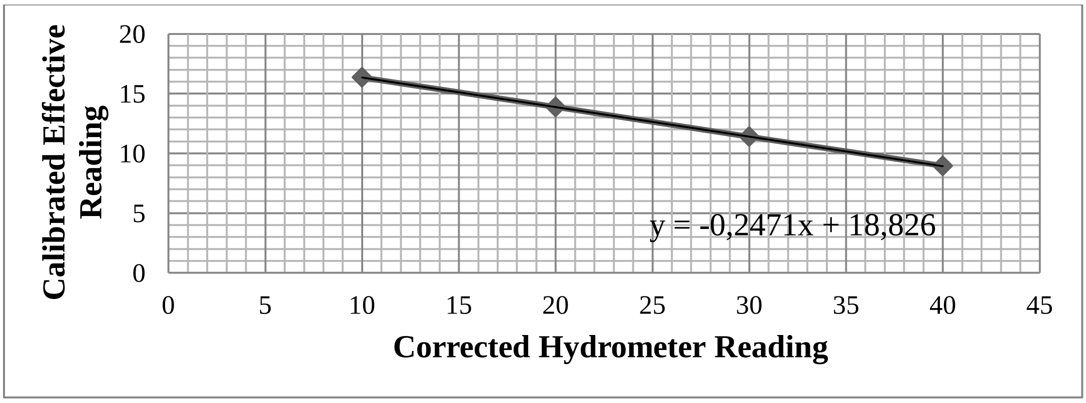

Figure 3.7 Calibration linear slope line with its equation.

Table 3.12 Percent finer and diameter calculation for sandy soil-1.

Sandy Soil-1						
Cm	Mt	B	Temperature		Dry Specimen Weight (gr)	
0.5	-0.5	10.25	17.1^{o}C		44.51	
Time (min)	(Rh)'	Rh=(Rh)'+Cm	Hr	Velocity (cm/sec)	Diameter (mm)	K(%)
1	29	29.5	11.5	0.192	0.046	84.9
2	26.5	27	12.2	0.101	0.034	76.4
4	23	23.5	13.0	0.054	0.024	64.5
8	20	20.5	13.8	0.029	0.0175	54.3
15	17	17.5	14.5	0.016	0.013	44.1
30	14.7	15.2	15.1	0.008	0.0092	36.3
60	13	13.5	15.5	0.004	0.0064	30.6
120	12	12.5	15.7	0.002	0.0045	27.2
248	10.9	11.4	16.0	0.001	0.00325	23.4
1696	8.8	9.3	16.5	0.0002	0.00145	16.3

Table 3.13 Percent finer and diameter calculation for sandy soil-2.

Sandy Soil-2						
Cm	Mt	B	Temperature		Dry Specimen Weight (gr)	
0.5	-0.4	10	17.7°C		44.24	
Time (min)	(Rh)'	Rh=(Rh)'+Cm	Hr	Velocity (cm/sec)	Diameter (mm)	K(%)
1	30.5	31	11.2	0.186	0.044	90.8
2	29	29.5	11.5	0.096	0.032	85.7
4	23.1	23.6	13.0	0.054	0.024	65.5
8	19.8	20.3	13.8	0.029	0.0188	54.3
15	6.4	6.9	17.1	0.019	0.014	8.5
30	6.1	6.6	17.2	0.010	0.01	7.4
60	6	6.5	17.2	0.005	0.007	7.1
120	6	6.5	17.2	0.002	0.0045	7.1
260	5.1	5.6	17.4	0.001	0.0032	4.0
1764	5.2	5.7	17.4	0.0002	0.0014	4.4

Table 3.14 Percent finer and diameter calculation for slurry tailing-1.

Slurry Tailing-1						
Cm	Mt	B	Temperature		Dry Specimen Weight (gr)	
0.5	-0.42	12.5	17.5°C		45.4	
Time (min)	(Rh)'	Rh=(Rh)'+Cm	Hr	Velocity (cm/sec)	Diameter (mm)	K(%)
1	29	29.5	11.5	0.192	0.05	90.2
2	26.1	26.6	12.3	0.102	0.037	79.8
4	21.5	22	13.4	0.056	0.027	63.2
8	17.3	17.8	14.4	0.030	0.02	48.1
15	14.6	15.1	15.1	0.017	0.015	38.4
30	12	12.5	15.7	0.009	0.0109	29.1
60	10.5	11	16.1	0.004	0.0071	23.7
120	9	9.5	16.5	0.002	0.005	18.3
240	8	8.5	16.7	0.001	0.0036	14.7
1789	5.7	6.2	17.3	0.0002	0.00155	6.4

Table 3.15 Percent finer and diameter calculation for slurry tailing-2.

Slurry Tailing-2						
Cm	Mt	B	Temperature		Dry Specimen Weight (gr)	
0.5	-0.48	12.75	17.2^{o}C		45.3	
Time (min)	(Rh)'	Rh=(Rh)'+Cm	Hr	Velocity (cm/sec)	Diameter (mm)	K(%)
1	29	28.5	11.8	0.196	0.0725	86.6
2	26.1	24	12.9	0.107	0.05	70.4
4	21.5	20	13.9	0.058	0.032	55.9
8	17.3	17	14.6	0.030	0.0225	45.1
15	14.6	14.5	15.2	0.017	0.014	36.1
30	12	12	15.9	0.009	0.0092	27.1
60	10.5	10	16.4	0.005	0.0065	19.9
120	9	8.5	16.7	0.002	0.0045	14.5
236	8	7.3	17.0	0.001	0.00325	10.2
1746	5.7	5.5	17.5	0.0002	0.001	3.7

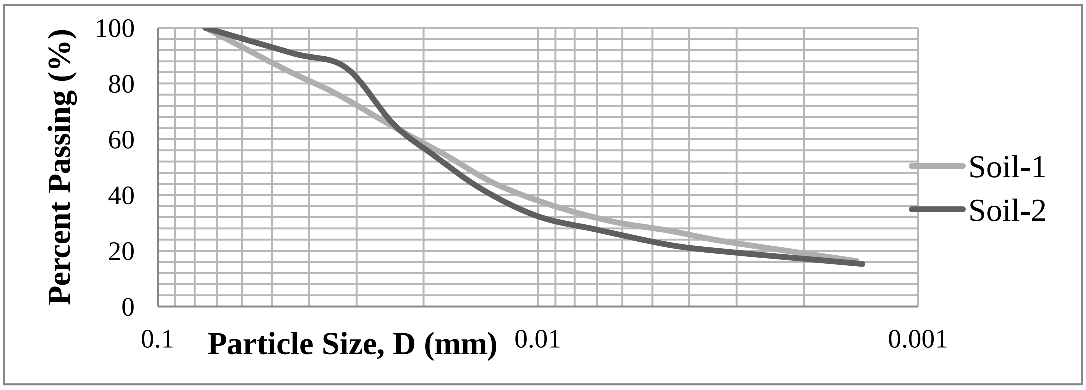

Figure 3.8 Sandy soil-1 and sandy soil-2 hydrometer analysis graph.

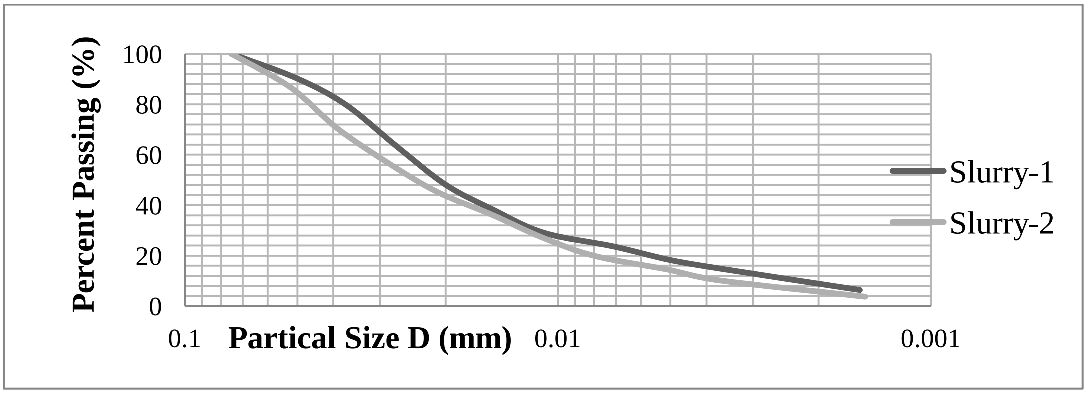

Figure 3.9 Slurry tailing-1 and slurry tailing-2 hydrometer analysis graph.

Two hydrometer tests are conducted on tailing specimens which are quartered from different samples. The results are so close to each other. D_{10}, D_{30}, D_{60}, values are 0.0035 mm 0.015 mm 0.0425 mm respectively, derived from average resultant curve. Its group symbol is ML and group name is silt with sand. The other two hydrometer tests are conducted on sandy soil specimens. The same specimen is used for both of them. Small amount of specimen is lost due to this reason. The results reflect slight differences but an idea can be owned by looking at the results, especially for some useful correlation such as hydraulic conductivity estimation.

The comments cannot be done regarding results of hydrometer tests because there are no acceptable criteria for criticizing accuracy and precision for hydrometer (Germaine, 2009). Likewise, there is no comment regarding results of sieve analyses of GW and SW-SM soils. Nevertheless, grain size distributions of the samples are reasonable as expected. At the field, the water is almost retained by the zone of sandy soil. Therefore, grain size of fine part of sandy soil is expected as smaller than tailing part. As can be seen, grain size distribution curve of fine part of sandy soil is above the tailing part.

3.6 **Direct Shear Tests**

The main purpos of these tests is to determine of the range of shear strength parameters for tailing samples. The tests are performed with 60 by 60 mm square direct shear device. The speed of shearing process is considered as 0.61 mm/min since dissipation of pore water pressure does not need too much time for the soils whose group name is silt with sand. Moreover, short primarily consolidation periods of specimens are also observed. Therefore, it is assumed that specimens have enough drainage conditions to allow proper dissipation of water with this rate. Besides, specimens are prepared at several different void ratios and moisture content to be sheared with this rate.

Firstly, required all dimensions are measured by compass to use necessary calculations. For instance, width of the gaps and height of the ribs in the grooved insert plate, are measured as 0.322cm, 0.13cm respectively. Length of the gaps is measured at three different locations and average value 5.99cm is used. Likewise, edge of the box is measured and average value 5.97cm is used for calculation of nominal specimen area. Mass of top plate, top cap, steel ball, hanger and external weights are carefully scaled for accurate calculations of normal stresses and used along all of the tests.

All specimens are prepared from air-dried sample which is laid in a container without any specially humidity protection. At that condition, their moisture contents are measured as %1.09 and used in further dry density calculations. During preparation of unsaturated specimens, %5, %7.5 and %10 percentages of sample weight of water are thoroughly mixed with samples. Afterwards, mixed specimens are waited in well sealed plastic cap to equalize water equilibrium. Also, at the end of the shearing process, water content of samples is determined to observe the relative differences.

Specimens are placed into the direct shear apparatus by the help of funnel with little amount of input energy as possible as. Funnel is slightly lifted along the axis of symmetry of the specimen so that drop height changes of specimens are eliminated. Hereby, the loosest state is obtained. In desired situations, less void ratio is achieved by squeezing the specimens with smooth glass plate. Afterwards, the surface is flatten and screwed direct shear apparatus are connected to gear mechanism. The first vertical displacement reading is taken as soon as top cape and steel ball are putted on the specimen. When the masses have been loaded, rapid settlements occur, after a few seconds, rate of downward movement have gradually slowed. Shearing processes have been initiated at after two hours for each saturated and unsaturated tests. Within this time, wet towel is covered around the shear box to minimize the undesired drying. While shearing and at the end of the shearing, vertical displacement and o-ring readings are recorded. Also, lateral displacements and elapsed time are recorded to check the average rate of shearing. Dilation rate have been calculated as ratio of vertical displacement to shear displacement. Dilation phenomenon does not occur in any case. This indicates that specimen are prepared in relatively loose state.

Maintaining the shear process under permanent normal stress is essential to achieve accurate linear relationship between normal stress and shear strength. However, incessant vertical displacements render it difficult. Horizontality of the moment arm is continuously controlled and shearing process is continued until the force begins to decline.

Acceptableness of the tests results is more complicated and obscure. According to ASTM D3080, there is no accepted reference to evaluate the direct shear test of soils under consolidated drained conditions yet. Likewise, Germaine (2009) states only some of the main problems which can be detected by evaluating the results. The results of the tests do not indicate any problems so that they are assumed as accurate and precise.

$$Vg = (Hr \times Wg \times Lr) \times Ng \tag{3.7}$$

Vg: Volume for the sand between the ribs of each grooved insert plate (cm^3),

Wg: Width of the gaps in the grooved insert plate (cm)

Hr: Height of the ribs in the grooved insert plate (cm),

Lr: Length of the gaps in the grooved insert plate (cm),

Ng: Number of the gaps (15 for this grooved insert plate).

$$Vt = (di - ds) \times Ab + 2 \times Vg \tag{3.8}$$

Vt: Total volume of the specimen (cm^3),

di: Initial depth to the top of the top cap with the specimen container empty (cm),

ds: Depth to the top of the top cap with the soil specimen in place (cm),

Ab: Area of specimen container (cm^2).

$$N = (Mc + 5 * Mw) * g \tag{3.9}$$

N: Normal force applied to the specimen, Mc: Mass of top plate, top cap, steel ball, and hanger,

g: Acceleration of gravity.

Mw: Mass of the weights added to the hanger.

$$Hps = (di - df) + Hr \tag{3.10}$$

Hps: Preshear height of the specimen (cm).

$$\Upsilon d = \frac{Ms/Vt}{1+W/100} \tag{3.11}$$

Υd: Dry density of the specimen (g/cm^3),

Ms: Mass of specimen (gr),

w: Water content (%).

$$e_o = (Gs*\Upsilon w/ \Upsilon d)-1 \tag{3.12}$$

e_o: void ratio before consolidation and loading process,

Gs: Specific gravity of soil,

Υw: Dry density of water (g/cm^3).

$$e_{start} = e_o - \frac{Dv*(1+e_o)}{10*Hps} \tag{3.13}$$

e_{start}: Initial void ratio just before shearing process,

Dv: Vertical displacement (mm).

Table 3.16 Direct shear result of slurry tailing at $e_{average}$=1.34 on air dry condition.

Angle of Friction (degree): 35.89 and Cohesion (kPa): 8				
Normal Stress (kPa)	51.78	120.4	230.12	395.68
Peak Shear Stress (kPa)	68	120.32	199.36	324.62
Initial Void Ratio	1.35	1.31	1.32	1.37

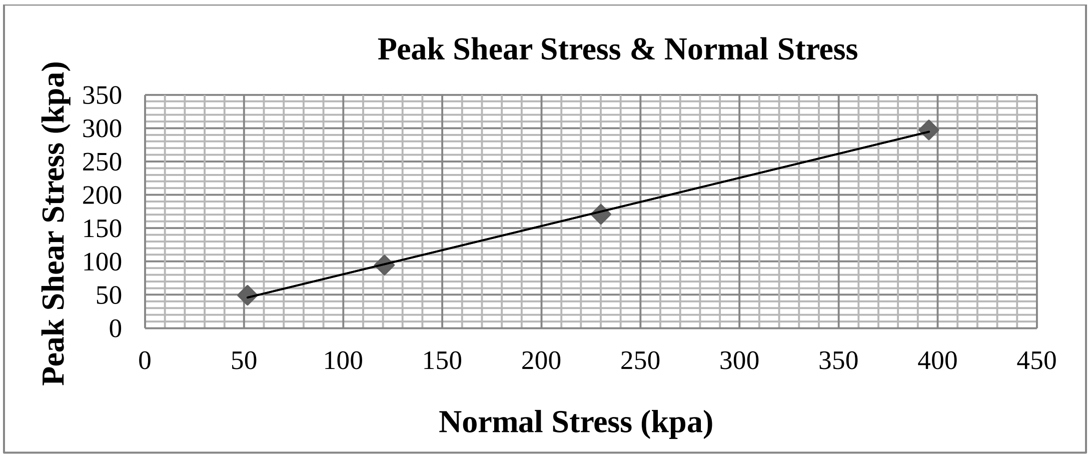

Figure 3.10 Peak shear stress versus normal stress for slurry tailing at $e_{average}$=1.34 on air dry condition.

Table 3.17 Direct shear result of slurry tailing at $e_{average}$=1.17 on air dry condition.

Angle of Friction (degree): 36.24 and Cohesion (kPa): 14.7				
Normal Stress (kPa)	51.77	120.87	230.09	395.61
Peak Shear Stress (kPa)	55.22	100.26	181.35	305.73
Initial Void Ratio	1.15	1.18	1.16	1.2

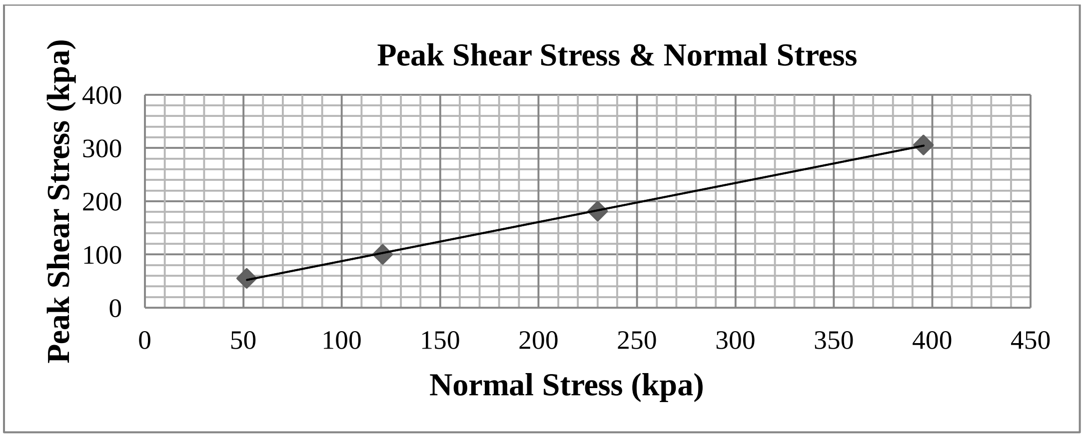

Figure 3.11 Peak shear stress versus normal stress for slurry tailing at $e_{average}$=1.17 on air dry condition.

Table 3.18 Direct shear result of slurry tailing at $e_{average}$=1.1 on air dry condition.

Angle of Friction (degree): 36.46 and Cohesion: 24 kPa				
Normal Stress (kPa)	51.77	120.87	230.09	395.61
Peak Shear Stress (kPa)	62.77	111.89	195.3	315.9
Initial Void Ratio	1.09	1.11	1.13	1.11

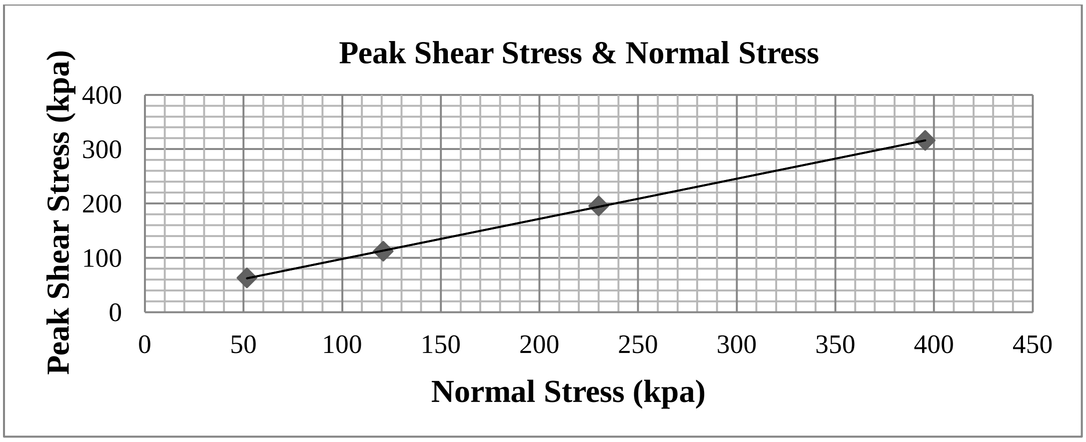

Figure 3.12 Peak shear stress versus normal stress for slurry tailing at $e_{average}$=1.11 on air dry condition.

Table 3.19 Direct shear result of slurry tailing at $e_{average}$=1 on air dry condition.

Angle of Friction (degree): 36.84 and Cohesion (kPa): 12.2				
Normal Stress (kPa)	51.77	120.87	230.09	395.61
Peak Shear Stress (kPa)	68.33	115.54	201.64	324.17
Initial Void Ratio	1.01	0.96	0.99	1.03

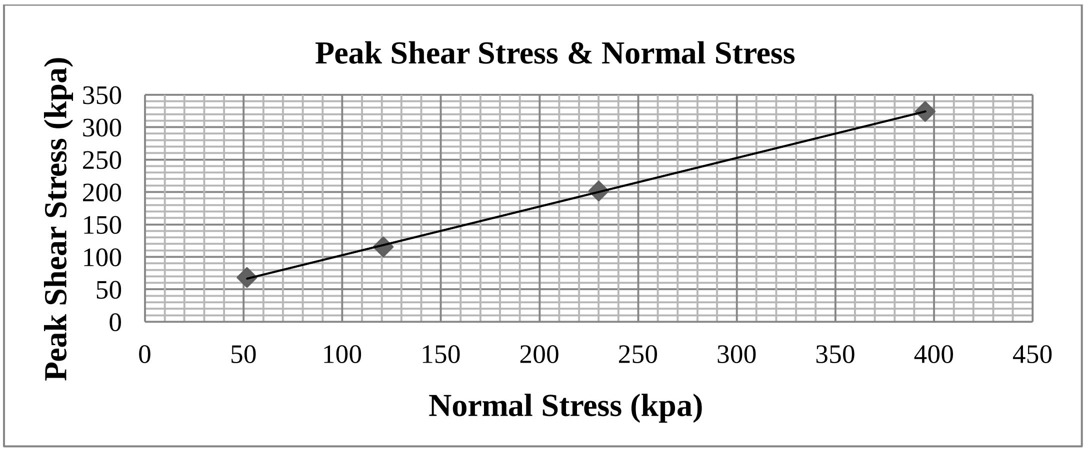

Figure 3.13 Peak shear stress versus normal stress for slurry tailing at $e_{average}$=1 on air dry condition.

Table 3.20 Direct shear result of slurry tailing at $e_{average}$=0.77 on air dry condition.

Angle of Friction (degree): 37.03 and Cohesion (kPa): 30				
Normal Stress (kPa)	51.77	120.87	230.09	395.61
Peak Shear Stress (kPa)	70.74	117.84	205.41	328.12
Initial Void Ratio	0.78	0.78	0.78	0.73

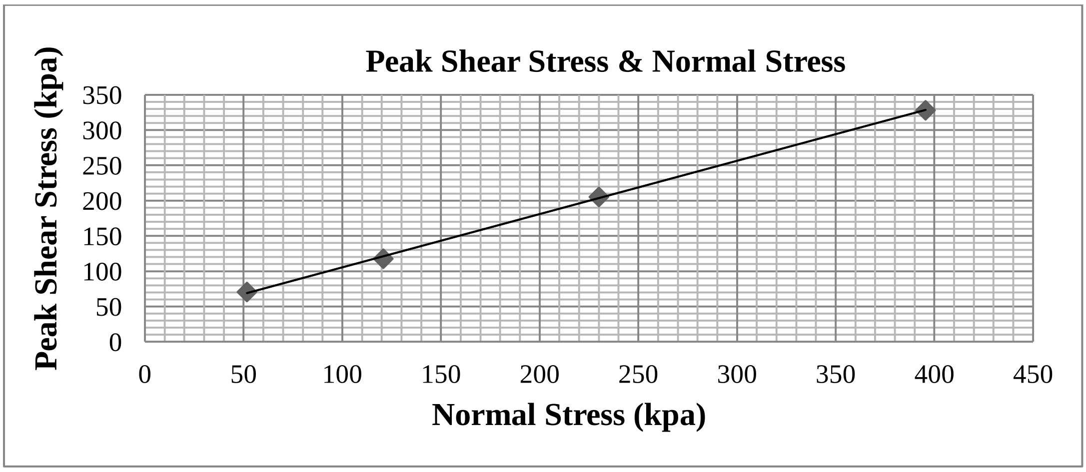

Figure 3.14 Peak shear stress versus normal stress for slurry tailing at $e_{average}$=0.77 on air dry condition.

Table 3.21 Direct shear result of unsaturated slurry tailing with initial water content=%6.16 at $e_{average}$=1.055.

Angle of Friction (degree): 34.52 and Cohesion (kPa): 30				
Normal Stress (kPa)	51,77	120.87	230.09	395.61
Peak Shear Stress (kPa)	60.45	115.67	193.26	298.47
Initial Void Ratio	1p1	1.03	1.11	0.98
Final Water Content (%)	6.08	6.01	5.97	5.90

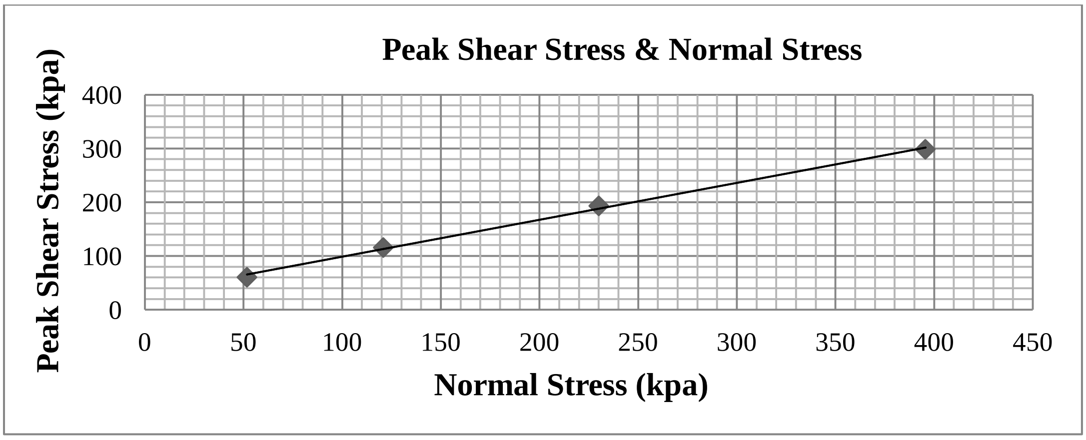

Figure 3.15 Peak shear stress versus normal stress for unsaturated slurry tailing with initial water content=%6.16 at $e_{average}$=1.055.

Table 3.22 Direct shear result of unsaturated slurry tailing with initial water content=%8.68 at $e_{average}$=0.885.

Angle of Friction (degree): 33.58 and Cohesion (kPa): 21				
Normal Stress (kPa)	51.76	120.87	230.03	395.68
Peak Shear Stress (kPa)	56.67	100.55	173.21	284.52
Initial Void Ratio	0.89	0.89	0.91	0.93
Final Water Content (%)	8.61	8.58	8.54	8.49

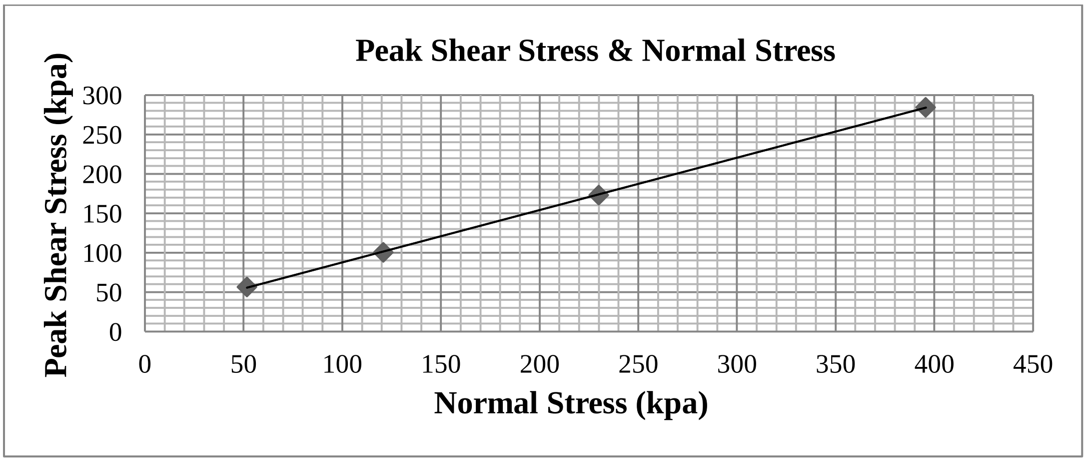

Figure 3.16 Peak shear stress versus normal stress for unsaturated slurry tailing with initial water content=%8.68 at $e_{average}$=0.885.

Table 3.23 Direct shear result of unsaturated slurry tailing with initial water content=%11.21 at $e_{average}$=0.953.

Angle of Friction (degree): 32.51 and Cohesion (kPa): 31				
Normal Stress (kPa)	51.74	120.76	230.23	395.49
Peak Shear Stress (kPa)	61.32	111.02	178.15	282.19
Initial Void Ratio	1.11	1.02	0.88	0.8
Final Water Content (%)	11.07	10.90	11.08	11.04

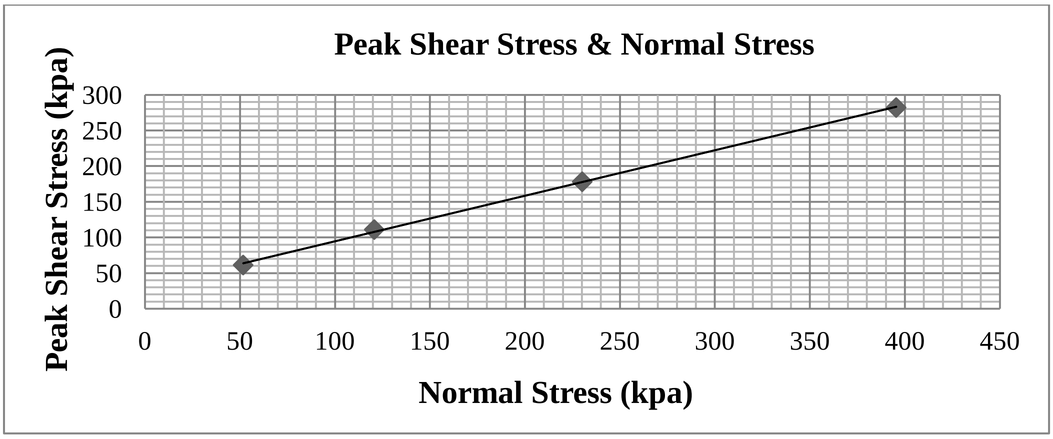

Figure 3.17 Peak shear stress versus normal stress for unsaturated slurry tailing with initial water content=%11.21 at $e_{average}$=0.953.

Table 3.24 Direct shear result of saturated slurry tailing at $e_{average}$=0.75.

Angle of Friction (degree): 30.35 and Cohesion (kPa): 8				
Normal Stress (kPa)	48.85	120.187	230.03	395.68
Peak Shear Stress (kPa)	38.91	75.01	145.93	239.46
Initial Void Ratio	0.81	0.75	0.69	0.75

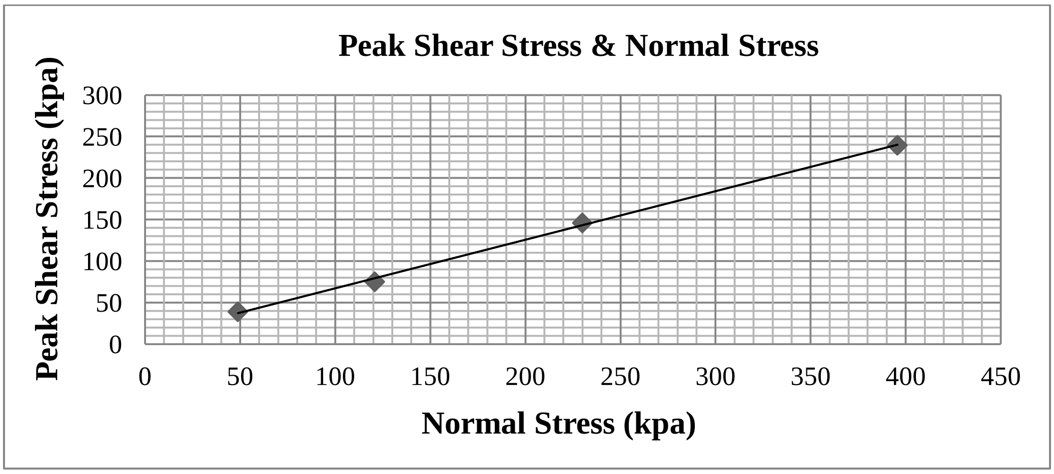

Figure 3.18 Peak shear stress versus normal stress for saturated slurry tailing at $e_{average}$=0.75.

The effective friction angles can be assessed as too high for soil which comprised of silt and sand, however according to Jantzer (2008) research on material properties of tailings from Swedish mines demonstrate that consolidated friction angles varies between 18^o and 46^o. According to Bjelkevik (2005), this reason is attributed to angularity of the tailings.

3.7 **Maximum Void Ratio**

Determination of maximum void ratio is done according to method mentioned in Yamamuro and Lade (1998). The funnel is filled with dry sample; during depositional process drop height is hold minimum to avoid rearrangement of particles. A container is swiftly filled with particles and excessive specimens are smoothly trimmed with spatula. Five successive tests are conducted and average value of void ratios are assign as e_{max} value.

Table 3.25 Determination of maximum void ratio with Yamamuro & Lade (1998).

Mass of container (gr)	57.01	57.09	57.13	57.15	57.16
Mass of container + Wet soil (gr)	386.52	387.99	384.02	385.75	383.9
Moist Density (gr/cm^3)	1.55	1.56	1.54	1.55	1.54
Dry Density (gr/cm^3)	1.54	1.54	1.52	1.53	1.52
Void Ratio	1.41	1.40	1.43	1.42	1.43
Note: Volume of container 212.29 cm^3 and air-dry soil water content 1.09%					

3.8 **Unconfined Axial Loading Test**

In this study, the reason of doing these tests is to determine a rough range for modulus of elasticity values of course tailings to use in PLAXIS slope stability analysis. The cylindrical specimens are compacted up to achieve average void ratios of layer in the dam. Also, all of them have 10 percent water content. A greater number of specimens cannot be prepared at looser state and several different amounts of water due to consistency. In other states, the specimens are not stable in form of cylindrical shape, whose diameter is 5cm and length is 10 cm. While axial stress calculation, area correction is done according to formula 3.14 by considering the change of volume is zero.

$$Ai = \frac{Ao}{1 - \frac{\varepsilon(\%)}{100}} \tag{3.14}$$

ε: Axial strain,

Ao: Initial cross sectional area,

Ai: Corrected cross sectional area with respect to axial strain,

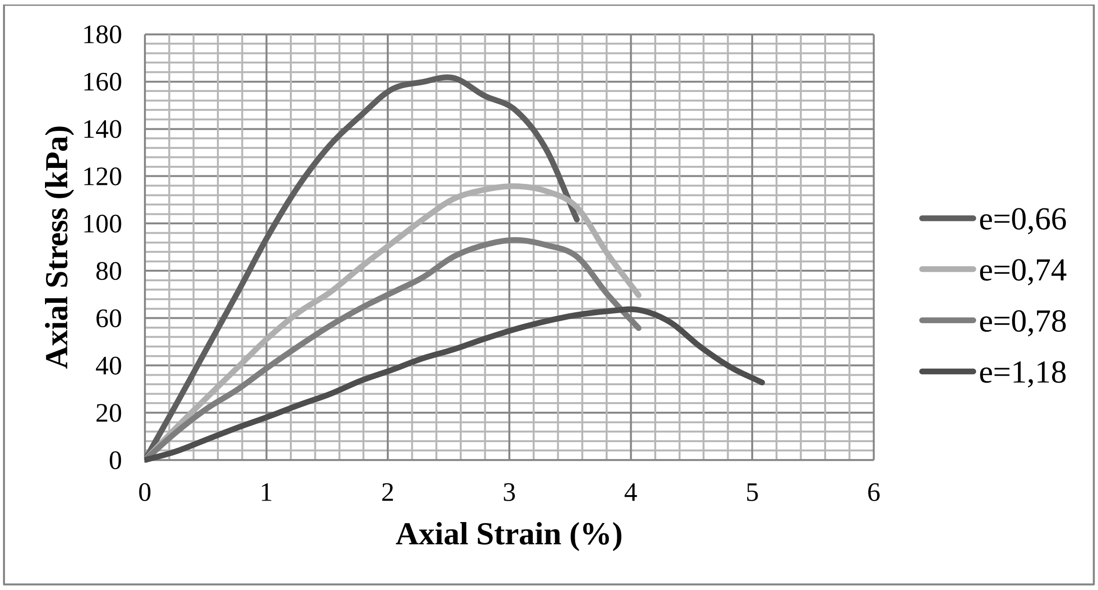

Figure 3.19 Unconfined axial loading curve of Küre coarse tailings at different void ratios (Water content: 10%).

CHAPTER 4

SEEPAGE and STABILITY ANALYSIS of KASTAMONU KÜRE COPPER TAILING DAMS

4.1 **Details of drained SLIDE Analyses**

The first slope stability analyses are done in SLIDE software. Sections of dam are drawn and geotechnical properties of the materials are assigned as determined in previous chapters. Three different scenarios are designed with respect to ponds' locations. The inputted shear strength parameters and saturated hydraulic conductivities of tailings are showed in tables 4.1 and 4.2. Unsaturated hydraulic conductivities of tailings and rock-fill part are plotted versus matrix suctions and putted in appendix-A chapter. Also, air entry values are read from figure 2.11 and 2.12 for sandy soils and tailings and used in unsaturated strength calculations. This value is 5 kPa for tailings and 1 kPa for sandy soil. The same shear strength values are used for both coarse and fine tailings as seen in table 4.1.

Table 4.1 Shear strength parameters of tailings.

	Effective Friction Angle (^{o})	**Cohesion (kPA)**	**Unsaturated Shear Strength ($\emptyset^b$)**
Mean	34.82	19.66	18.5
Max	37.03	30	24
Min	24	8	14
SD	2.28	9.78	1

Table 4.2 Revised saturated hydraulic conductivity of tailings according to depth.

Adjusted Saturated Hydraulic Conductivity (m/s) with Void Ratio		
Depth (m)	**Mean Void Ratio**	**Fine Tailing (Ks)**
0-15	1.18	4.84969E-09
15-30	0.78	1.30103E-09
30-45	0.74	1.14062E-09
45-90	0.66	8.76712E-10

For rock-fill part, it is assumed that the permeability is governed by sandy soil fraction and shear strength is governed by coarser than sand fractions. Thus, unsaturated hydraulic conductivity properties of sandy-soil are assigned to rock-fill part. Also, its statistical characteristics are hypothetically determined with assuming that its average grain size is corresponding to gravel; the values are tabulated in table 4.3. The last layer, bed-rock, is actually designed as the least permeable layer and under water table at every scenario so that simple model is used with 10^{-10} m/s saturated hydraulic conductivity value. Additionally, it is stretched to 25 m below ground surface with 45^{o} effective friction angle and zero cohesion, to search whether presence of possible critical slip surface extension reach out nearby.

Table 4.3 Shear strength parameters of rock-fill part.

	Effective Friction Angle (^{o})	**Cohesion (kPa)**
Mean	42	2.5
Max	44	5
Min	40	1
SD	1	1

Note: Typical SD values are larger. In this study, we assumed small values that does not influence the results much.

Saturated unit weights of the tailings are derived from their void ratios and listed in table 4.4. The saturated unit weights of all of rock-fill parts are set to same values due to lack of published data regarding their void ratio. While choosing, its maximum, minimum, mean and standard deviation values, especially attention is paid to stay in close to probabilistic parameters of the tailings. Consequently, the values are 26 kN/m^3, 24 kN/m^3, 25 kN/m^3 and 1 kN/m^3 are assigned to maximum, minimum, mean and standard deviation values respectively.

Table 4.4 Statistical parameters of saturated unit weight of tailings with depth.

Saturated Unit Weight (kN/m^3)				
Depth (m)	**Mean**	**Max**	**Min**	**SD**
0-15	21.96	26.36	20.84	2.54
15-30	24.68	26.78	22.92	2.54
30-45	25.03	26.26	23.67	1.85
45-90	25.76	26.26	25.29	0.94

Three scenarios are written with respect to pond's positions. The phreatic surfaces and pore-water pressures are determined by the help of finite element methods for each scenario. Afterwards, probabilistic slope stability analyses are done with limit equilibrium method and factor of safeties are calculated by Spencer Method.

Three slope stability analyses are done for each scenario with different (Ko/Ks) ratios which are 1, 10 and 100. In each subtitle, the critical slip surfaces, mean and deterministic factor of safeties, reliability indexes are showed in figures for all (Ko/Ks) conditions.

The mean factors of safeties (FOS) are plotted versus Ko/Ks values. The regression lines and correlation coefficients are derived from the scatters for each scenario.

The amounts of water, seep through the cross sections of the first embankments, are established in tables for each Ko/Ks conditions. These values are functional indicator for supervision on progression of seepage analyses.

The equations of the linear regression trend lines and their correlation coefficients are listed in (Tables 4.6-4.3, Tables 4.15-4.22 and Tables 4.24-4.31) for each scatter of FOS values and parameters. These scatters are derived from 1000 values of parameters which determined by the help of Monte Carlo method versus calculated FOS values.. These equations and correlation coefficients are used in the result and discussion chapter while evaluating the contributions of the parameters to FOS. Also, by the help of them, unique evaluation factors for each scenario in drained condition are determined.

Table 4.5 General view of derivation of the parameters used in analyses.

		Coarse Tailings	Fine Tailings	Sandy Soil	Rock-fill	Bedrock
Void Ratio	**e_{min}**	Assumed	Assumed	-	Assumed	Assumed
	e_{max}	LT	LT	-	Assumed	Assumed
	According Depth Interval	Blight (2010)	Blight (2010)	-	-	-
Specific Gravity (Gs)		LT	LT	LT	Assumed	Assumed
Hydraulic Conductivity (k_x,k_y)		Derived by the help of Ko/Ks	Abolfazl (2007) Taylor (1948)	-	Assumed	Assumed
Effective Friction Angle		LT	LT	-	Zardari (2011)	Assumed
Cohesion		LT	LT	-	Zardari (2011)	Assumed
Unsaturated Shear Strength Parameter ($Ø_b$)		Assumed	Assumed	-	Assumed	-
Modulus of Elasticity (E)		Gurbuz (2007)	Zardari (2011) Assumed	-	Zardari (2011)	Assumed
Undrained Shear Strength (Su)		LT	Gurbuz (2007)	-	-	-
SWCC		Zapata (2000) Fredlund (1994)	Zapata (2000) Fredlund (1994)	Zapata (2000) Fredlund (1994)	-	-
Unsaturated Hydraulic Conductivity		Leong (1997)	Leong (1997)	Leong (1997)	-	-

Note: LT= Laboratory tests, Assumed= Assumptions are done, “-“= It is not considered in this study.

4.1.1 **Scenario-1 for SLIDE**

In the first scenario, the water layer is defined as triangular shape and initiated from the point (214 m, 90 m), which is 10 meters away from edge of the crest and the polygon is closed at the point (350 m, 87 m) on the right boundary of the cross section. The deepest point of the pond is located at the furthest distance from spigot point and the depth is taken as same as the height of the last raised part.

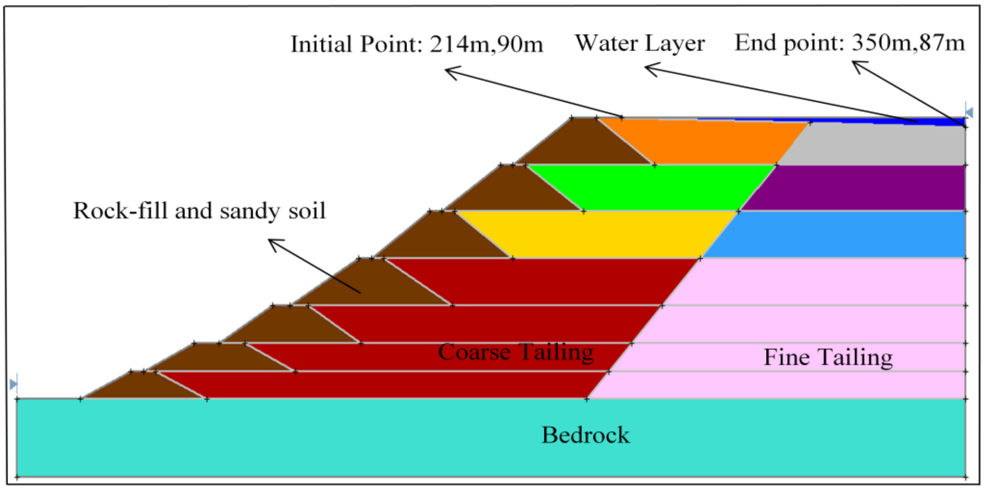

Figure 4.1 Cross sectional details of Kastamonu Küre tailing dam for scenario-1.

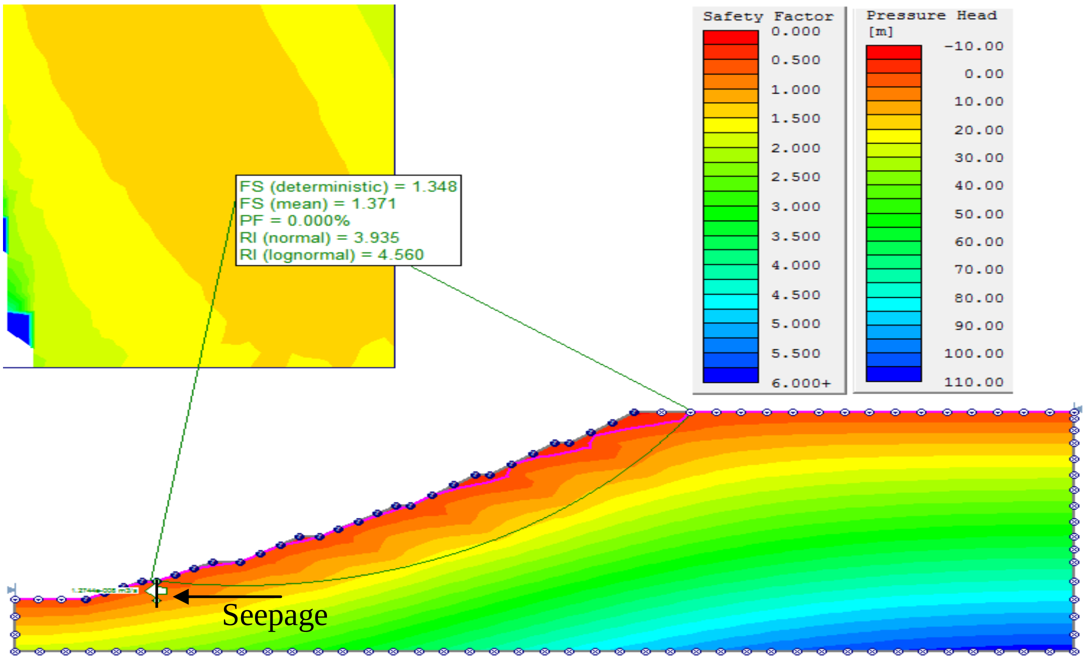

Figure 4.2 Critical slip surface and pore pressures when Ko/Ks=1 for scenario-1.

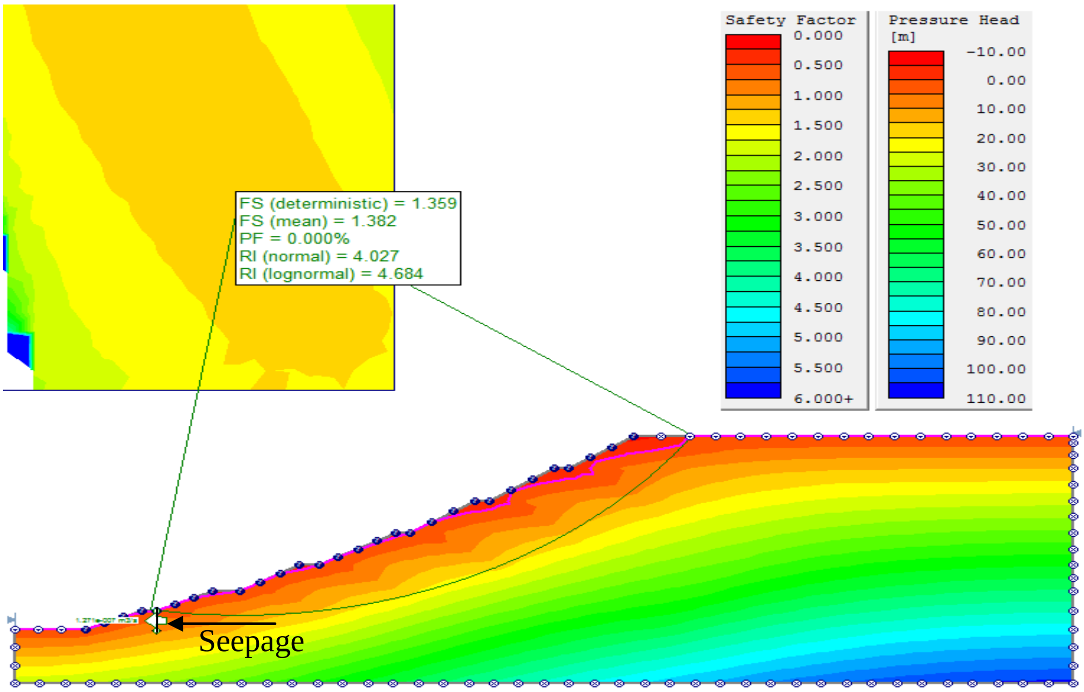

Figure 4.3 Critical slip surface and pore pressures when Ko/Ks=10 for scenario-1.

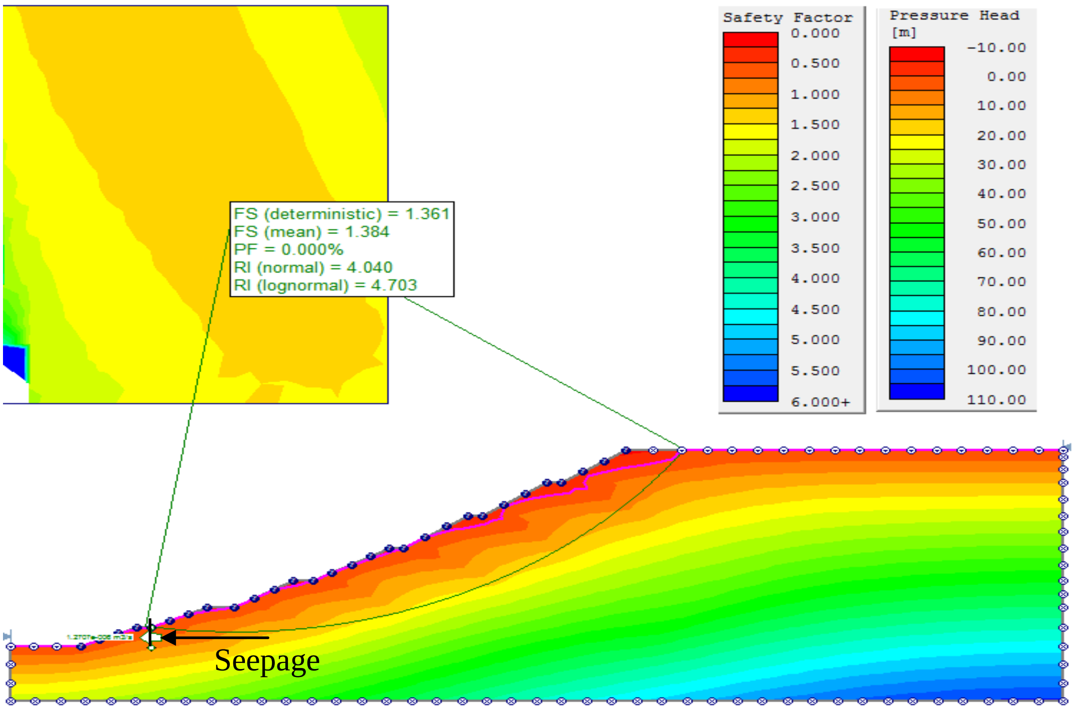

Figure 4.4 Critical slip surface and pore pressures when Ko/Ks=100 for scenario-1.

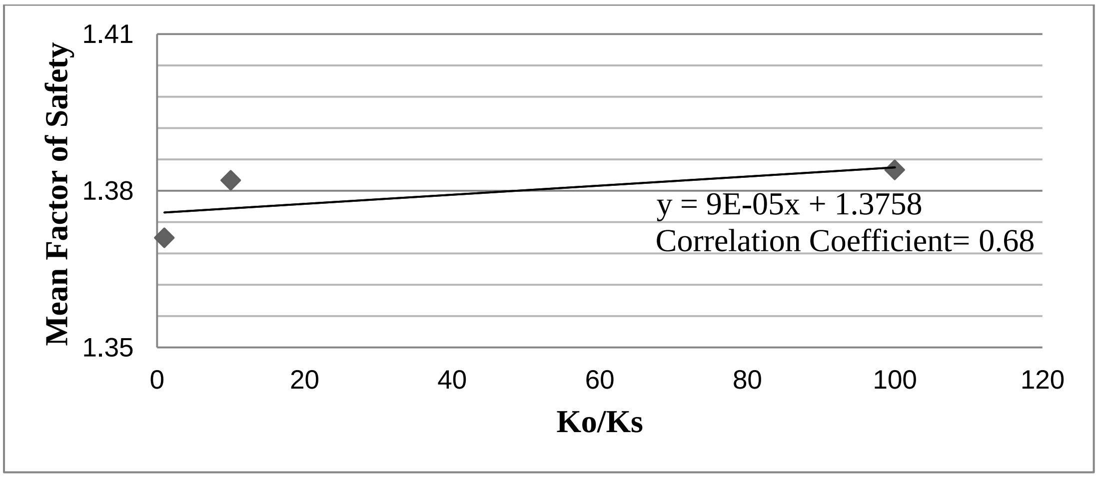

Figure 4.5 Equations of the trend lines and correlation coefficients between Ko/Ks and mean factor of safeties for scenario-1.

Table 4.6 Amounts of seepage from the first embankment for scenario-1.

Amounts of seepage (m^3/s) from first embankment	
Ko/Ks	Q (m^3/s)
1	1.2744×10^{-8}
10	1.271×10^{-7}
100	1.2707×10^{-6}

Table 4.7 Equations of the trend lines and correlation coefficients between cohesions of dam parts and factor of safeties under Ko/Ks=1 and scenario-1 conditions.

Cohesion & Factor of Safety				
Condition	**Type**	**Depth (m)**	**Equation**	**Correlation Coefficient**
Ko/Ks=1 with Water layer from (214m,90m) to (350m,87m)	Coarse Tailing	0-15	y= 0.0004x+1.3608	0.034598
		15-30	y= 0.0002x+1.3653	0.019604
		30-45	y= 0.0008x+1.3537	0.057597
		45-90	y= 0.0038x+1.2821	0.299414
	Fine Tailing	0-15	y= 0.0002x+1.3673	0.012342
		15-30	y= 0.00007x+1.3693	0.005748
		30-45	y= -0.0005x+1.3834	-0.041481
		45-90	y= 0.0003x+1.3639	0.024005
	Rock-Fill	0-90	y= 0.0028x+1.3629	0.24545

Table 4.8 Equations of the trend lines and correlation coefficients between cohesions of dam parts and factor of safeties under Ko/Ks=10, Ko/Ks=100 and scenario-1 conditions.

Cohesion & Factor of Safety				
Condition	**Type**	**Depth (m)**	**Equation**	**Correlation Coefficient**
Ko/Ks=10 with Water layer from (214m,90m) to (350m,87m)	Coarse Tailing	0-15	y= 0.0005x+1.3715	0.035468
		15-30	y= 0.0002x+1.3715	0.019203
		30-45	y= 0.0007x+1.3648	0.057261
		45-90	y= 0.0038x+1.293	0.298146
	Fine Tailing	0-15	y= 0.0002x+1.3782	0.012846
		15-30	y= 0.00008x+1.3802	0.006493
		30-45	y= -0.0005x+1.3945	-0.041091
		45-90	y= 0.0003x+1.37484	0.024351
	Rock-Fill	0-90	y= 0.0028x+1.37421	0.023727
Ko/Ks=100 with Water layer from (214m,90m) to (350m,87m)	Coarse Tailing	0-15	y= 0.0005x+1.3732	0.035522
		15-30	y= 0.0002x+1.3781	0.019175
		30-45	y= 0.0008x+1.3664	0.057195
		45-90	y= 00038x+1.29462	0.29792
	Fine Tailing	0-15	y= 0.0002x+1.3798	0.012845
		15-30	y= 0.00008x+1.38186	0.006257
		30-45	y= -0.0005x+1.3961	-0.041131
		45-90	y= 0.0003x+1.37652	0.024222
	Rock-Fill	0-90	y= 0.0027x+1.37581	0.023841

Table 4.9 Equations of the trend lines and correlation coefficients between effective friction angles of dam parts and factor of safeties under Ko/Ks=1 and scenario-1 conditions.

Effective Friction Angle & Factor of Safety				
Condition	**Type**	**Depth (m)**	**Equation**	**Correlation Coefficient**
Ko/Ks=1 with Water layer from (214m,90m) to (350m,87m)	Coarse Tailing	0-15	y= 0.0018x+1.30975	0.042889
		15-30	y= 0.0013x+1.32681	0.0330696
		30-45	y= 0.0054x+1.1814	0.130884
		45-90	y= 0.0389x+0.01365	0.938753
	Fine Tailing	0-15	y= -0.0016x+1.4261	-0.037644
		15-30	y= 0.0031x+1.2643	0.074708
		30-45	y= 0.0018x+1.3072	0.046224
		45-90	y= 0.00004x+1.36956	0.001029
	Rock-Fill	0-90	y= 0.0015x+1.309	0.015887

Table 4.10 Equations of the trend lines and correlation coefficients between effective friction angles of dam parts and factor of safeties under Ko/Ks=10, Ko/Ks=100 and scenario-1 conditions.

Effective Friction Angle & Factor of Safety				
Condition	**Type**	**Depth (m)**	**Equation**	**Correlation Coefficient**
Ko/Ks=10 with Water layer from (214m,90m) to (350m,87m)	Coarse Tailing	0-15	y= 0.0018x+1.3205	0.042865
		15-30	y= 0.0013x+1.3369	0.03116
		30-45	y= 0.0055x+1.1895	0.132097
		45-90	y= 0.0391x+0.015	0.939432
	Fine Tailing	0-15	y= -0.0016x+1.4375	-0.037593
		15-30	y= 0,0031x+1.2734	0.075635
		30-45	y= 0.0018x+1.3184	0.045878
		45-90	y= 0.00003x+1.3184	0.000759
	Rock-Fill	0-90	y= 0.0015x+1.3177	0.016372
Ko/Ks=100 with Water layer from (214m,90m) to (350m,87m)	Coarse Tailing	0-15	y= 0.0018x+1.3223	0.042691
		15-30	y= 0.0013x+1.3382	0.031424
		30-45	y= 0.0055x+1.1907	0.132294
		45-90	y= 0.0392x+0.0153	0.93953
	Fine Tailing	0-15	y= -0.0016x+1.4392	-0.037582
		15-30	y= 0.0031x+1.2750	0.075572
		30-45	y= 0.0018x+1.3202	0.04574
		45-90	y= 0.00004x+1.3825	0.000905
	Rock-Fill	0-90	y= 0.0015x+1.3194	0.016348

Table 4.11 Equations of the trend lines and correlation coefficients between unit weights of dam parts and factor of safeties under Ko/Ks=1 and scenario-1 conditions.

Unit Weight & Factor of Safety				
Condition	**Type**	**Depth (m)**	**Equation**	**Correlation Coefficient**
Ko/Ks=1 with Water layer from (214m,90m) to (350m,87m)	Coarse Tailing	0-15	y= 0.00008x+1.3693	0.002078
		15-30	y= 0.0007x+1.3530	0.019302
		30-45	y= -0.0022x+1.4267	-0.044912
		45-90	y= 0.0121x+1.0596	0.116197
	Fine Tailing	0-15	y= -0.0013x+1.3986	-0.033915
		15-30	y= 0.0017x+1.33	0.043981
		30-45	y= 0.0024x+1.3108	0.047231
		45-90	y= -0.0046x+1.48913	-0.0465
	Rock-Fill	0-90	y= 0.098x+1.1261	0.103829

Table 4.12 Equations of the trend lines and correlation coefficients between unit weights of dam parts and factor of safeties under Ko/Ks=10, Ko/Ks=100 and scenario-1 conditions.

Unit Weight & Factor of Safety				
Condition	**Type**	**Depth (m)**	**Equation**	**Correlation Coefficient**
Ko/Ks=10 with Water layer from (214m,90m) to (350m,87m)	Coarse Tailing	0-15	y= 0.00009x+1.3802	0.002311
		15-30	y= 0.0007x+1.36406	0.019235
		30-45	y= -0.0023x+1.4394	-0.045889
		45-90	y= 0.0120x+1.0722	0.114869
	Fine Tailing	0-15	y= -0.0013x+1.4106	-0.034807
		15-30	y= 0.0017x+1.33412	0.043601
		30-45	y= 0.0024x+1.32091	0.047647
		45-90	y= -0.0046x+1.5015	-0.046695
	Rock-Fill	0-90	y= 0.0095x+1.1433	0.100592
Ko/Ks=100 with Water layer from (214m,90m) to (350m,87m)	Coarse Tailing	0-15	y= 0.00009x+1.3818	0.002367
		15-30	y= 0.0007x+1.3656	0.019295
		30-45	y= -0.023x+1.4413	-0.046072
		45-90	y= 0.012x+1.0744	0.114668
	Fine Tailing	0-15	y= -0.0013x+1.4124	-0.034969
		15-30	y= 0.0017x+1.3426	0.043807
		30-45	y= 0.0024x+1.3224	0.047695
		45-90	y= -0.0047x+1.50355	-0.046822
	Rock-Fill	0-90	y= 0.0095x+1.14579	0.100148

Table 4.13 Equations of the trend lines and correlation coefficients between unsaturated shear strengths ($\emptyset^b$) of dam parts and factor of safeties under Ko/Ks=1 and scenario-1 conditions.

Unsaturated Shear Strength & Factor of Safety				
Condition	**Type**	**Depth (m)**	**Equation**	**Correlation Coefficient**
Ko/Ks=1 with Water layer from (214m,90m) to (350m,87m)	Coarse Tailing	0-15	y= -0.0044x+1.4521	-0.0444
		15-30	y= -0.0008x+1.38665	-0.009133
		30-45	y= 0.00374x+1.30185	0.04145
		45-90	y= 0.0012x+1.348	0.012928
	Fine Tailing	0-15	y= -0.0006x+1.3815	-0.005956
		15-30	y= -0.0022x+1.4108	-0.022548
		30-45	y= -0.0008x+1.38509	-0.007898
		45-90	y= 0.0039x+1.2996	0.041514

Table 4.14 Equations of the trend lines and correlation coefficients between unsaturated shear strengths ($\emptyset^b$) of dam parts and factor of safeties under Ko/Ks=10, Ko/Ks=100 and scenario-1 conditions.

Unsaturated Shear Strength & Factor of Safety				
Condition	**Type**	**Depth (m)**	**Equation**	**Correlation Coefficient**
Ko/Ks=10 with Water layer from (214m,90m) to (350m,87m)	Coarse Tailing	0-15	y= -0.0044x+1.4643	-0.044698
		15-30	y= -0.0009x+1.3993	-0.009956
		30-45	y= 0.0037x+1.3134	0.040933
		45-90	y= 0.0013x+1.3582	0.013331
	Fine Tailing	0-15	y= -0.0005x+1.3918	-0.005486
		15-30	y= -0.0022x+1.4232	-0.02312
		30-45	y= -0.0008x+1.3965	-0.008
		45-90	y= 0.0039x+1.3095	0,041886
Ko/Ks=100 with Water layer from (214m,90m) to (350m,87m)	Coarse Tailing	0-15	y= -0.044x+1.4658	-0.044556
		15-30	y= -0.0009x+1.4006	-0.009763
		30-45	y= 0.0037x+1.3149	0.040964
		45-90	y= 0.0013x+1.3598	0.013349
	Fine Tailing	0-15	y= -0.0005x+1.3934	-0.00543
		15-30	y= -0.0022x+1.4249	-0.023141
		30-45	y= -0.0008x+1.3983	-0.008108
		45-90	y= 0.0039x+1.3112	0.04185

4.1.2 **Scenario-2 for SLIDE**

In the second scenario, the water layer is initiated at the middle of layer of upper coarse tailing. It is stretched from the point (247 m, 90 m) to (350 m, 87 m) on the right boundary of the cross section. Similarly, the deepest point of the pond is located at the furthest distance from spigot point and the depth is taken as same as the height of the last raised part.

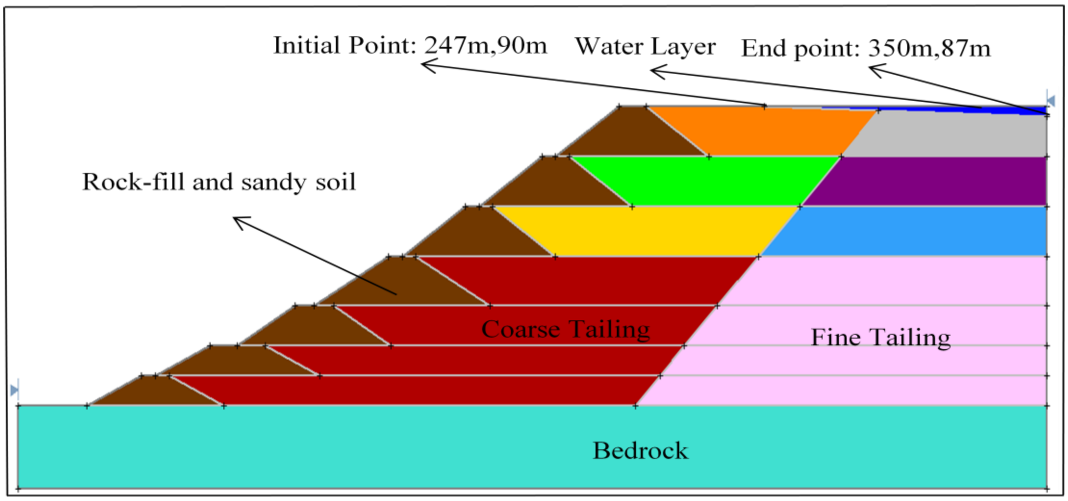

Figure 4.6 Cross sectional details of Kastamonu Küre tailing dam for scenario-2.

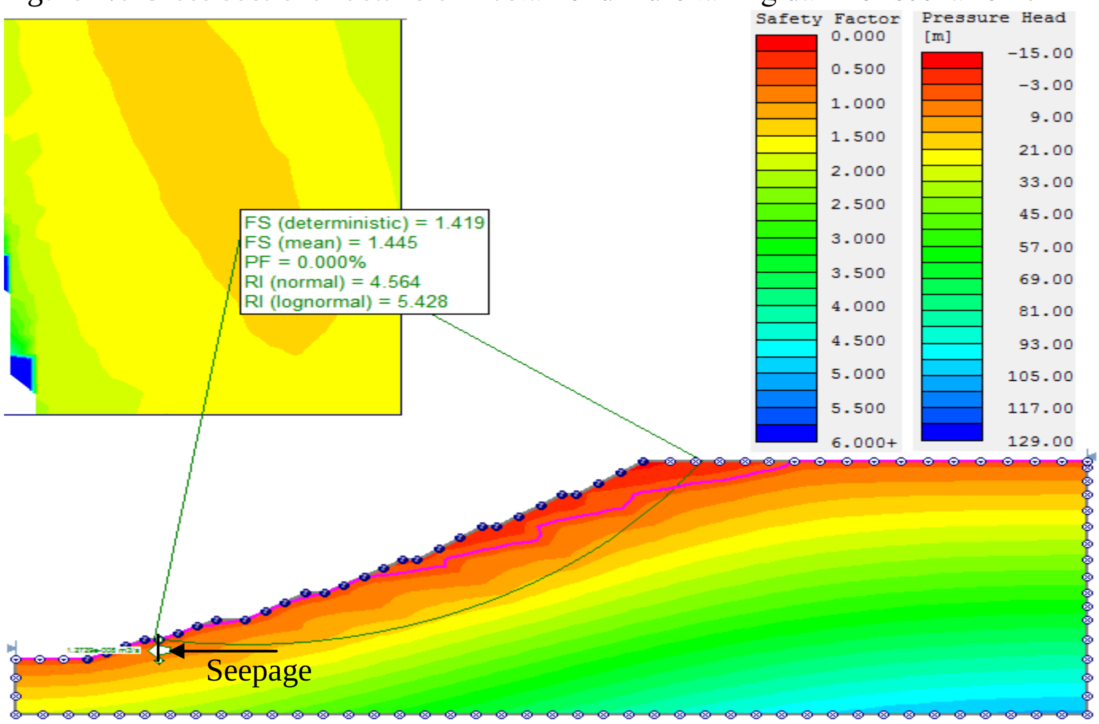

Figure 4.7 Critical slip surface and pore pressures when Ko/Ks=1 for scenario-2.

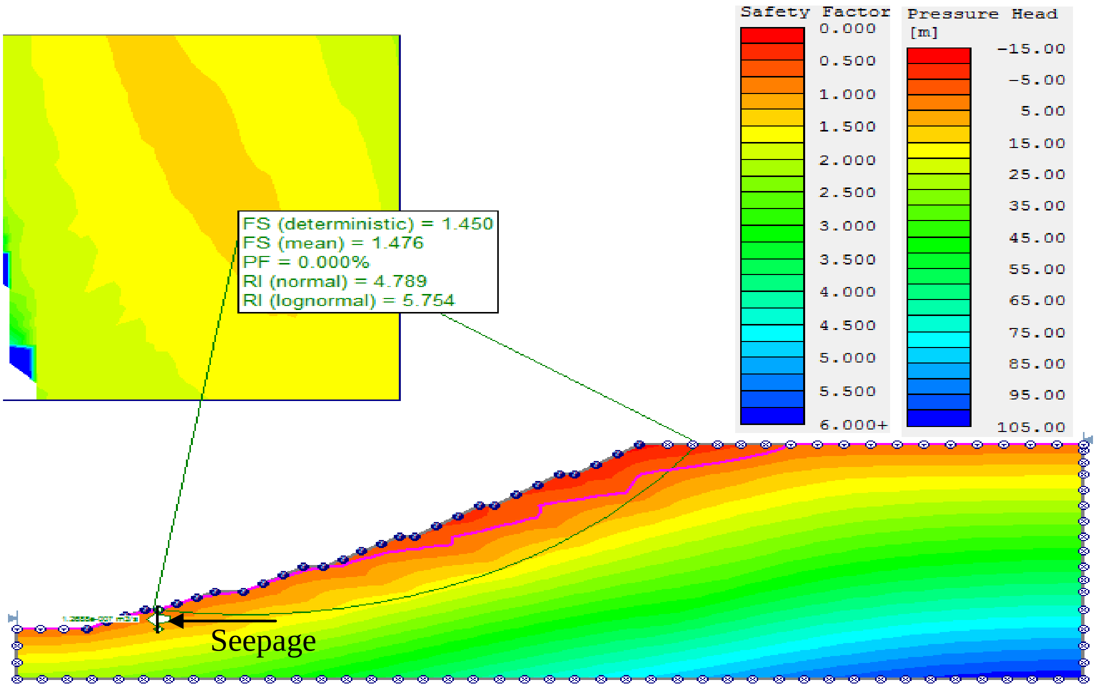

Figure 4.8 Critical slip surface and pore pressures when Ko/Ks=10 for scenario-2.

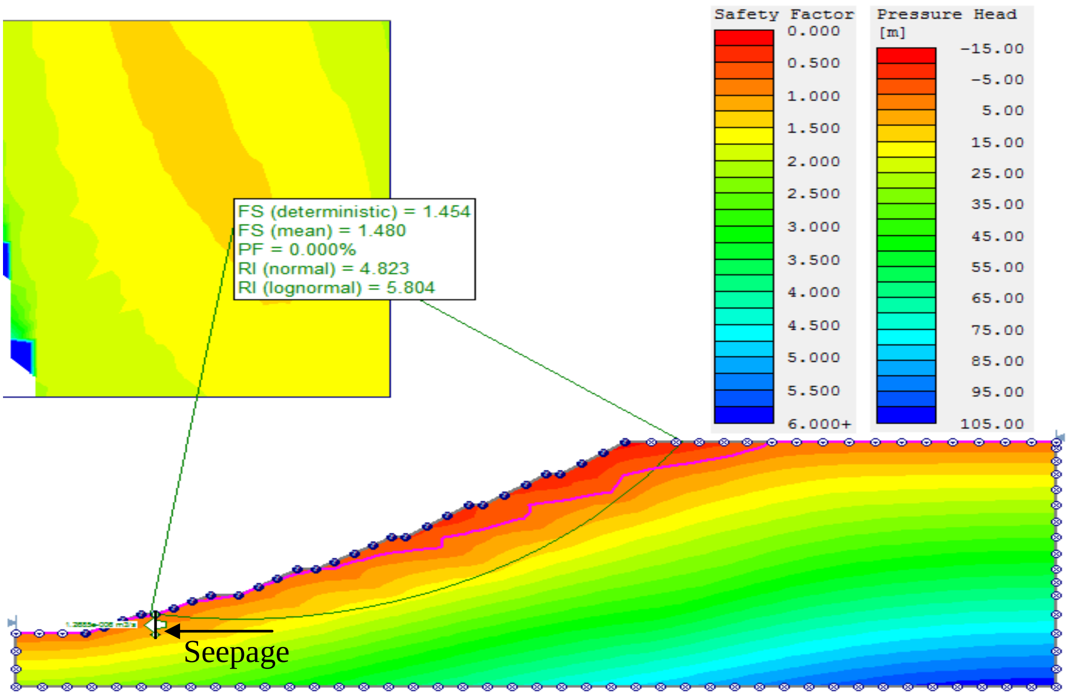

Figure 4.9 Critical slip surface and pore pressures when Ko/Ks=100 for scenario-2.

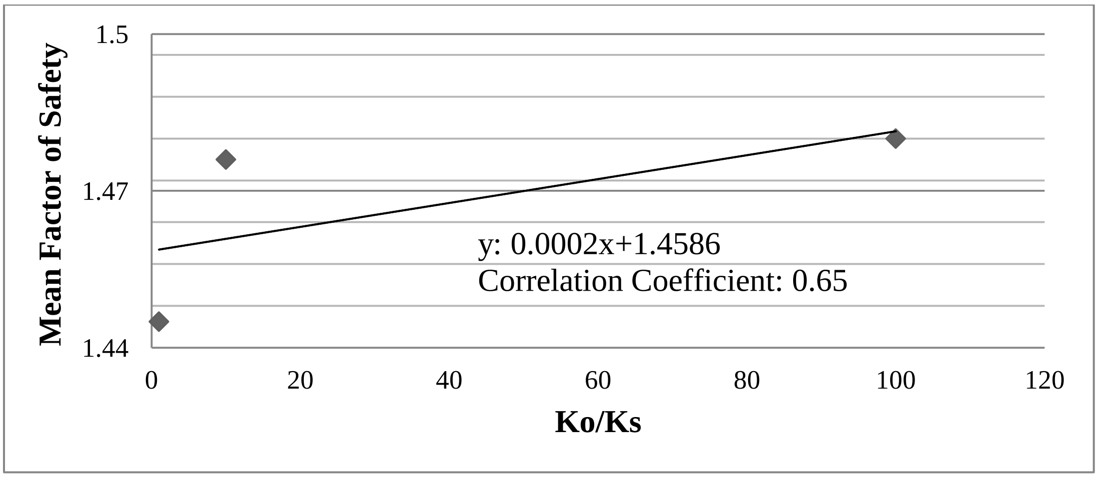

Figure 4.10 Equations of the trend lines and correlation coefficients between Ko/Ks and mean factor of safeties for scenario-2.

Table 4.15 Amounts of seepage from the first embankment according to Ko/Ks ratio for scenario-2.

Amounts of seepage (m^3/s) from first embankment	
Ko/Ks	Q (m^3/s)
1	$1.2729x10^{-8}$
10	$1.2688x10^{-7}$
100	$1.2685x10^{-6}$

Table 4.16 Equations of the trend lines and correlation coefficients between cohesions of dam parts and factor of safeties under Ko/Ks=1 and scenario-2 conditions.

Cohesion & Factor of Safety				
Condition	**Type**	**Depth (m)**	**Equation**	**Correlation Coefficient**
Ko/Ks=1 with Water layer from (247m,90m) to (300m,87m)	Coarse Tailing	0-15	y= 0.00005x+1.4332	0.037465
		15-30	y= 0.0003x+1.4384	0.020595
		30-45	y= 0.00081x+1.426	0.059932
		45-90	y= 0.0039x+1.35342	0.297205
	Fine Tailing	0-15	y= 0.0002x+1.4403	0.013614
		15-30	y= 0.00007x+1.443	0.005192
		30-45	y= -0.0005x+1.4573	-0.041082
		45-90	y= 0.0003x+1.4372	0.024326
	Rock-Fill	0-90	y= 0.0031x+1.4357	0.026077

Table 4.17 Equations of the trend lines and correlation coefficients between cohesions of dam parts and factor of safeties under Ko/Ks=10, Ko/Ks=100 and scenario-2 conditions.

Cohesion & Factor of Safety				
Condition	**Type**	**Depth (m)**	**Equation**	**Correlation Coefficient**
Ko/Ks=10 with Water layer from (247m,90m) to (300m,87m)	Coarse Tailing	0-15	y= 0.0005x+1.4644	0.036939
		15-30	y= 0.0003x+1.4698	0.019761
		30-45	y= 0.0008x+1.4568	0.060212
		45-90	y= 0.0039x+1.38433	0.29257
	Fine Tailing	0-15	y= 0.0002x+1.4713	0.014398
		15-30	y= 0.00008x+1.474	0.005924
		30-45	y= -0.0006x+1.4890	-0.041641
		45-90	y= 0.0003x+1.4681	0.025182
	Rock-Fill	0-90	y= 0.0033x+1.4665	0.027192
Ko/Ks=100 with Water layer from (247m,90m) to (300m,87m)	Coarse Tailing	0-15	y= 0.0005x+1.4686	0.037205
		15-30	y= 0.0003x+1.4742	0.01976
		30-45	y= 0.0008x+1.4613	0.059686
		45-90	y= 0.0039x+1.3888	0.291446
	Fine Tailing	0-15	y= 0.0002x+1.4755	0.014658
		15-30	y= 0.00008x+1.4784	0.006
		30-45	y= -0.0006x+1.49322	-0.041179
		45-90	y= 0.0003x+1.47252	0.024681
	Rock-Fill	0-90	y= 0.0034x+1.4706	0.027576

Table 4.18 Equations of the trend lines and correlation coefficients between effective friction angles of dam parts and factor of safeties under Ko/Ks=1 and scenario-2 conditions.

Friction Angle & Factor of Safety				
Condition	**Type**	**Depth (m)**	**Equation**	**Correlation Coefficient**
Ko/Ks=1 with Water layer from (247m,90m) to (300m,87m)	Coarse Tailing	0-15	y= 0.0018x+1.3804	0.0043535
		15-30	y= 0.0016x+1.3883	0.037882
		30-45	y= 0.006x+1.2359	0.139411
		45-90	y= 0.04x+0.0399	0.940302
	Fine Tailing	0-15	y= -0.0016x+1.50058	-0.037021
		15-30	y= 0.0032x+1.3337	0.075155
		30-45	y= 0.002x+1.37578	0.048272
		45-90	y= 0.0001x+1.4405	0.002875
	Rock-Fill	0-90	y= 0.0017x+1.3743	0.017412

Table 4.19 Equations of the trend lines and correlation coefficients between effective friction angles of dam parts and factor of safeties under Ko/Ks=10, Ko/Ks=100 and scenario-2 conditions.

Friction Angle & Factor of Safety				
Condition	**Type**	**Depth (m)**	**Equation**	**Correlation Coefficient**
Ko/Ks=10 with Water layer from (247m,90m) to (300m,87m)	Coarse Tailing	0-15	y= 0.0018x+1.4121	0.042351
		15-30	y= 0.0017x+1.4182	0.038056
		30-45	y= 0.0061x+1.2614	0.140486
		45-90	y= 0.0411x+0.0395	0.942559
	Fine Tailing	0-15	y= -0.0016x+1.5325	-0.036656
		15-30	y= 0.0033x+1.3623	0.075476
		30-45	y= 0.002x+1.40602	0.048048
		45-90	y= 0.0001x+1.4718	0.002816
	Rock-Fill	0-90	y= 0.0017x+1.4043	0.017385
Ko/Ks=100 with Water layer from (247m,90m) to (300m,87m)	Coarse Tailing	0-15	y= 0.0018x+1.4164	0.04235
		15-30	y= 0.0016x+1.4232	0.037524
		30-45	y= 0.0061x+1.2658	0.140175
		45-90	y= 0.0412x+0.0403	0.94304
	Fine Tailing	0-15	y= -0.0016x+1.537	-0.036708
		15-30	y= 0.0032x+1.3675	0.074725
		30-45	y= 0.002x+1.4107	0.047725
		45-90	y= 0.0001x+1.1323	0.002317
	Rock-Fill	0-90	y= 0.0001x+0.0023	0.017311

Table 4.20 Equations of the trend lines and correlation coefficients between unit weights of dam parts and factor of safeties under Ko/Ks=1 and scenario-2 conditions.

Unit Weight & Factor of Safety				
Condition	**Type**	**Depth (m)**	**Equation**	**Correlation Coefficient**
Ko/Ks=1 with Water layer from (247m,90m) to (300m,87m)	Coarse Tailing	0-15	y= 0.00008x+1.4428	0.002084
		15-30	y= 0.0006x+1.4299	0.015317
		30-45	y= -0.0026x+1.50944	-0.0505751
		45-90	y= 0.0116x+1.1445	0.108359
	Fine Tailing	0-15	y= -0.0014x+1.4752	-0.036392
		15-30	y= 0.0017x+1.40314	0.043047
		30-45	y= 0.0024x+1.3840	0.045949
		45-90	y= -0.0047x+1.5651	-0.045897
	Rock-Fill	0-90	y= 0.0082x+1.2405	0.08376

Table 4.21 Equations of the trend lines and correlation coefficients between unit weights of dam parts and factor of safeties under Ko/Ks=10, Ko/Ks=100 and scenario-2 conditions.

Unit Weight & Factor of Safety				
Condition	**Type**	**Depth (m)**	**Equation**	**Correlation Coefficient**
Ko/Ks=10 with Water layer from (247m,90m) to (300m,87m)	Coarse Tailing	0-15	y= 0.00008x+1.4741	0.00205
		15-30	y= 0.0006x+1.4622	0.013928
		30-45	y= -0.0003x+1.5438	-0.05194
		45-90	y= 0.0115x+1.17927	0.105001
	Fine Tailing	0-15	y= -0.0014x+1.5076	-0.036914
		15-30	y= 0.0017x+1.4329	0.043806
		30-45	y= 0.0025x+1.4122	0.047391
		45-90	y= -0.0048x+1.599	-0.045995
	Rock-Fill	0-90	y= 0.0075x+1.2883	0.075455
Ko/Ks=100 with Water layer from (247m,90m) to (300m,87m)	Coarse Tailing	0-15	y= 0.00005x+1.479	0.001402
		15-30	y= 0.00005x+1.479	0.013072
		30-45	y= -0.0028x+1.54949	-0.052851
		45-90	y= 0.0114x+1.1846	0.104454
	Fine Tailing	0-15	y= -0.0014x+1.51208	-0.037053
		15-30	y= 0.0017x+1.4372	0.043718
		30-45	y= 0.0026x+1.4162	0.047515
		45-90	y= -0.0047x+1.6021	-0.045439
	Rock-Fill	0-90	y= 0.0074x+1.2952	0.07428

Table 4.22 Equations of the trend lines and correlation coefficients between unsaturated shear strengths ($\emptyset^b$) of dam parts and factor of safeties under Ko/Ks=1 and scenario-2 conditions.

Unsaturated Shear Strength & Factor of Safety				
Condition	**Type**	**Depth (m)**	**Equation**	**Correlation Coefficient**
Ko/Ks=1 with Water layer from (247m,90m) to (300m,87m)	Coarse Tailing	0-15	y= -0.0043x+1.5245	-0.042322
		15-30	y= -0.0009x+1.462	-0.009815
		30-45	y= 0.0036x+1.3789	0.038103
		45-90	y= 0.0014x+1.4184	0.014271
	Fine Tailing	0-15	y= -0.0004x+1.4517	-0.003877
		15-30	y= -0.0024x+1.4891	-0.02439
		30-45	y= -0.0007x+1.4587	-0.0007665
		45-90	y= 0.0041x+1.3695	0.042233

Table 4.23 Equations of the trend lines and correlation coefficients between unsaturated shear strengths ($\emptyset^b$) of dam parts and factor of safeties under Ko/Ks=10. Ko/Ks=100 and scenario-2 conditions.

Unsaturated Shear Strength & Factor of Safety				
Condition	**Type**	**Depth (m)**	**Equation**	**Correlation Coefficient**
Ko/Ks=10 with Water layer from (247m,90m) to (300m,87m)	Coarse Tailing	0-15	y= -0.0045x+1.5584	-0.042856
		15-30	y= -0.001x+1.4948	-0.0104507
		30-45	y= 0.0035+1.4107	0.037074
		45-90	y= 0.0015x+1.4488	0.014462
	Fine Tailing	0-15	y= -0.0003x+1.4817	-0.003116
		15-30	y= -0.0026x+1.5243	-0.02603
		30-45	y= -0.0008x+1.4915	-0.00832156
		45-90	y= 0.0041x+1.4003	0.0416961
Ko/Ks=100 with Water layer from (247m,90m) to (300m,87m)	Coarse Tailing	0-15	y= -0.0045x+1.5632	-0.042979
		15-30	y= -0.001x+1.4990	-0.010397
		30-45	y= 0.0036x+1.4144	0.0373704
		45-90	y= 0.0015x+1.4523	0.014884
	Fine Tailing	0-15	y= -0.0003x+1.48634	-0.003289
		15-30	y= -0.0026x+1.52849	-0.0258832
		30-45	y= -0.0008x+1.4953	-0.008
		45-90	y= 0.004x+1.4056	0.041076

4.1.3 **Scenario-3 for SLIDE**

In the third scenario. the water layer is specified at the intersection point of coarse and fine tailings. It is extended from the point (290 m, 90 m) to (350 m,87 m) so that entire pond is grounded on upper fine tailing part. Likewise. the deepest point of the pond is located at the furthest distance from spigot point and the depth is increasingly deepened as closing this point.

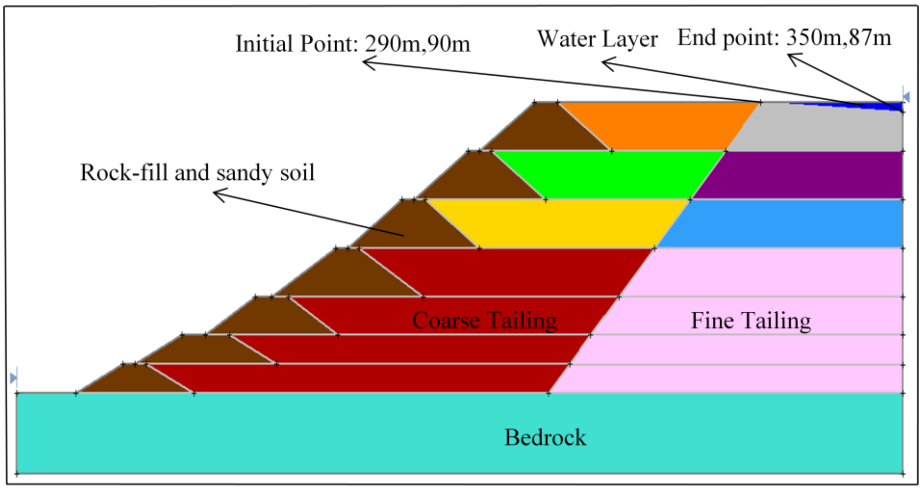

Figure 4.11 Cross sectional details of Kastamonu Küre tailing dam for scnerio-3.

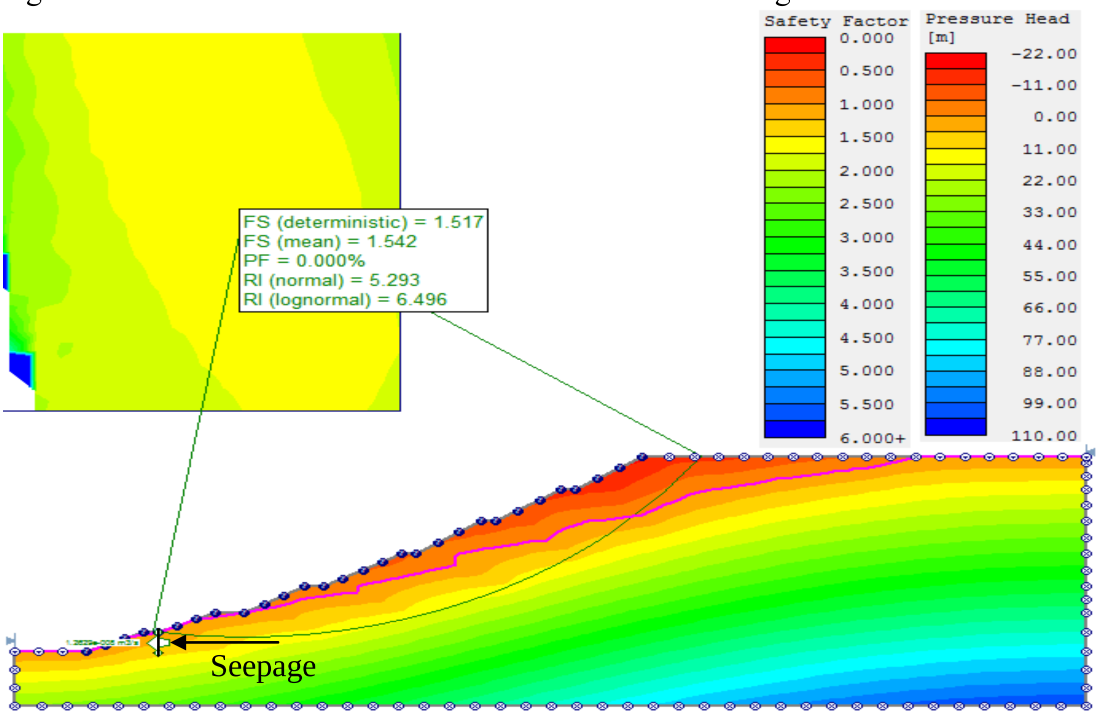

Figure 4.12 Critical slip surface and pore pressures when Ko/Ks=1 for scenario-3.

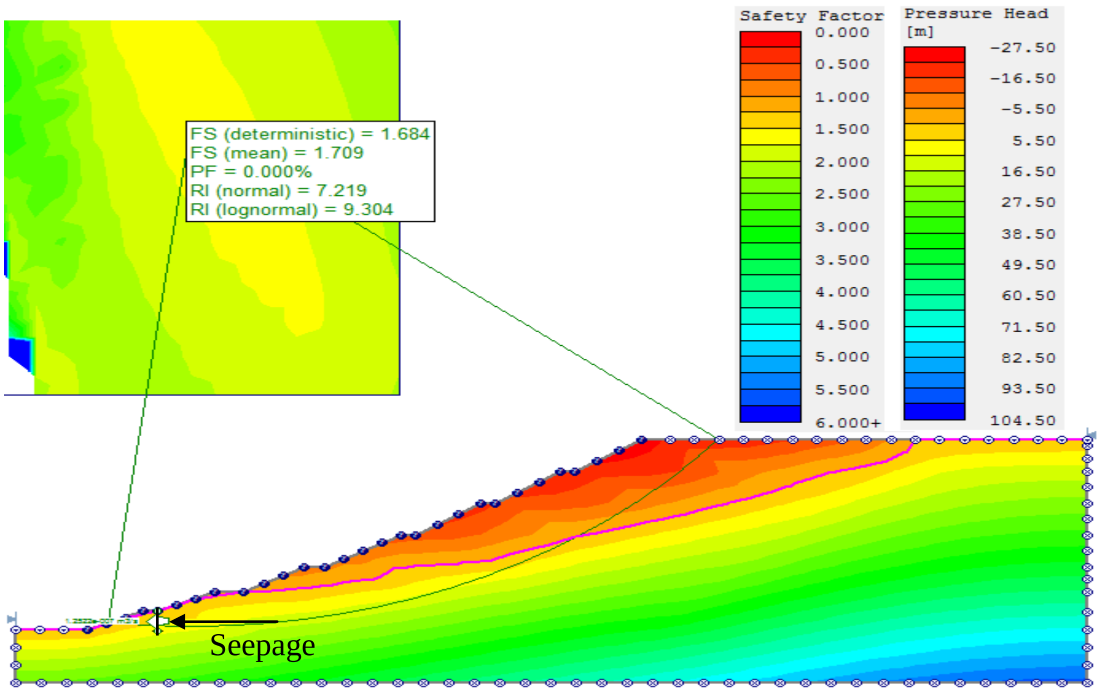

Figure 4.13 Critical slip surface and pore pressures when Ko/Ks=10 for scenario-3.

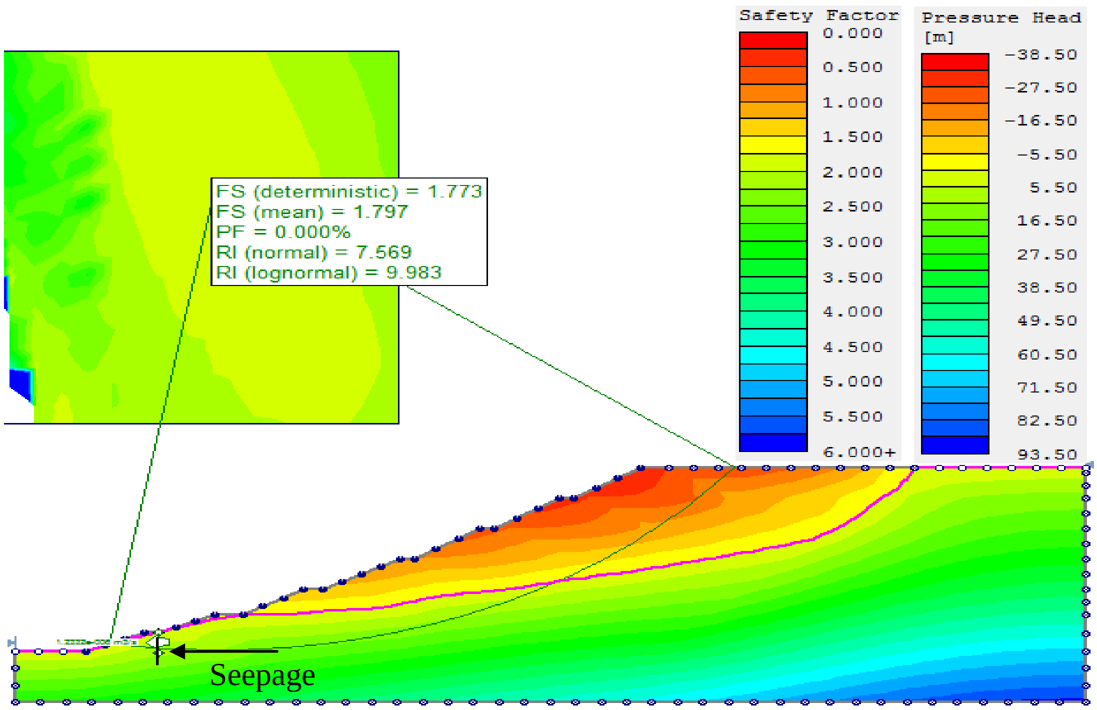

Figure 4.14 Critical slip surface and pore pressures when Ko/Ks=100 for scenario-3.

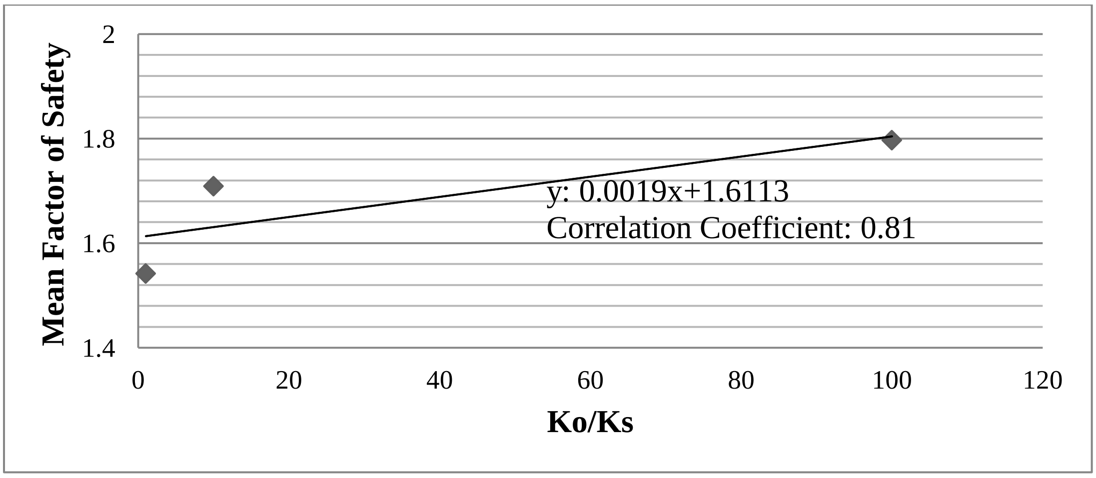

Figure 4.15 Equations of the trend lines and correlation coefficients between Ko/Ks and mean factor of safeties for scenario-3.

Table 4.24 Amounts of seepage from the first embankment according to Ko/Ks ratio for scenario-3.

Amounts of seepage (m^3/s) from first embankment	
Ko/Ks	Q (m^3/s)
1	1.2629×10^{-8}
10	1.2522×10^{-7}
100	1.2332×10^{-6}

Table 4.25 Equations of the trend lines and correlation coefficients between cohesions of dam parts and factor of safeties under Ko/Ks=1 and scenario-3 conditions.

Cohesion & Factor of Safety				
Condition	**Type**	**Depth (m)**	**Equation**	**Correlation Coefficient**
Ko/Ks=1 with Water layer from (290m,90m) to (350m,87m)	Coarse Tailing	0-15	y= 0.0006x+1.78229	0.045341
		15-30	y= 0.0003x+1.79075	0.019992
		30-45	y= 0.0008x+1.7783	0.056361
		45-90	y= 0.0029x+1.7293	0.204837
	Fine Tailing	0-15	y= 0.0002x+1.7927	0.013459
		15-30	y= 0.0001x+1.7946	0.008106
		30-45	y= -0.0006x+1.8108	-0.0407042
		45-90	y= 0.0004x+1.7886	0.026065
	Rock-Fill	0-90	y= 0.0042x+1.7854	0.0321137

Table 4.26 Equations of the trend lines and correlation coefficients between effective friction angles of dam parts and factor of safeties under Ko/Ks=10. Ko/Ks=100 and scenario-3 conditions.

Cohesion & Factor of Safety				
Condition	**Type**	**Depth (m)**	**Equation**	**Correlation Coefficient**
Ko/Ks=10 with Water layer from (290m,90m) to (350m,87m)	Coarse Tailing	0-15	y= 0.0006x+1.69529	0.044445
		15-30	y= 0.0003x+1.70186	0.023469
		30-45	y= 0.0008x+1.6896	0.06193
		45-90	y= 0.0031x+1.635	0.239057
	Fine Tailing	0-15	y= 0.0002x+1.7047	0.0136385
		15-30	y= 0.00008x+1.7071	0.006061
		30-45	y= -0.0005x+1.7217	-0.040819
		45-90	y= 0.0003x+1.7012	0.0251107
	Rock-Fill	0-90	y= -0.0093x+1.2657	0.037096
Ko/Ks=100 with Water layer from (290m,90m) to (350m,87m)	Coarse Tailing	0-15	y= 0.0005x+1.5299	0.038116
		15-30	y= 0.0002x+1.5362	0.01873
		30-45	y= 0.0009x+1.5221	0.0611266
		45-90	y= 0.0039x+1.4505	0.283949
	Fine Tailing	0-15	y= 0.0002x+1.5372	0.014787
		15-30	y= 0.00009x+1.5401	0.0062568
		30-45	y= -0.0006x+1.5556	-0.041505
		45-90	y= 0.0004x+1.5336	0.026512
	Rock-Fill	0-90	y= 0.0035x+1.5321	0.02793

Table 4.27 Equations of the trend lines and correlation coefficients between effective friction angles of dam parts and factor of safeties under Ko/Ks=1 and scenario-3 conditions.

Friction Angle & Factor of Safety				
Condition	**Type**	**Depth (m)**	**Equation**	**Correlation Coefficient**
Ko/Ks=1 with Water layer from (290m,90m) to (350m,87m)	Coarse Tailing	0-15	y= 0.0018x+1.4801	0.039954
		15-30	y= 0.0018x+1.4781	0.040913
		30-45	y= 0.0064x+1.3171	0.143001
		45-90	y= 0.0425x+0.0559	0.946159
	Fine Tailing	0-15	y= -0.0016x+1.5989	-0.035716
		15-30	y= 0.0034x+1.4236	0.076393
		30-45	y= 0.002x+1.4731	0.046057
		45-90	y= 0.0002x+1.5361	0.004
	Rock-Fill	0-90	y= 0.0015x+1.4780	0.015105

Table 4.28 Equations of the trend lines and correlation coefficients between effective friction angles of dam parts and factor of safeties under Ko/Ks=10. Ko/Ks=100 and scenario-3 conditions.

Friction Angle & Factor of Safety				
Condition	**Type**	**Depth (m)**	**Equation**	**Correlation Coefficient**
Ko/Ks=10 with Water layer from (290m,90m) to (350m,87m)	Coarse Tailing	0-15	y= 0.0018x+1.64575	0.042485
		15-30	y= 0.0023x+1.6294	0.053092
		30-45	y= 0.0074x+1.4521	0.170206
		45-90	y= 0.0409x+0.2794	0.949066
	Fine Tailing	0-15	y= -0.0017x+1.7675	-0.038378
		15-30	y= 0.0032x+1.5965	0.075582
		30-45	y= 0.002x+1.6411	0.047232
		45-90	y= 0.00009x+1.7059	0.002147
	Rock-Fill	0-90	y= 0.0069x+1.4201	0.071042
Ko/Ks=100 with Water layer from (290m,90m) to (350m,87m)	Coarse Tailing	0-15	y= 0.0021x+1.7232	0.046386
		15-30	y= 0.0024x+1.7152	0.051
		30-45	y= 0.0072x+1.5465	0.154902
		45-90	y= 0.0442x+0.2527	0.956124
	Fine Tailing	0-15	y= -0.0018x+1.8606	-0.038734
		15-30	y= 0.0034x+1.6779	0.074831
		30-45	y= 0.0021x+1.7251	0.046798
		45-90	y= 0.00004x+1.7959	0.00086
	Rock-Fill	0-90	y= 0.0066x+1.5202	0.063531

Table 4.29 Equations of the trend lines and correlation coefficients between unit weights of dam parts and factor of safeties under Ko/Ks=1 and scenario-3 conditions.

Unit Weight & Factor of Safety				
Condition	**Type**	**Depth (m)**	**Equation**	**Correlation Coefficient**
Ko/Ks=1 with Water layer from (290m,90m) to (350m,87m)	Coarse Tailing	0-15	y= 0.0001x+1.5397	0.002706
		15-30	y= 0.0005x+1.5301	0.011821
		30-45	y= -0.0031x+1.6202	-0.05789
		45-90	y= 0.0112x+1.2519	0.099669
	Fine Tailing	0-15	y= -0.0016x+1.5765	-0.038918
		15-30	y= 0.0426x+0.8057	0.042638
		30-45	y= 0.0017x+1.4989	0.0467031
		45-90	y= -0.005x+1.6698	-0.04627
	Rock-Fill	0-90	y= 0.0058+1.3973	0.056599

Table 4.30 Equations of the trend lines and correlation coefficients between unit weights of dam parts and factor of safeties under Ko/Ks=10. Ko/Ks=100 and scenario-3 conditions.

Unit Weight & Factor of Safety				
Condition	**Type**	**Depth (m)**	**Equation**	**Correlation Coefficient**
Ko/Ks=10 with Water layer from (290m,90m) to (350m,87m)	Coarse Tailing	0-15	y= -0.0004x+1.717	-0.01037
		15-30	y= -0.0001x+1.7125	-0.00372
		30-45	y= -0.0035x+1.7965	-0.067682
		45-90	y= 0.0105x+1.4379	0.097075
	Fine Tailing	0-15	y= -0.0017x+1.7472	0.0451
		15-30	y= 0.0016x+1.6701	0.040004
		30-45	y= 0.0027x+1.6413	0.050919
		45-90	y= -0.0049x+1.8351	-0.047654
	Rock-Fill	0-90	y= 0.0042x+1.6043	0.042574
Ko/Ks=100 with Water layer from (290m,90m) to (350m,87m)	Coarse Tailing	0-15	y= -0.0011x+1.8225	-0.028085
		15-30	y= -0.0011x+1.8241	-0.025865
		30-45	y= -0.0045x+1.9097	-0.081094
		45-90	y= 0.0116x+1.4967	0.100365
	Fine Tailing	0-15	y= -0.002x+1.8407	-0.047768
		15-30	y= 0.0017x+1.7556	0.04
		30-45	y= 0.0029x+1.7257	0.050183
		45-90	y= -0.0053x+1.9338	-0.048124
	Rock-Fill	0-90	y= 0.0052x+1.6678	0.049115

Table 4.31 Equations of the trend lines and correlation coefficients between unsaturated shear strengths ($\emptyset^b$) of dam parts and factor of safeties under Ko/Ks=1 and scenario-3 conditions.

Unsaturated Shear Strength & Factor of Safety				
Condition	**Type**	**Depth (m)**	**Equation**	**Correlation Coefficient**
Ko/Ks=1 with Water layer from (290m,90m) to (350m,87m)	Coarse Tailing	0-15	y= -0.0045x+1.6255	-0.042012
		15-30	y= -0.001x+1.5612	-0.010256
		30-45	y= 0.0037x+1.4743	0.037437
		45-90	y= 0.0016x+1.5132	0.014965
	Fine Tailing	0-15	y= -0.0004x+1.5489	-0.003541
		15-30	y= -0.0029x+1.5952	-0.027703
		30-45	y= -0.001x+1.5602	-0.009345
		45-90	y= 0.0041x+1.4659	0.040754

Table 4.32 Equations of the trend lines and correlation coefficients between unsaturated shear strengths ($\emptyset^b$) of dam parts and factor of safeties under Ko/Ks=10. Ko/Ks=100 and scenario-3 conditions.

Unsaturated Shear Strength & Factor of Safety				
Condition	**Type**	**Depth (m)**	**Equation**	**Correlation Coefficient**
Ko/Ks=10 with Water layer from (290m,90m) to (350m,87m)	Coarse Tailing	0-15	y= -0.0043x+1.7881	-0.041569
		15-30	y= -0.0007x+1.7225	-0.007574
		30-45	y= 0.0035x+1.644	0.037377
		45-90	y= 0.002x+1.6714	0.020285
	Fine Tailing	0-15	y= -0.00009x+1.7106	-0.000888
		15-30	y= -0.0032x+1.7687	-0.032453
		30-45	y= -0.0013x+1.7321	-0.012439
		45-90	y= 0.004x+1.6356	0.040902
Ko/Ks=100 with Water layer from (290m.90m) to (350m.87m)	Coarse Tailing	0-15	y= -0.0041x+1.8729	-0.0370567
		15-30	y= -0.0002x+1.8006	-0.001746
		30-45	y= 0.0041x+1.7211	0.040851
		45-90	y= 0.0022x+1.7565	0.020519
	Fine Tailing	0-15	y= -0.0005x+1.806	-0.004445
		15-30	y= -0.0032x+1.8571	-0.030337
		30-45	y= -0.0014x+1.8238	-0.0133006
		45-90	y= 0.0043x+1.7187	0.040835

4.2 **Calculation Details of the Evaluation Parameters for Drained Analyses**

Slopes of linear regression lines' equations and their correlation coefficients are used in calculation of percent contributions of the parameters for each scenario. The percentages and squared correlation of variations of the parameters are listed in table 4.32 and table 4.33 respectively.

Table 4.33 Percent contributions of the parameters for each scenario.

	Scenario-1	**Scenario-2**	**Scenario-3**
Cohesion	3.37 %	2.95 %	1.76 %
Effective Friction Angle	85.12 %	87.84 %	70.36 %
Unit Weight	7.28 %	5.27 %	3.58 %
Unsaturated Shear Strength ($\emptyset^b$)	2.99 %	1.35 %	1.17 %
Ko/Ks	1.24 %	2.59 %	23.12 %

Table 4.34 Squared COV values of the parameters for all scenarios.

Cohesion	0.247
Effective Friction Angle	0.004
Unit Weight	0.005
Unsaturated Shear Strength ($\emptyset^b$)	0.003
Ko/Ks	2.189

Unique evaluation factors for each scenario are extrapolated by the help of the percentages and COVs. These evaluation factors are entered in table 4.34.

Table 4.34 Unique evaluation factor according to three scenarios in SLIDE.

	Scenario-1	**Scenario-2**	**Scenario-3**
Hj	4	7	51

4.3 **Details of undrained SLIDE Analysis**

In this analysis. the factors of safeties are researched in case of tailings are in totally undrained conditions. The properties of rock-fill part are kept but only mean values are used for the tailings except their unit weights. The aim of making this analysis is looking over consequent situations when the tailings in undrained conditions. Actually. making consideration about stability of the dam with assuming that the shear strength of the tailings are utterly governed by undrained conditions. is pretty over conservative. Since. the dam has been raised for nearly 30 years. hence ignoring the validation of steady state flow conditions. completion of deeper layers' consolidations and dissipation of excess pore water pressures can mislead the results. Deterministic undrained shear strengths of the tailings are listed in table 4.35. Constant undrained shear strength criteria is preferred and the water is defined from upper boundary of coarse and fine tailings to the toe. The probability of failure. critical slips surface and factor of safeties are showed in figure 4.16.

Table 4.35 Undrained shear strength of the layers in SLIDE analyses.

Undrained Shear Strength (su) (kN/m^2)				
Depth (m)	0-15	15-30	30-45	45-90
Coarse Tailing	30	45	60	80
Fine Tailing	15	30	45	65

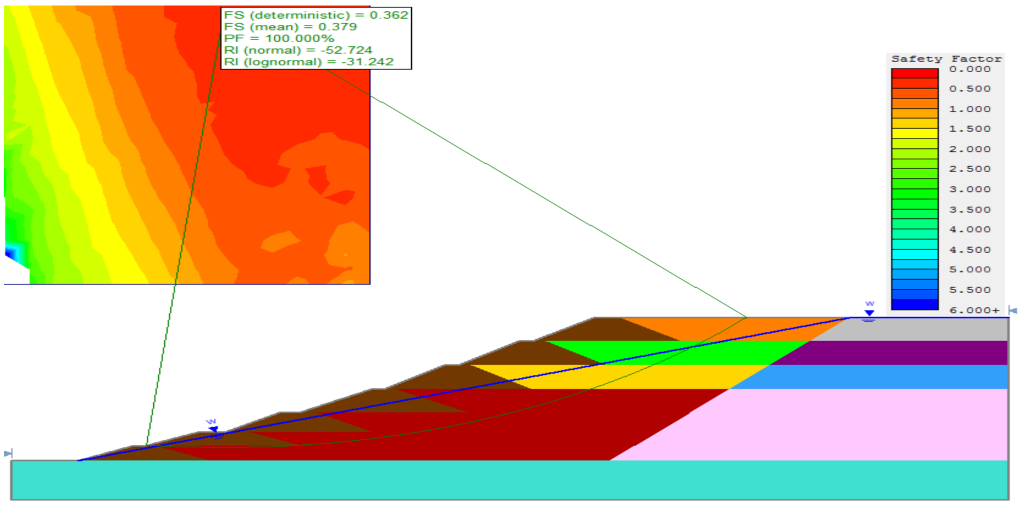

Figure 4.16 Critical slip surface and pore pressures under undrained condition.

4.4 **Staged Construction Analyses at PLAXIS**

In this analysis. the tailing dam is constructed stage by stage on bed-rock layer with 3m/yr of rising rate. Firstly. the rock-fill part is risen to 3 meters in 15 days. afterwards. the tailings are dumped and consolidated in 350 days. The average properties of the layers are used in the analysis and Ko/Ks ratio is taken 10. In each increment stages of the tailings. the water table is also risen. The phreatic surface is initiated to down from the intersection point of coarse and fine tailings and stretched to the toe. During the whole analyses. only saturated hydraulic conductivities of the layers are utilized and kx/ky ratio is taken as 2. As nature of consolidation analyses. the initial voids are significant for shear strength increases for drain layer. reduction of hydraulic conductivities and amounts of settlement. The average void ratios of the tailings are assigned as initial values. also 0.5 is preferred for rock-fill and bedrock. The main properties for the layers are enrolled as in table 4.36.

Table 4.37 Properties of the layers used in PLAXIS analysis.

Parameter	Rock-Fill	Bedrock	Fine Tailing (0-15)	Fine Tailing (15-30)	Fine Tailing (30-45)	Fine Tailing (45-90)	Coarse Tailing (0-15)	Coarse Tailing (15-30)	Coarse Tailing (30-45)	Coarse Tailing (45-90)
Material Model	MC	MC	MC	MC	MC	MC	MC	MC	MC	MC
Material Type	drained	drained	undrained	undrained	undrained	undrained	undrained	undrained	undrained	undrained
ϒdry	21.75	25	16.65	20.38	20.86	21.86	16.65	20.38	20.86	21.86
ϒsat	25	25	21.96	24.68	25.03	25.76	21.96	24.68	25.03	25.76
Kx (m/s)	$2x10^{-8}$	2	$9.7x10^{-9}$	$2.6x10^{-9}$	$2.2x10^{-9}$	$1.7x10^{-9}$	$9.7x10^{-8}$	$2.6x10^{-8}$	$2.2x10^{-8}$	$1.7x10^{-8}$
Ky (m/s)	10^{-8}	1	$4.8x10^{-9}$	$1.3x10^{-9}$	$1.1x10^{-9}$	$8.7x10^{-10}$	$4.8x10^{-8}$	$1.3x10^{-8}$	$1.1x10^{-8}$	$8.7x10^{-9}$
E (kN/m^2)	40000	10^6	3000	6000	9000	13000	6000	9000	12000	16000
v	0.33	0.2	0.33	0.33	0.33	0.33	0.33	0.33	0.33	0.33
c' (kN/m^2)	2.5	100	15	19.66	19.66	19.66	30	19.66	19.66	19.66
Ø' (^{o})	43	45	0	34.82	34.82	34.82	0	34.82	34.82	34.82

Note: ϒdry is dry unit weight, ϒsat is saturaed unit weight. kx is the hydraulic conductivity in horizontal direction, ky is the hydraulic conductivity in vertical direction, E is the Young's modulus, c' is the effective cohesion and Ø' is the effective friction angle.

The material type of rock-fill and bedrock is submitted as drained. during the consolidation process. the increments are allowed in strength of these materials. The increases in strength are prevented for other layers. Therefore. their materials type is selected as undrained. Mohr-Coulomb is used as shear strength criteria for all of the layers. The effective shear strength parameters are assigned for all of the layers expect for surface layers which are extended from surface to 15 meters depth. Undrained shear strength parameters (su) are used for both of the surface layers. In other words. it is assumed that the tailings reach drained condition in five years. After the last calculation. the deformed shape is showed in figure 4.17.

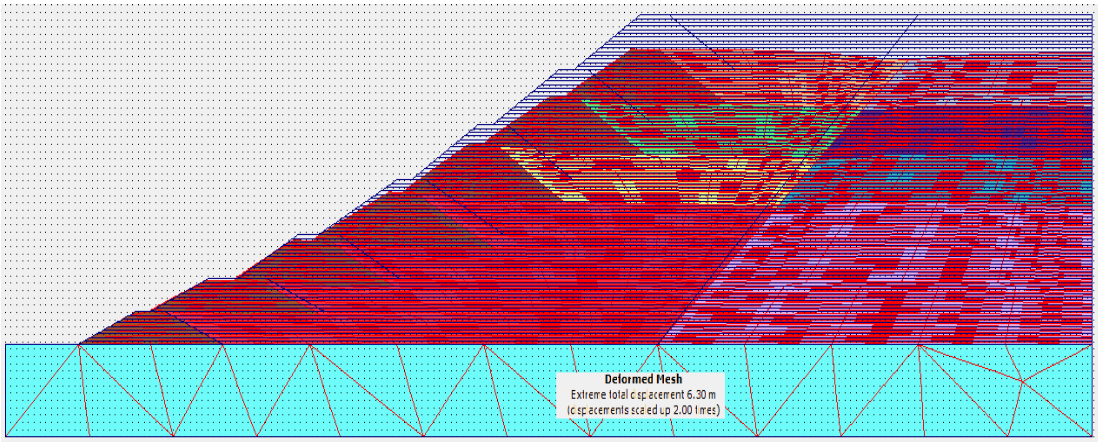

Figure 4.17 Deformed shape of after the last increment.

The displacements are not be set to zero. so that 6.30 meters displacement is cumulative extreme displacement at 90 meters height. The displacements are drastically increased as the dam raise. There are not substantial deformations in bedrock as desired. to provide that modulus of elasticity is chosen really high than others. Also. 0.2 is assigned as its poison ratio like as concrete. The poison ratios for other layers are cited from Zardari (2011).

The vertical total displacements are showed in figure 4.18. The maximum vertical displacement is about 6 meters at the middle of upper tailing as expected. Even this high values. when the iterative procedure is adjusted as standard setting the calculation are not halted.

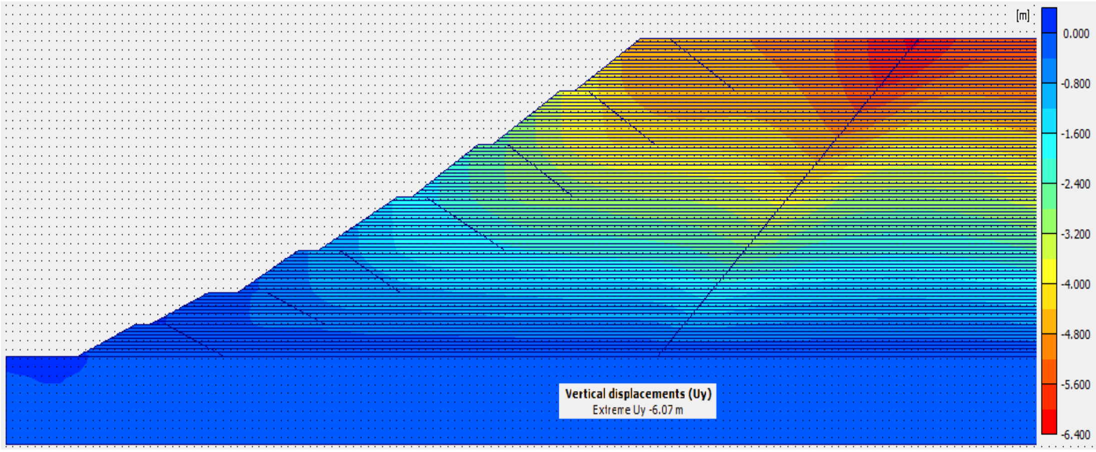

Figure 4.18 Vertical displacements after last increment.

The horizontal total displacements are showed in figure 4.19. The maximum horizontal displacement is occurred at upper boundaries of coarse and fine tailing. The inclination of rock-fill is moving to left. on the other hand. fine tailing is moving to right. This moving is directly related with direction of flow. All of the boundaries allow the flow of the excess water expect the layer at the bottom of the bedrock.

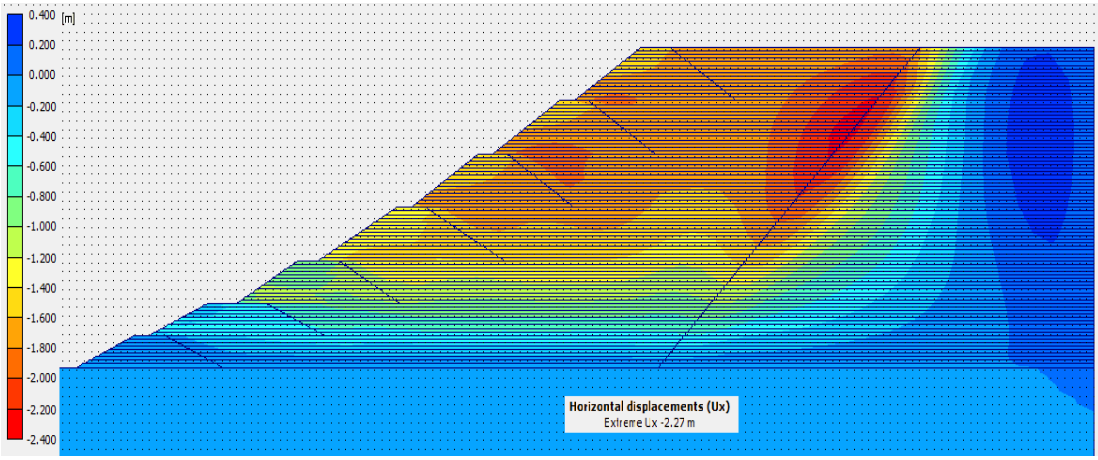

Figure 4.19 Horizontal displacements after last increment.

The total incremental displacements are showed in figure 4.20. This shaded figure indicates that possible slip surfaces. The shapes of the surfaces are disrupted and are not circular at the top of the dam due to the layers whose shear strength is relative less than others.

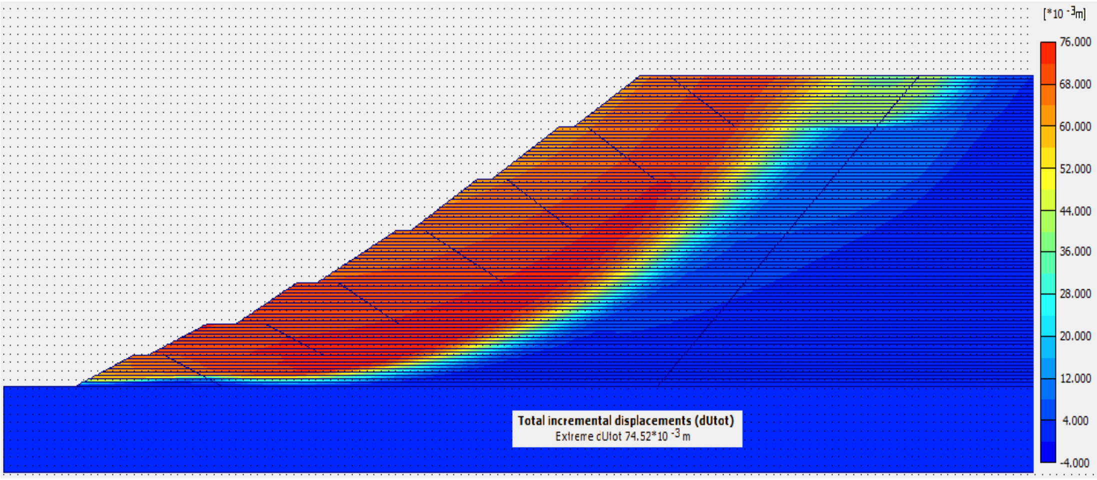

Figure 4.20 Slip surfaces of after the last increment.

The reduction factors are calculated at several different heights while the dam is being raised. The direction of regression line is down as excepted. the reduction factor downs below one when the height is reach to 106 meters. It is maximum critical height for the dam under these conditions.

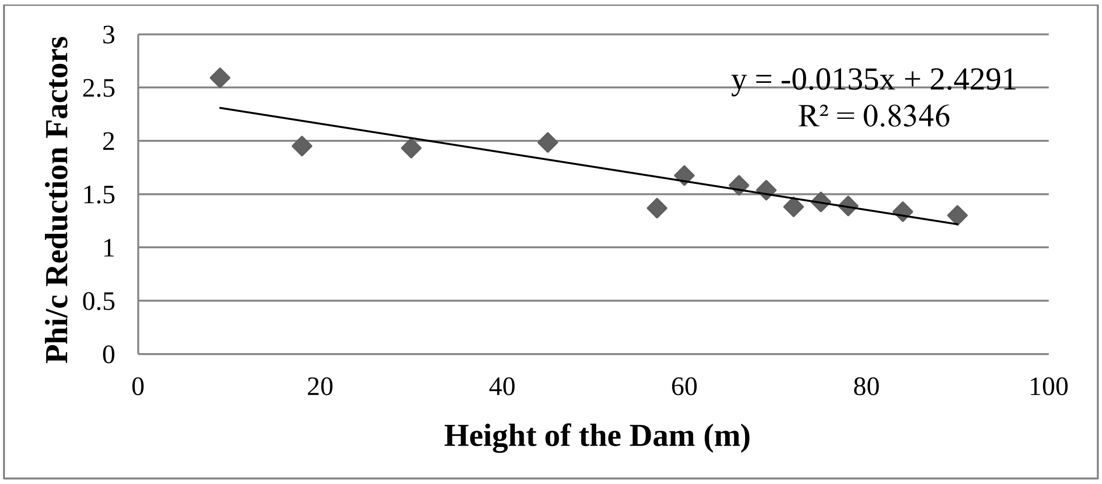

Figure 4.21 Phi/c reduction factors versus height of the dam.

As can be seen from figure 4.21 as height of the dam increases, strength reduction factor decreases. For determining critical maximum height of tailings dams such plots could be useful.

CHAPTER 5

RESULTS AND CONCLUSION

5.1 **Results of SLIDE Analyses**

Two types of extreme conditions drained and undrained are considered in SLIDE analyses. Three scenarios are made up for drained condition. In drained analyses not only factor of safeties are calculated but also the contribution of several parameters to the results are investigated to make comparisons among the reliability of the analyses. According to Sowers (1979) the slope stability of the dam can be categorized as safe. When the pond level gets closer to the rock-fill stability decreases.

Table 5.1 Mean factor of safeties according to scenarios in drained analyses.

Ko/Ks	Scenario-1	Scenario-2	Scenario-3
1	1.371	1.445	1.542
10	1.382	1.476	1.709
100	1.384	1.48	1.797

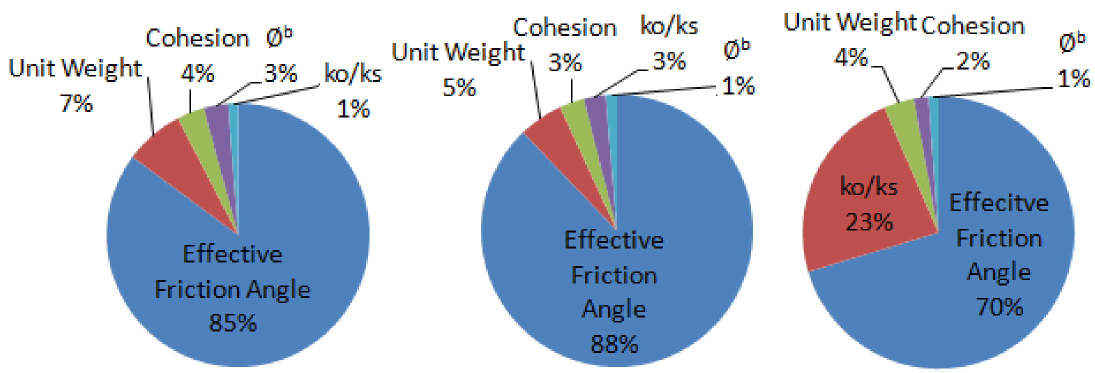

Figure 5.1 Relative contributions of the parameters to the factor of safety according to scenario-1. scenario-2 and scenario-3 respectively.

The reliability of the analyses directly relate with uncertainties of the parameters used in the calculations. The uncertainty of Ko/Ks parameter is substantially more than the others. Also its share drastically increases in scenario-3. Hence scenario-3 is the least reliable analysis among each other and scenario-2 is coming second in ranking.

5.2 **Results of PLAXIS Analyses**

In the plaxis analysis both drained and undrained conditions are included in the calculation. The dam is raised step by step. The results show that strength reduction factors (which can be considered similar to a factor of safety) do not gradually decrease due to changes in the slope of the dam body. As can be seen in figure 4.21 as the height of the dam is increased factor of safety decreases. and the minimum value is 1.3 after the last increment.

5.3 **Conclusions**

In this study, samples of the tailing and natural soil are obtained from a copper tailing dam in Kastamonu, Turkey. Laboratory tests are conducted on these samples to determine geotechnical material properties. Slope stability of the tailing dam is analyzed using PLAXIS and SLIDE softwares according to several scenarios for different conditions. Moreover elaborate literature survey about stability problems and failures of tailing dams all over the world is done. Also general geotechnical characteristics of the copper tailings are investigated. As a result of all these studies some conclusions are deduced.

- In tailing dams, one of the most important reasons for failures and accidents all over the world is undoubtedly slope stability.
- The rate of occurrences of slope stability problems in tailing dams constructed by upstream-method is the highest compared to tailing dams constructed by downstream- or centerline-method of construction.

- While the tailing dam is being raised, drained and undrained conditions (and partially drained) develop together.
- In pure drained conditions, friction angle is overwhelmingly the most significant parameter for slope stability, as expected. Its effect on stability is between 70% and 88%. Other parameters that effect stability and the shares of these parameters are 1%-23% for Ko/Ks ratio (ratio of permeability of tailings at the discharge point at the crest of the dam to their permeability at the pond level at slimes zone), 4%-7% for unit weight of tailing, 2%-4% for cohesion and finally 1%-3% for unsaturated shear strength of tailings.
- The relationship between factor of safety and phreatic surface is obvious and it is largely governed by location of the pond (clean water) at the upper layers.
- Especially, in case of the pond is located on the boundary of coarse and fine tailings, the effects of Ko/Ks ratio on safety factors exceed 20%.
- Amount of seepage is gradually decreased while the location of the pond is being moved away from the dam body, and consequently factor of safety increases.
- On the other hand, amount of seepage are gradually increased as Ko/Ks ratio increase for all scenarios. As Ko/Ks ratio increase the factor of safeties are increased, it is attributed to the fact that the phreatic level decreases.
- According to unique evaluation of factors, there are many uncertainties in analyses of Scenarios-3 than others. Moreover, the most reliable analyses belong to scenarios-1 among three scenarios.
- Determining material properties in the field and in the lab (at the same conditions as in the field) is very important for tailing dams. In addition, obtained geotechnical material properties should be checked with the properties of similar mine tailings (with similar deposition and construction methods) in the literature. Based on laboratory/field obtained and correctly judged geotechnical parameters; conducting seepage, stability (by limit equilibrium method) and deformation analysis (for example by finite element method) is compulsory for each and every increase in tailing dams or in the

tailing level, or for any other planned change in the geometry of tailing dams. Tailing dams contructed by upstream-construction method are the most crticial structures, especially in the seismically active countries such as Turkey. Upstream-construction method of tailing dams should not be preferred.

REFERENCES

Abolfazl, S., Ali. P., Mohyeddin, S. B., Amir Hossein, A. S. (2007). Geotechnical characteristics of coppers mine tailings: A case study. Geotechnical Geology. Engineer. vol.25. pp:591-602.

Andy Fourie. (2009). Preventing catastrophic failures and mitigating environmental impacts of tailings storage facilities. Procedia earth and planetary science. vol.1. pp:1067-1070.

Ang, A. H. S. and Tang, W. H. (2007). Probability Concepts in Engineering Emphasis on Applications to Civil and Environmental Engineering. 2ndEdition. John Wiley& Sons.

ASCE. (2002). American Society of Civil Engineers Los Angeles section geotechnical group. Recommended procedures for implementation of DMG special publication 117: Guidelines for analyzing and mitigating landslide hazards in California. Southern California Earthquake Center.

ASTM. (2008). Standard test method for direct shear test of soils under consolidated drained conditions (D3080-98). Annual book of ASTM Standards. vol.04.08.

ANCOLD. (2011). Australian National committee on Large Dams. Guidelines on tailings dams: planning. design. construction. operation and closure.

Bagarello, V., Sferlazza, Sgroi, A. (2009). Testing laboratory methods to determine the anisotropy of saturated hydraulic conductivity in a sandy-loam soil. Geoderma 154. pp:52-58.

Bear, J. (1972). Dynamics of the fluids in porous media. Dover Publications. Inc.. New York.

Bjelkevik, A., Knutsson, S. (2005). Swedish Tailings – Comparison of mechanical properties between tailings and natural geological materials. Proceedings of "Securing the future. international conference on mining and the environment. Metals and Energy Recovery". Skelleftea. Sweden. June 27-July 1.

Blight, G. (2010). Geotechnical engineering mine waste storage facilities. Schwartz & Wade Books. ISBN: 9780375958991.

Chamber of mining engineering press release dated 10.09.2004. Mine accident in Kastamonu Küre.

Cubrinovski, M., Ishihara, K. (2002). Maximum and minimum void ratio characteristics of sands. JGS. vol.42. pp: 65-78.

Davies, M. P. and Martin, T. E. (2000). Upstream constructed tailings dams - A review of the basics. In proceedings of tailings and mine waste '00. Fort Collins. Balkema Publishers. January. pp:3-15.

Davies, M. P., McRoberts, E. C., Martin, T. E. (2002). Static liquefaction of tailings and fundamentals and case histories. In proceedings tailings dams ASDSO/USCOLD. Las Vegas.

EPA. (1994). Technical report design and evaluation of tailings dams. U.S environmental protection agency office of solid waste special waste branch. 401M Street. SW Washington. DC 20460.

Fredlund, D. G., Xing, A., Fredlund, M. D. and Borbour, S. L. (1995). The relationships of the unsaturated soil shear strength to the soil-water characteristic curve. Canadian Geotechnical Journal. vol.32. pp:440-448.

Fredlund, D. G. and Xing, A. (1994). Equations for soil-water characteristic curve. Canadian Geotechnical Journal. vol.31 (4). pp:521-532.

Frelund, D. G. and Rahardjo, H. (1993). An overview of unsaturated soil behavior. In proceedings of ASCE specialty series on unsaturated soil properties.

Fredlund, D. G., Krahn. J. (1997). Comparison of slope stability methods of analysis. Canadian Geotechnical Journal. 14(3). pp:429-439.

Fredlund, D. G., Morgenstern, N.R., Widger, A. (1978). Shear strength of unsaturated soils. Canadian Geotechnical Journal. vol.15. pp:313–321.

Germaine, J. T. and Germaine, A. Geotechnical laboratory measurements for engineers. John Wiley & Sons. Inc.. 2009.

Google Earth, last accessed on 10/04/2011.

Guangzhi, Y., Guanzhi, L., Zuoan, W., Ling, W., Guohong, S., Xiaofei, J. (2011). Stability analysis of a copper tailing dam via laboratory model tests: Chinese case study. Mineral Engineering. vol.24. pp:122-130.

Gurbuz, A. (2007). The uncertainty in the displacement evaluation of deep foundation.

ICOLD and UNEP. (2001). Tailings dams - risk of dangerous occurrences. lessons learnt from practical experiences. Bulletin 121. ISSN 0534-8293.

Jantzer, I., Bjelkevik, A., Pousette, K. (2008). Material properties of tailings from Swedish mines. Nordic Geotechnical Meeting NGM 15. Sandefjord. Norway. 3–6 September. pp: 229–235.

Johnson, R. H., Blowes, D. W., Robertson, W.D., Jambor, J. L. (2000). The hydro geochemistry of the nickel rim mine tailings impoundment. Sudbury. Ontario. Journal of Contaminant Hydrology. vol.41. pp:49-80.

Lade, P. V., Liggio, C. D., Yamamuro, J. A. (1998). Effects of non-plastic fines on minimum and maximum void ratios of sand. Geotechnical Testing Journal. vol.21 (4). December. pp:336-347.

Leong, E. C., Rahardjo, H. (1997). Permeability functions for unsaturated soils. J. Geotechnical and Geoenvironmental engineering. pp:1118-1126.

Lighthall, P. C., Watts, B. D., Rice, S. (1989). Deposition methods for construction of hydraulic fill tailings dams. in geotechnical aspects of tailings disposal and acid mine drainage. Vancouver Geotechnical Society. Vancouver. British Columbia. May 26.

Marshall, T. J. (1958). A relation between permeability and size distribution of pores. J. Soil Sci.. vol.9. pp:1-8.

Mittal, H. K., Morgenstern, N. R. (1976). Design and performance of tailings dams. ASCE conference on geotechnical practice for disposal of solid waste materials.

Michael. P., Davies, M. P. (2002). Tailing impoundment failures: Are geotechnical engineers listening?. Geotechnical News. September. pp:31-36.

Ning, S. J., Yao, L. H. and Zhao, Y. N. (2008). Application of improved decimal strings genetic algorithm to searching for the most critical slip surface of soil slope. Journal of Engineering Geology. vol.16. no.01. pp.109-115.

Pockoski, M., Michael Duncan, J. (2000). Comparison of computer programs for analysis of reinforced slopes. Virginia tech center for geotechnical practice and research.

Saxena, M., Dhimole, L. K. (2006). Utilization and value addition of copper tailing as extender for development of paints. Journal of hazardous materials B129. pp: 50-57.

Rocscience Inc.. (1989-2003). Slide 2D limit equilibrium slope stability for soil and rock slopes. user's guide part-2.

Sowers, G. F. (1979). Introductory soil mechanics and foundations. Macmillan. pp:587.

Taylor, D. W. (1948). Fundamental of soil mechanics. John Wiley & Sons. New York.

The landside blog, (www.landslideblog.org). Dave Petley. Last accessed on 10/04/2011.

United Nations environmental program division of technology. industry and economics (UNEP). (2000). Mining and sustainable development II challenges and perspectives. vol.23.

United States committee on large dams (USCOLD). (1996). Tailings Dam Incidents. Denver. CO.

United Nations environment program (UNEP). (1996). Tailings Dams Incidents 1980-1996. Mining Journal Ltd.. London.

Wahler, W. A. (1974). Evaluation of mill tailings disposal practices and potential dam stability problems in Southwestern United States. U.S. Bureau of Mines. OFR 50(1)-75–OFR 50(5)-75.

Wise-uranium. http://www.wise-uranium.org. last accessed on 10/04/2011.

Vick, S. G. (1990). Planning. design. and analysis of tailings dams. BiTech Publishers Ltd.. Vancouver. Canada. 1990. ISBN:0-921095-12-0.

Vick, S. G. (1983). Planning. design and analysis of tailings dams. Wiley & Sons. New York. pp:369. ISBN 0-471-89829-5.

Volpe, R. (1979). Physical and engineering properties of copper tailings. current geotechnical practice in mine waste disposal. ASCE. pp:242–260.

Yerbilimleri. http://www.yerbilimleri.com. last accessed on 10/04/2011.

Yin, Guangzhi., Wei, Zuoan, Xu Jiang. (2004). Fine tailings and its dam stability analysis. Chongqing University Publishing House. pp:1–4 (in Chinese).

Zardari, M. A. (2011). Stability of tailing dams focus on numerical modeling. Licentiate thesis. Lulea university of technology.

Zapata, C. E., Houston, W. N., Houston, S. L., Walsh, K. D. (2000). Soil-water characteristic curve variability. Advances in Unsaturated Geotechnics. ASC-Geo institute geotechnical special publication. no.99. C.D. Shackelford. S.L. Houston and N-Y Chang. editors.

Zuoan, W., Guangzhi, Y., Guangzhi, L., Wang, J.G., Ling, W., Louyan, S. (2009). Reinforced terraced fields' method for fine tailings disposal. Minerals Engineering. vol.22. pp:1053-1059.

APPENDIX A

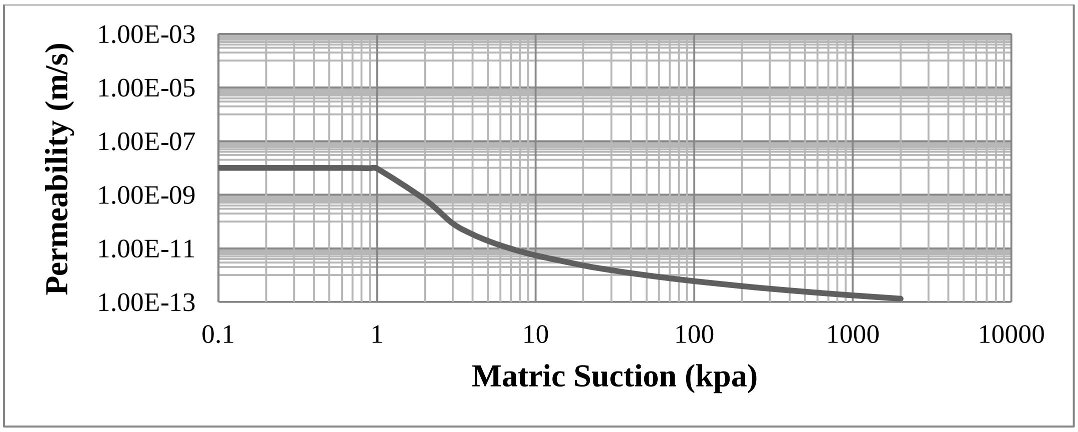

Figure A.1- Graph of matric suction against permeability of rock-fill part when Ko/Ks is equal to 1 .

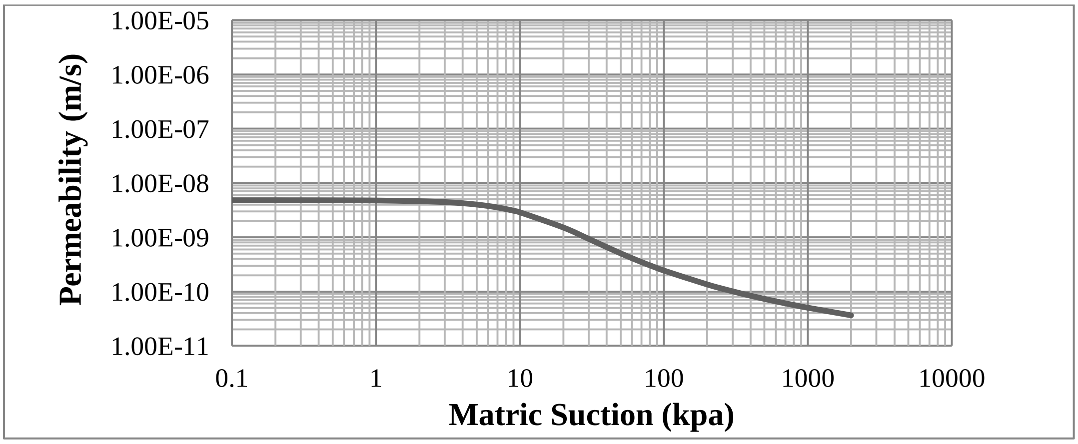

Figure A.2- Graph of matric suction against permeability of both coarser (Ko) and finer (Ks) tailings at interval (0m-15m) when Ko/Ks is equal to 1.

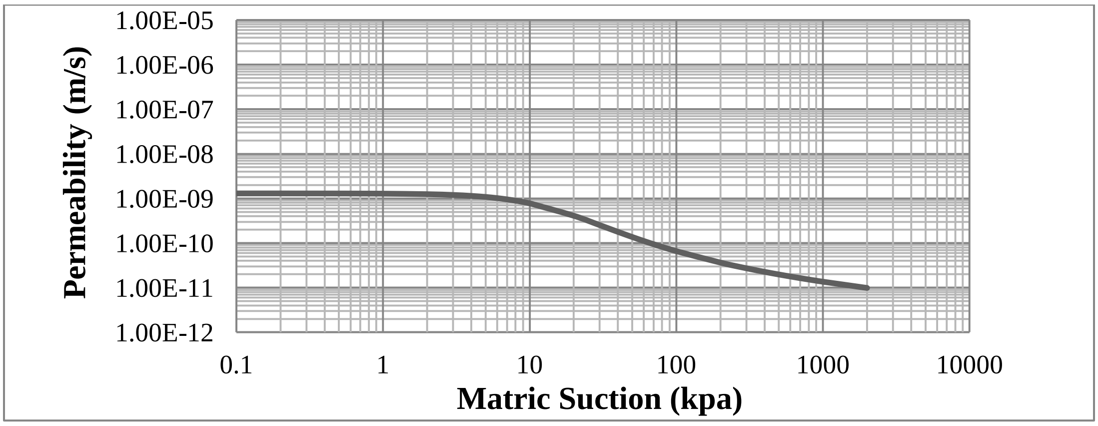

Figure A.3- Graph of matric suction against permeability of both coarser (Ko) and finer (Ks) tailings at interval (15m-30m) when Ko/Ks is equal to 1.

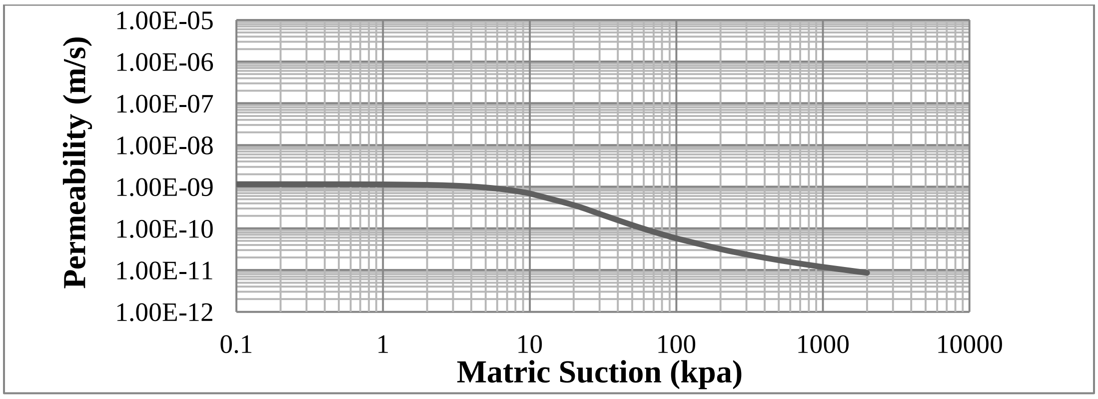

Figure A.4- Graph of matric suction against permeability of both coarser (Ko) and finer (Ks) tailings at interval (30m-45m) when Ko/Ks is equal to 1.

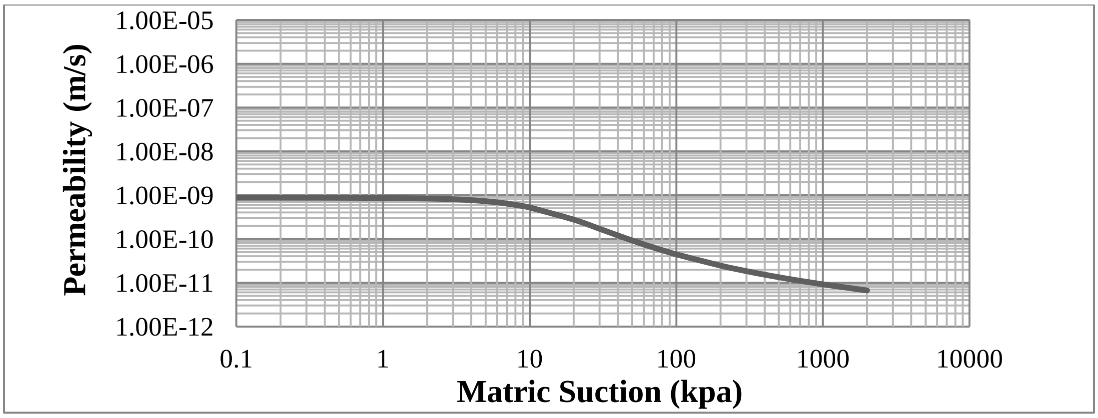

Figure A.5- Graph of matric suction against permeability of both coarser (Ko) and finer (Ks) tailings at interval (45m-90m) when Ko/Ks is equal to 1.

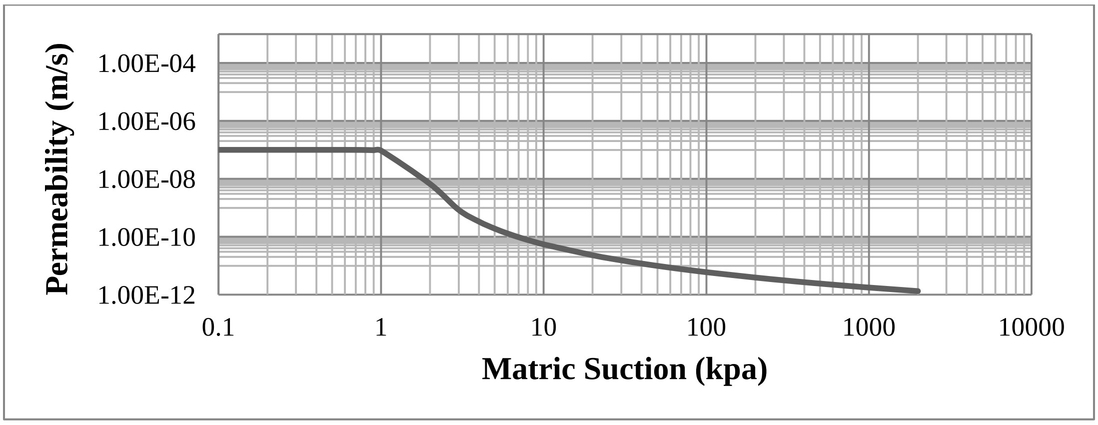

Figure A.6- Graph of matric suction against permeability of rock-fill part when Ko/Ks is equal to 10.

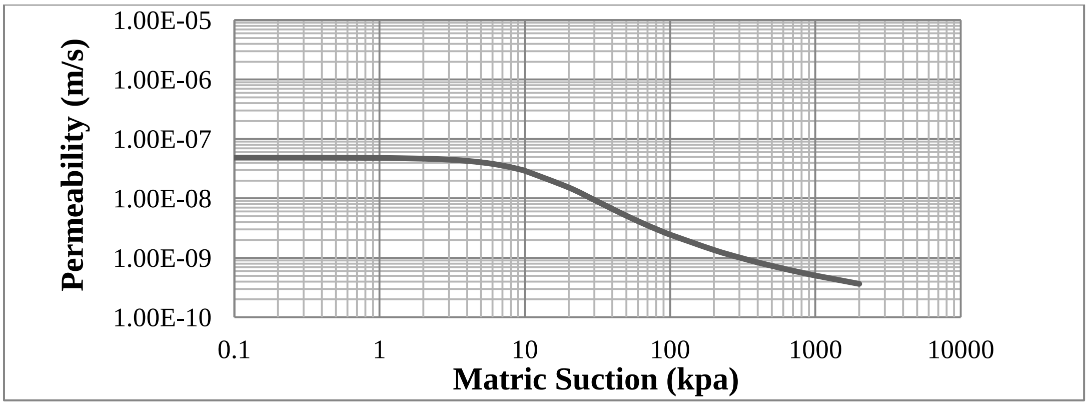

Figure A.7- Graph of matric suction against permeability of coarser tailings (Ko) at interval (0m-15m) when Ko/Ks is equal to 10.

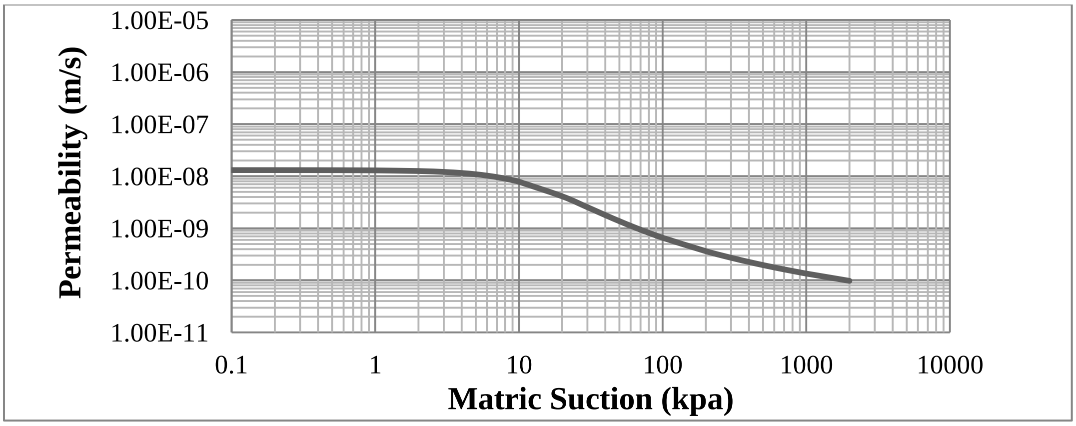

Figure A.8- Graph of matric suction against permeability of coarser tailings (Ko) at interval (15m-30m) when Ko/Ks is equal to 10.

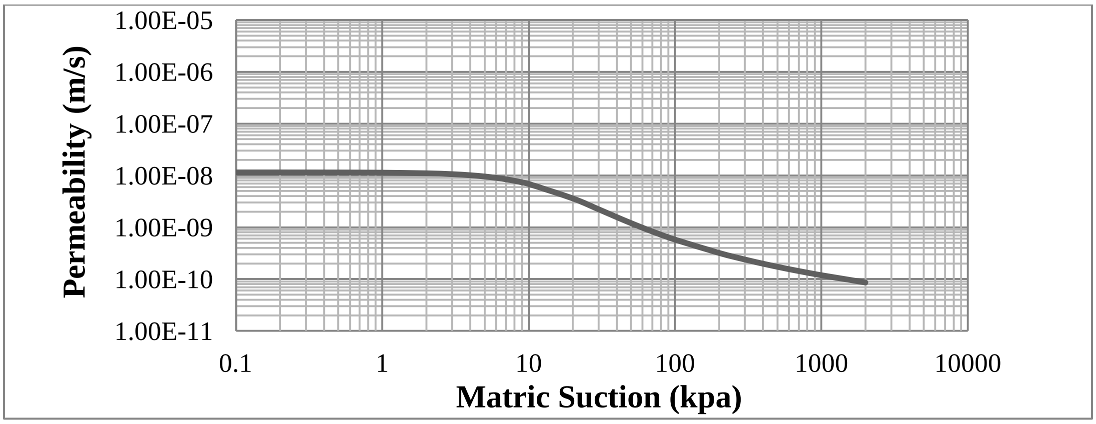

Figure A.9- Graph of matric suction against permeability of coarser tailings (Ko) at interval (30m-45m) when Ko/Ks is equal to 10.

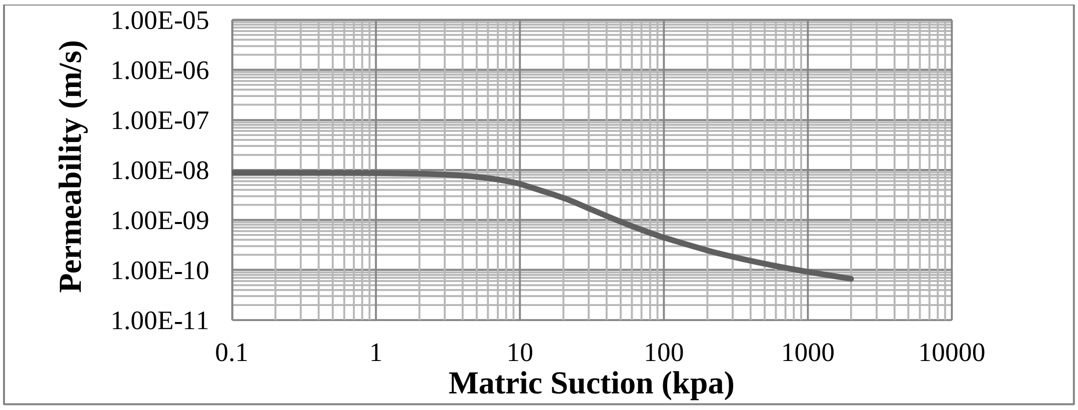

Figure A.10- Graph of matric suction against permeability of coarser tailings (Ko) at interval (45m-90m) when Ko/Ks is equal to 10.

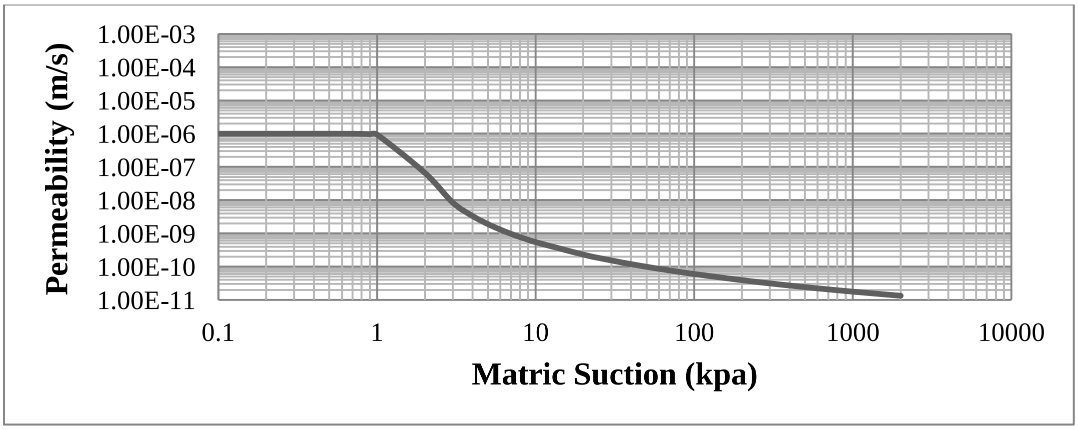

Figure A.11- Graph of matric suction against permeability of rock-fill part when Ko/Ks is equal to 100.

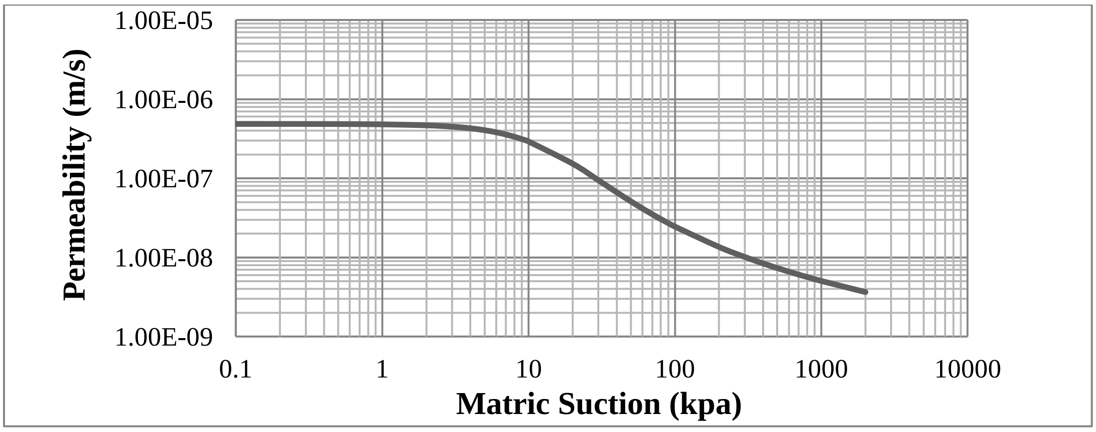

Figure A.12- Graph of matric suction against permeability of coarser tailings (Ko) at interval (0m-15m) when Ko/Ks is equal to 100.

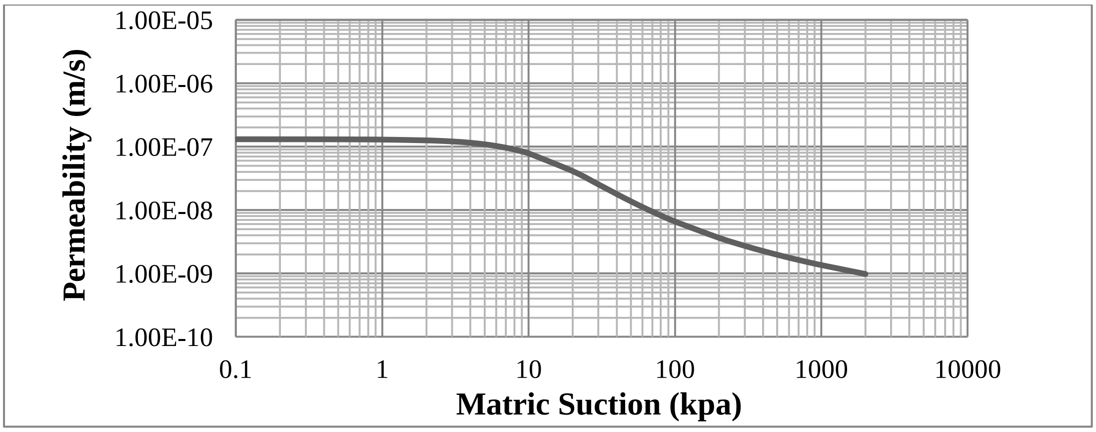

Figure A.13- Graph of matric suction against permeability of coarser tailings (Ko) at interval (15m-30m) when Ko/Ks is equal to 100.

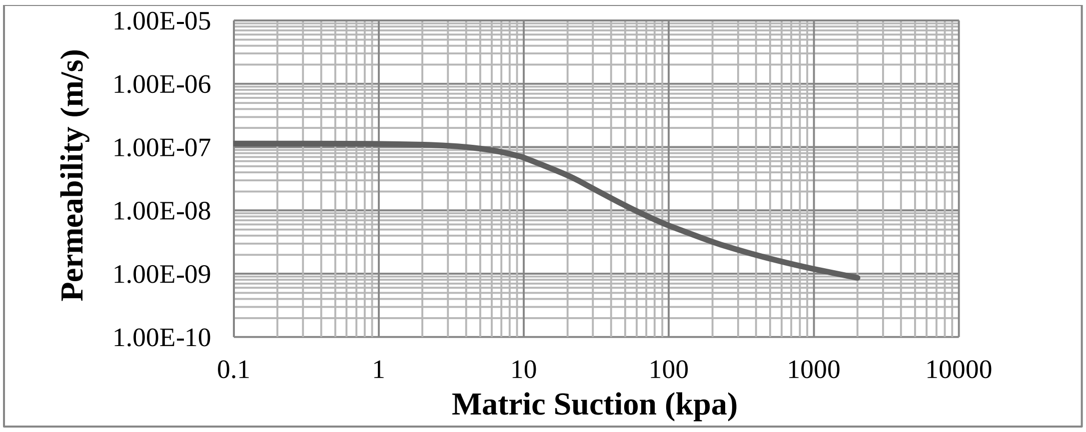

Figure A.14- Graph of matric suction against permeability of coarser tailings (Ko) at interval (30m-45m) when Ko/Ks is equal to 100.

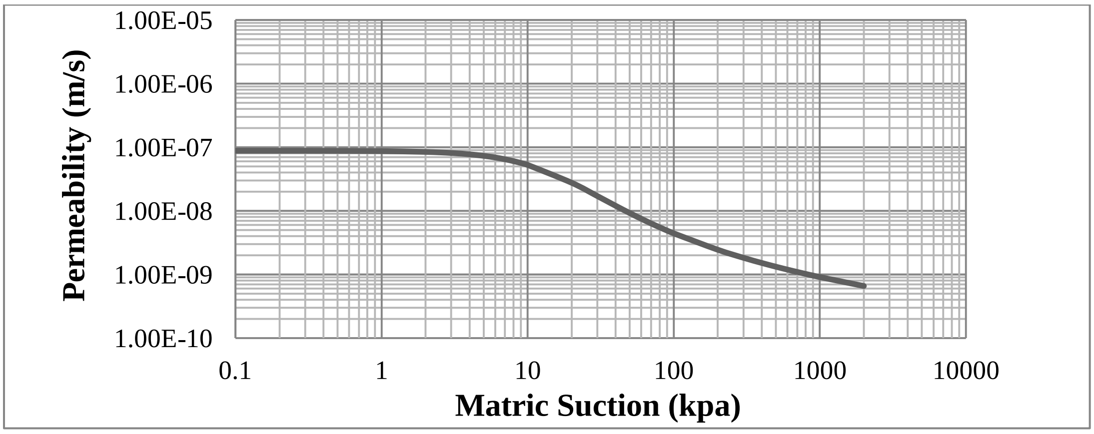

Figure A.15- Graph of matric suction against permeability of coarser tailings (Ko) at interval (45m-90m) when Ko/Ks is equal to 100.